# Hybrid Granitoid Rocks of the Southern Snake Range, Nevada

GEOLOGICAL SURVEY PROFESSIONAL PAPER 668

# Hybrid Granitoid Rocks of the Southern Snake Range, Nevada

*By* DONALD E. LEE *and* RICHARD E. VAN LOENEN

GEOLOGICAL SURVEY PROFESSIONAL PAPER 668

*A study of assimilation and the resulting systematic and interrelated differences in chemistry and mineralogy within a well-exposed granitoid outcrop area of 20 square miles*


UNITED STATES GOVERNMENT PRINTING OFFICE, WASHINGTON : 1971

UNITED STATES DEPARTMENT OF THE INTERIOR

ROGERS C. B. MORTON, *Secretary*

GEOLOGICAL SURVEY

William T. Pecora, *Director*

Library of Congress catalog-card No. 72-611324

For sale by the Superintendent of Documents, U.S. Government Printing Office
Washington, D.C. 20402

# CONTENTS



# ILLUSTRATIONS

## TABLES

# HYBRID GRANITOID ROCKS OF THE SOUTHERN SNAKE RANGE, NEVADA

By DONALD E. LEE and RICHARD E. VAN LOENEN


## ABSTRACT

A detailed field and laboratory study of igeneous rocks exposed a few miles north of the Mount Wheeler mine in the southern Snake Range of Nevada showed many well-defined and interrelated differences in the chemistry and mineralogy of the granitoid rocks within an outcrop area of about 20 square miles. Chemical controls were established by major- and minor-element analyses of 133 granitoid rocks; mineralogical controls were established by modal analyses of all the analyzed rocks and by mineral separation work on 30 of them.

The well-exposed granitoid rocks range in composition from granodiorite with 4.5 percent CaO (63 percent $SiO_2$) to quartz monzonite with 0.5 percent CaO (76 percent $SiO_2$). For various reasons, we relate mineralogical and other chemical trends to CaO instead of to $SiO_2$, but the major-element chemistry of these rocks is that expected in a series of magmatic differentiates. Amounts of essential minerals (quartz, feldspars, micas) in these rocks also fit the idea of differentiation.

In a field setting less ideal for a detailed study, it would indeed seem best to appeal to the process of differentiation to explain the gross chemistry and mineralogy of these rocks. However, in the study area of this report, it is obvious that the equivalent of a large part of the classic differentiation sequence formed through assimilation of chemically distinct host rocks, which are Prospect Mountain Quartzite, Pioche Shale, and Pole Canyon Limestone, all of Cambrian age. The case for assimilation is supported by several positive arguments based on field relations and on separate lines of chemical and mineralogical evidence. Some of the most obvious clues are provided by accessory-mineral data resulting from systematic mineral-separation work on analyzed rocks.

A few square miles of the intrusive outcrop displays large crystals of muscovite and is otherwise chemically and mineralogically distinct from the rest of the igneous exposure. This rock intruded the Osceola Argillite of Misch and Hazzard (1962), and its distinctive nature resulted from assimilation of the argillite.

The chemistry of the intrusive rocks is similar in some respects to that of alkalic rocks and carbonatites and seems to offer new support to the limestone syntexis hypothesis for the origin of these odd rock types. Allanites from the most lime rich rocks show a pronounced concentration of the most basic rare earths; and whole-rock concentrations of rare constituents such as total cerium earths, Zr, P, Ti, Ba, Sr, and F increase sympathetically with whole-rock calcium.

The granitoid rocks described are exposed just beneath the surface of a thrust fault, and the eastern part of the intrusive outcrop has been cataclastically deformed by movement on the thrust. The main intrusive phase and some associated aplite crystallized during Middle Jurassic time (about 160 million years ago), but the nonpegmatite beryllium mineralization at the Mount Wheeler mine probably resulted from hydrothermal activity related to a middle Tertiary (28–33 million years ago) aplite phase.


## LOCATION AND GEOLOGIC SETTING

The area studied is about 50 miles southeast of Ely, Nev., in the southern part of the Snake Range of Nevada, a prominent north-south range just west of the Utah boundary, in the eastern part of the Basin and Range province (fig. 1). Together with its southern continuation, the Wilson Creek Range, and its northern extension, the Deep Creek Range of Utah, the Snake Range as a geographic unit is about 150 miles long.

The granitoid rocks are exposed a few miles north and east of the Mount Wheeler mine. These rocks intruded part of a lower Paleozoic miogeosynclinal sequence of predominantly quartzite and carbonate rocks; they are east of the Mississippian Antler orogenic belt (Gilluly, 1963, p. 139, 140) and just west of the Cretaceous Sevier orogenic belt (Armstrong, 1968, p. 436). The sedimentary rocks exposed in intrusive contact with these granitoid rocks are the Shingle Creek Quartzite and Osceola Argillite (Misch and Hazzard, 1962) of Precambrian age, and the Prospect Mountain Quartzite, Pioche Shale, and Pole Canyon Limestone, all of Cambrian age. A comprehensive account of the depositional history of east-central Nevada was given by Drewes (1967, p. 86–88).

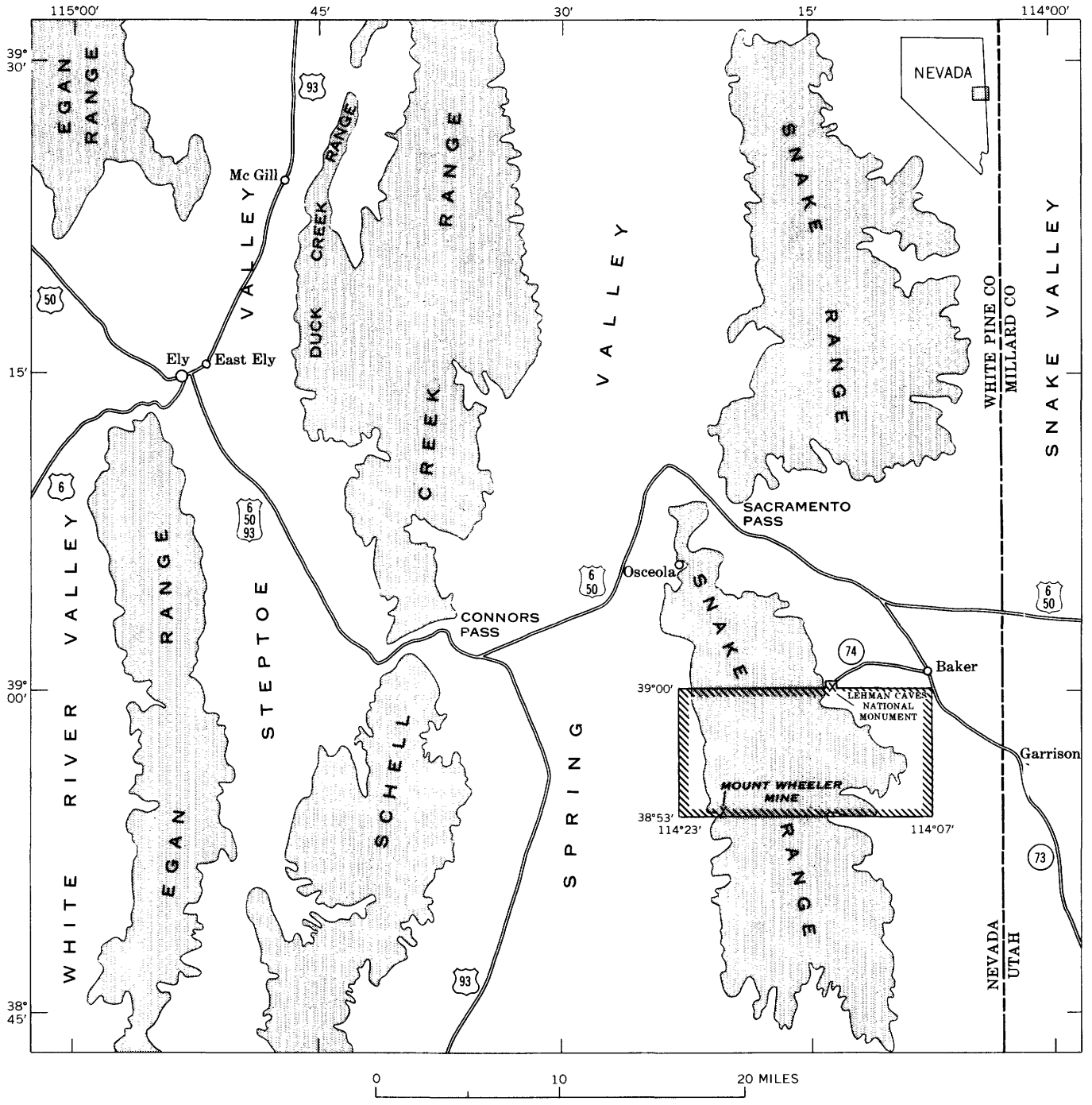


FIGURE 1.—Map showing location of report area.

## PREVIOUS WORK AND PURPOSE OF THIS PAPER

Geologists of the Wheeler Survey visited the area and published some general observations on the Snake Range (Howell, 1875, p. 240–242). About 30 years later, Spurr (1903, p. 25–36) made a reconnaissance of the area. This was followed by a more detailed study of part of the southern Snake Range by Weeks (1908), who described the geology and mineral resources of the Osceola mining district, about 10 miles north of the present study area and about 14 miles north of the Pole Canyon adit of the Mount Wheeler mine.

The granitoid rocks described in this report were first mapped by Drewes (1958) as part of a reconnaissance of about 250 square miles of the adjacent Wheeler Peak (Nevada) and Garrison (Nevada-Utah)

15-minute quadrangles. Later, a more comprehensive study of these two quadrangles was carried out by Whitebread, Griggs, Rogers, and Mytton (1962, 1970). Much of the area between these two quadrangles and the Osceola mining district was mapped by Misch and Hazzard (1962).

The nonpegmatite beryllium mineralization at the Mount Wheeler mine was discussed by Stager (1960) and Whitebread and Lee (1961). The present study was started to test the hypothesis of a genetic relation between this beryllium mineralization and the granitoid rocks exposed a few miles to the north. It soon became clear that the texture and mineralogy of the intrusive vary widely from place to place; this led to the suggestion (Lee and Bastron, 1962) that more than one intrusive phase might be present within the 20-square-mile outcrop area. Later results (Lee and Dodge, 1964) showed that chemical and mineralogical differences in the intrusive rocks were controlled primarily by variations in the nature of the host rock. Intrusive rocks in the study area have compositional ranges from granodiorite (host rock Cambrian Pole Canyon Limestone) to quartz monzonite (host rock Cambrian Prospect Mountain Quartzite). Further work (Lee and Bastron, 1967) disclosed that these granitoid rocks are chemically similar in some respects to alkalic rocks and carbonatites. Analyses of the rare-earth contents of accessory allanites and monazites show concentration of the most basic rare earths to be directly related to calcium content of the rock. Moreover, whole-rock concentrations of rare constituents such as total cerium earths, Zr, P, Ti, Ba, and Sr increase sympathetically with whole-rock calcium content. Later (Lee and others, 1968), 25 accessory zircon fractions recovered from these granitoid rocks were described. The crystal morphology, physical properties, and minor-element contents of these zircons support the idea that the large compositional range and systematic chemical gradients found in the granitoid rocks result more from assimilation of sedimentary host rocks than from differentiation of magma. More recent studies describe the sphene (Lee and others, 1969), biotite (Lee and Van Loenen, 1970), and epidote (Lee and others, 1971) from these granitoid rocks. Radiometric ages for many minerals from these rocks are discussed by Lee, Marvin, Stern, and Peterman (1970).

This paper describes the intrusive types exposed north and east of the Mount Wheeler mine and presents the field evidence on which we base our conclusion that compositional differences among these types are due mainly to assimilation of chemically distinct host rocks. Sample locality data and major- and minor-element data for each of 133 granitoid and 34 sedimentary rock samples are included. This study also sets the stage for additional papers on the detailed mineralogy and geochemistry of individual mineral suites separated from these intrusive rocks.

The following is a review of a few terms, all of which are in general use. *Assimilation* is the process of interaction between a magma and its host rocks. A magma that assimilates foreign material undergoes a chemical change, or *contamination*, and such contaminated magma will crystallize as a *hybrid* rock. Assimilation always implies contamination. *Granitoid* is a term applied to igneous rocks with the texture of a granite, without concern for composition. The term usually is reserved for rocks that are nearly uniform in grain size, whether fine or coarse. In the present report, the term also is applied to some intrusive rocks that are porphyritic but are nevertheless genetically related to the granitoid rocks.

A study such as this is dependent in large measure on analytical results provided by our colleagues in the laboratories. Each contributor is specifically acknowledged by name in the tables of analytical data accompanying the report, but we take this opportunity to thank them as a group for their careful and essential work.

## INTRUSIVE STRUCTURES, FORM, AND CONTACT EFFECTS

Petrologically and structurally, these intrusive rocks fall into three separate study units: the Snake Creek-Williams Canyon area, the Pole Canyon-Can Young Canyon area, and the Young Canyon-Kious Basin area. The aplite types are a separate category and are discussed later in this paper.

The influence of host rock on chemistry and mineralogy of the intrusive rocks, as described by Lee and Dodge (1964) and Lee and Bastron (1967), is most clearly shown in the Snake Creek-Williams Canyon area. There the intrusive is undeformed, probably has not been eroded to a depth of much more than 1,000 feet, and is well exposed in contact with host rocks ranging in composition from limestone to quartzite.

The Pole Canyon-Can Young Canyon area intrusive is exposed almost entirely in contact with quartzite. However, this intrusive is very different from the granitoid rock in contact with quartzite in the Snake Creek-Williams Canyon area, the intrusive distinguished in part by the presence of large muscovite phenocrysts, many of which contain euhedral crystals of biotite. Evidence presented in the following section shows that the distinctive nature of this intrusive reflects the influence of the Osceola Argillite. As in the Snake Creek-Williams Canyon area, the nature of the granitoid rock resulted mainly from assimilation.

The Young Canyon-Kious Basin area intrusive consists of sheared and unsheared parts separated by a fault that probably represents the location of the Cambrian Pioche Shale before the advent of the intrusive. The shearing and deformation so apparent in part of this intrusive have been caused by regional thrust faulting. Although this deformation has obscured the original nature of much of the intrusive outcrop, bulk-rock analyses reflect host-rock influence here, too, on the chemistry of the intrusive rock.

### SNAKE CREEK-WILLIAMS CANYON AREA

The eroded roof of the granitoid body (pl. 1) probably was not much higher than the present intrusive as exposed in peaks in the Snake Creek area (Drewes, 1958, p. 231). Thus, the intrusive itself probably has not been anywhere unroofed to a depth of much more than 1,000 feet. This point is important to the major- and minor-element chemistry of these granitoid rocks.

This intrusive is essentially domelike (Drewes, 1958, p. 231) and roughly concordant with bedding in the overlying sedimentary rocks. Both the general concordance and the most notable discordance are well shown where the intrusive crops out on the crest of the range between Snake Creek and Williams Canyon. At the northern edge of this outcrop, beneath Pyramid Peak, the intrusive contact nearly parallels the bedding of the overlying quartzite, but at the southern edge of this outcrop, the intrusive contact cuts across about 1,000 feet of quartzite bedding at a very high angle.

Locally along steep contacts, the host rock has been dragged upward and appears to have been shouldered aside (Drewes, 1958, p. 231). This is apparent in the extreme eastern part of the outcrop (pl. 1, section *B–B′*), where Pioche Shale and Pole Canyon Limestone have been folded into an overturned syncline. However, just north of this shale outcrop an apophysis of the intrusive has engulfed part of the limestone. This, as well as the discordant intrusive-rock–quartzite contact at the crest of the range, indicates that some stoping took place.

The eastern half of the intrusive outcrop in Snake Creek drainage contains many xenoliths—fragments of Pioche Shale that are partly assimilated (Lee and Bastron, 1962). The smallest of these is the size and shape of a walnut; the largest crops out over an area of about 2 acres (pl. 1, section *B–B′*). In several places where the largest xenoliths are about 1 foot long, they aggregate as much as 5 percent of the intrusive. These xenoliths tend to be ellipsoidal and to stand out on a weathered surface, so usually the strike and at least the general angle of dip can be determined. Strikes tend to parallel the nearest intrusive contact, and dips usually are within 20° of vertical (pl. 1). From this we infer that at least this part of the intrusive must have undergone magmatic flow before solidification. West of the 2.0-percent-CaO isopleth (pl. 1), the intrusive is almost devoid of xenoliths.

The rock is well jointed (Lee and Bastron, 1962), and the sets within the system, in order of consistency, typically have these strikes and dips: (1) N. 40° E., steep SE. to 90°, (2) N. 40° W., moderate NE. or SW. to 90°, and (3) E., moderate N. or S. to 90°. Joints are not as well developed where CaO content of the rock is less than about 2.0 percent. In the more calcium rich part of the intrusive, many of the northeast-trending joint surfaces are silicified and stand out above the adjacent rock. Joint attitudes have been omitted from the map (pl. 1) for the sake of simplicity.

Above Johnson Lake, at the head of Snake Creek, scheelite-bearing quartz veins in the intrusive were mined. These quartz veins, as much as 3 feet wide, strike northeast and dip 80°–90° SE. The late Mr. Alfred Johnson, who discovered this deposit in 1907 and worked it intermittently for about 40 years, found seven of these quartz veins near the crest of the range (oral commun., 1961). There has been little alteration of the intrusive adjacent to these veins.

North of Williams Canyon (pl. 1) on the west side of the range, most of the intrusive is strongly altered and carries many quartz veins that are continuously exposed over a horizontal distance of 1,000 feet or more. Many of these veins are several feet wide and, in places, swell to 10 feet. Commonly, the intrusive near the quartz veins contains cubes of iron oxide pseudomorphous after pyrite. A few (one in particular) of these quartz veins were worked for wolframite at the Hub mine during World War I. Many aplites also cut the intrusive in this area. Most of the aplites are less than 1 foot wide but are continuously exposed over hundreds of feet. Both the quartz veins and the aplites are controlled by a very well developed and persistent set of joints that strike N. 60°–75° E. and dip 60°–90° SE. Locally, other joint sets also are evident, but the east-northeast set is everywhere dominant and even influences the topography.

Drewes (1958, p. 221, 223) noted that there is little evidence of contact metasomatism around the intrusive exposed in the Snake Creek–Williams Canyon area. The texture of most of the Pole Canyon Limestone is metamorphic (Drewes, 1958, p. 226), but as discussed later in the present report, this probably results more from a low-grade regional metamorphism than from the intrusive activity. In addition, it is not uncommon for the limestone to be gnarled and deformed within a few yards of the intrusive contact, but there is virtually no skarn.

Contact action on the Pioche Shale is no more impressive. Within a few feet of the igneous rock, the shale may be baked and recrystallized, but there is no evidence of metasomatism. The thin limestone in the lower part of the Pioche, the Wheeler limestone of local usage, shows a sparse development of scheelite and light-green amphibole and pyroxene near the intrusive contact at the crest of the range, near the eroded roof of the intrusive.

The intrusive's effect on the Prospect Mountain Quartzite is difficult to study because the quartzite-intrusive contact is exposed only in a few places owing to the tendency of the quartzite to form talus over the intrusive. Micropegmatitic apophyses were observed, however, along bedding and jointing in the quartzite. Contact action on the Osceola Argillite is more pronounced. In places, the rock is metamorphosed to spotted hornfels (Whitebread and others, 1962).

### POLE CANYON-CAN YOUNG CANYON AREA

In the Pole Canyon-Can Young Canyon area, the intrusive body (pl. 1) is domal in form, except for its northwestern extension, where flanking sedimentary beds dip gently toward, instead of away from, the igneous rock. This intrusive is exposed in contact with Prospect Mountain Quartzite, but it differs markedly from the granitoid intrusive that is in contact with this quartzite in the Snake Creek-Williams Canyon area.

The Pole Canyon-Can Young Canyon area intrusive actually consists of two main phases that are subequal in outcrop area—a "host" intrusive and late aplitic and pegmatitic material. The "host" intrusive is coarse grained and porphyritic, with phenocrysts of muscovite and feldspar as much as 1 inch across. Although degree of friability varies, no really massive sample of this rock was found. Good outcrops are scattered, with rubble slopes common except where the earlier phase has been invaded and now is sustained by aplitic and micropegmatitic rock. Where observed, joints in the host intrusive strike either northeast or northwest and dip steeply. The aplites tend to follow the better developed northeast-trending set, but many crosscutting relations are exposed. This also is true of the quartz veinlets that are present and closely associated with the aplites in many places.

The aplitic-pegmatitic dikes are as much as 6 feet wide. Where they occur in swarms, they all but obliterate any vestige of the host intrusive. Some of the large dikes display multiple and symmetrical banding, but there is no consistent relation between grain size of the various bands and their position within the dike. Much of this aplitic and pegmatitic material contains garnets.

In contrast to the Snake Creek-Williams Canyon granitoid rocks, the Pole Canyon-Can Young Canyon intrusive does not contain xenoliths. Moreover, chemical differences in the rock from place to place are relatively small, with no systematic spatial distribution of values for either major or minor elements.

Two additional structural features merit description. The eastern part of the igneous outcrop in Can Young Canyon displays a gross platy jointing that strikes north and dips about 35° E., roughly comformable to the bedding of the overlying quartzite. Also, two areas of sheared intrusive were found about 3,000 feet apart (pl. 1). The larger of these areas (section $A$–$A'$) is 30 feet wide and is continuously exposed for more than 100 feet along the strike (N. 10° W.) of the shears, most of which dip moderately to the west. These outcrops of sheared material are similar in every respect to the large exposure of deformed intrusive that includes parts of Young Canyon and Kious Basin, where the shearing is obviously a result of regional thrust faulting.

Because the host intrusive does not stand up well in outcrop and because quartzite talus tends to spill down over this intrusive, contact features are very poorly exposed in the Pole Canyon-Can Young Canyon area. Contacts involving apophyses of aplitic material in quartzite were seen in several places.

We attribute the distinctive nature of the intrusive rocks in this area to assimilation of the Osceola Argillite. This idea originally stemmed from an interesting mineralogical detail noted during mineral-separation work on these rocks. On the west side of the range where the intrusive is in contact with argillite, some of the zircon in the rock is present as acicular inclusions in apatite. This mode of occurrence was not found in any other part of the Snake Creek-Williams Canyon intrusive outcrop area. In the Pole Canyon-Can Young Canyon area, however, the same feature is so well developed that nearly all the zircon occurs as such inclusions.

The intrusive in the Pole Canyon-Can Young Canyon area appears to be near the stratigraphic position of the Osceola Argillite. The Osceola is probably 750–800 feet thick (Weeks, 1908; Misch and Hazzard, 1962), although Drewes (1958, fig. 2) showed a lesser thickness. In the same section, Drewes showed the top of the Osceola Argillite to be about 3,000 feet below the top of the Prospect Mountain Quartzite, whereas Misch and Hazzard (1962, p. 302–306) indicated that it may be almost 4,000 feet below. Regardless of which figure is accepted, we conclude that the intrusive rocks exposed in the Pole Canyon-Can Young Canyon area must be near the projected position of the argillite (pl. 1, section $A$–$A'$).

## YOUNG CANYON-KIOUS BASIN AREA

The Young Canyon-Kious Basin area is significant from the standpoint of the regional geology and tectonics, and it also provides special evidence bearing on the overall problem of the intrusive rocks under study. Intrusive contacts are roughly concordant with the bedding in the overlying sedimentary rocks although, locally, relations are somewhat obscured by the faults and cataclasis that make knowledge of this area so vital to an understanding of regional history.

Most of the intrusive rocks of the Young Canyon-Kious Basin area have been sheared and brecciated (pl. 1). Shears strike consistently about N. 15° W. Some shears dip northeast, but most (many of which are not plotted) dip southwest, commonly at about 25°. Slickensides normal to the direction of strike are very well developed on many of the shear surfaces, and in some places the direction of (latest) movement can be determined. We have not systematically determined these directions, but in many places the hanging wall of the shear has moved up with respect to the footwall, especially where the shear dips northeast. Here and there the intersection of these shears effects a gross lineation in the intrusive. This lineation strikes about N. 15° W., and plunges northwestward, commonly at 10°–15°. Regarding the regional thrust faulting, Drewes (1958, p. 230) stated: "The direction of movement and movement sense on these * * * thrust faults * * * is such that the upper plates moved relatively east-northeastward." The N. 15° W. strike of the shears described above is about perpendicular to the direction of thrusting deduced by Drewes, largely from his study of drag folds associated with the thrust faulting. Both the shears and the related lineation in these intrusive rocks result, then, from the regional thrust faulting, and they support Drewes' ideas regarding direction of fault movement.

About 1,200 feet west-southwest of locality P8 (pl. 1), another type of lineation was found in a mass of Pioche Shale surrounded by intrusive very near both the intrusive contact and the thrust surface. This shale has been recrystallized but has undergone little or no metasomatism. Crinkles and minor fold axes in the Pioche strike about N. 10° W. and are almost horizontal.

In a few localities where crushing has been most pronounced, as at locality 113 (pl. 1), the intrusive contains dikelike forms of pseudotachylite as much as 1 foot wide. These have about the same strike as the shears, and most have a southwest dip. In localities where deformation has been least pronounced, masses of relatively undeformed intrusive are suspended in the more contorted rock. These masses may involve tens of cubic feet; where best exposed, they are bounded by shears and cut by an intricate network of fractures marked by iron stains. One exposure of remarkably fresh-looking intrusive (loc. 111, pl. 1) more than 100 feet across displays no directional elements. The rock seems to be out of place in this environment until it is seen in thin section, where quartz and feldspar show much evidence of pronounced strain.

Where shear zones in the Young Canyon-Kious Basin area intrusive rock are intense over a distance of 30–40 feet normal to strike, they may contain barren milky-white bull quartz interfingering with the broken intrusive or forming massive veins several feet wide. Aplitic material is garnet free and only sparse within the main mass of the sheared material. There are a few scattered unsheared xenoliths (pl. 1, loc. 85; table 5, sample 85) that appear to be identical with those in the Snake Creek area and must be fragments of partly assimilated Pioche Shale. Some recognizable faults occur in the area of sheared intrusive, but displacements along them probably were small. Joints are present locally; although attitudes are not very systematic, strikes tend to be either east-northeast or west-northwest, and dips, steep.

Petrographic evidence (p. 40) indicates that the intrusive rock was rather well crystallized and "dry" at the time of deformation. Field evidence, such as the lack of pronounced offset along contacts and the presence of some ellipsoidal xenoliths, certainly suggests that although shears are ubiquitous over about 3 square miles of intrusive outcrop area, movement along any one of them probably was minor, perhaps not more than a few inches.

The sheared intrusive is separated from unsheared intrusive by a normal fault that probably represents the location of the Pioche Shale before the advent of the intrusive—that is, a bedding-plane fault that strikes about N. 50° W. and probably dips about 40° NE. (pl. 1, section *B–B'*). Near the head of Kious Basin, this fault is intersected by another that strikes about N. 20° W., subparallel to the strike of the shears in the intrusive to the east. Even though we cannot show the displacement to have been very great along either fault, the two faults are significant both because they separate sheared from unsheared material and because the wedge-shaped area of intrusive between them is made up of aplitic material.

The most extensive development of skarn found within the entire area is in Pole Canyon Limestone adjacent to sheared aplitic material on the northwest side of Can Young Canyon (pl. 1). Even so, the skarn is not impressive. Epidote and garnet are present in a lenticular body 6–18 inches wide and about 100 feet long.

The small area of unsheared intrusive exposed in contact with quartzite southwest of the projected Pioche Shale (pl. 1) contrasts sharply with the deformed intrusive to the northeast. In the unsheared area, the best developed joints strike N. 10°–30° W. and dip steeply northeast. There are a few scattered aplites and quartz veinlets and a few xenoliths of Pioche Shale. The contact is obscured by quartzite talus.

### SUMMARY OF INTRUSIVE ROCKS

In order to set the stage for the section on rock chemistry, we have distinguished petrologically and structurally the three intrusive types. Nonetheless, the total intrusive outcrop area involved is only about 20 square miles, so the features described reflect a single general geologic environment.

The intrusive rocks have not been deeply eroded anywhere. Sedimentary rocks rest on some of the highest parts of the intrusive exposure. Clearly, the top of the intrusive chamber was generally flat and concordant with the bedding of overlying Cambrian sedimentary rocks. Relations are as shown in the fence diagram by Drewes (1958, p. 1231) and as described by him. At the outer margins of the intrusive, where contacts are steeper, there is some discordance. The overall picture presented is one of a broad sedimentary dome overlying the granitic rocks.

Whether or not this doming was actually caused by the intrusion, it helped to meet some of the space requirements of the granitoid rocks. However, as stated by Drewes (1958, p. 233), "Stoping, accompanied by assimilation and perhaps by foundering, is a mechanism necessary to explain the missing part of Prospect Mountain quartzite, Pioche Shale, and less commonly also part of the Pole Canyon limestone."

Stoping also is indicated by some of the discordant contacts; and in the middle reaches of Snake Creek (pl. 1), about 50 acres of Pole Canyon Limestone was partly stoped by a large apophysis of the intrusive.

Contact effects are slight. Spurr (1903, p. 27) first noted that "the intrusive phenomena are of minor importance * * *" and used this fact to support his hypothesis that the intrusive was older (Archean) than the Cambrian sedimentary rocks. Drewes (1958, p. 233) wrote: "Evidence for contact metasomatism is meager."

Along with this lack of contact action, Drewes (1958, p. 233) called attention to the fact that some members of the Cambrian Pole Canyon Limestone have been recrystallized, and he suggested a low-grade regional metamorphism as one possible explanation of these marbleized limestones. Misch and Hazzard (1962) recognized a Mesozoic regional metamorphism in the area. Eight metamorphic micas recovered from Cambrian Prospect Mountain Quartzite give potassium-argon ages younger than Mesozoic (Lee and others, 1970), but these ages were reset by stresses related to late activity along the Snake Range décollement and thus neither prove nor disprove a Mesozoic age for the regional metamorphism.

The tendency for granitoid rocks in the area to be present at or near the Snake Range décollement was mentioned by Misch and Hazzard (1962), and Whitebread (1968, p. 346) said: "At several places the décollement truncates a granitic intrusive body * * *." In other words, the thrust faults and intrusive rocks are spatially related and probably penecontemporaneous, but the most recent movement on the thrust was later than the main instrusive activity. Directional elements in the cataclastic (eastern) part of the intrusive are consistent with the direction of movement on the thrust as deduced by Drewes (1958) from his study of drag folds. Farther west and as much as several hundred feet below the level of the thrusting, a few scattered exposures of directional elements attest that stresses resulting from later movement on the thrust were manifest locally throughout an appreciable part of the crystallized intrusive rock (Lee and others, 1970).

Inclusions are rare except in a relatively small part of the intrusive outcrop area which contains many partly assimilated xenoliths of Pioche Shale. The systematic orientation of these xenoliths must have resulted from magmatic flow.

## CHEMISTRY OF THE SEDIMENTARY ROCKS

Major and minor elements were determined for a total of 34 sedimentary rock samples: four samples of Prospect Mountain Quartzite, six samples of the Osceola Argillite, 15 samples of the Pioche Shale (including six samples of the Wheeler limestone of local usage), and nine samples of Pole Canyon Limestone (tables 1, 2). Sample localities are shown on plate 1; approximate stratigraphic positions of the samples analyzed are shown in figure 2, along with stratigraphic intervals intruded by the three main intrusive types at the present level of erosion.

As noted earlier, the Osceola Argillite is about 750 feet thick, and its top is about 3,500 feet below the top of the Prospect Mountain Quartzite. This argillite and the quartzite just below it are the oldest sedimentary rocks exposed in contact with the intrusive rocks to be described, and the argillite itself is the host rock that shows most clearly the effect of contact action. Some of the rocks represented in table 1 have been thermally metamorphosed; for example, samples Ar1 and Ar2 are actually spotted schists, and Ar5 is an epidote-rich rock. But the recrystallization of these rocks appears to have been essentially isochemical, and accordingly the analyses in table 1 are considered representative of the composition of the argillite before contact metamor-

TABLE 1.—*Analytical data for Osceola Argillite of Misch and Hazzard, 1962, Prospect Mountain Quartzite, and Pioche Shale*

[All samples were grab samples. Localities shown on plate 1; samples in each group are numbered from west to east. Approximate stratigraphic positions shown in figure 2 Samples Q3 and Q4 from about 1½ miles north of mapped area (pl. 1), at 39°01'20" N., 114°16'11" W., and 39°01'14" N., 114°15'05" W., respectively. Samples S1, S2, and S3 collected underground in the Mount Wheeler mine. Sample S1 from lateral 1, about 200 feet from the mouth of the Pole Canyon adit. Samples Q2, Q3, and Q4 included in study by Lee and Van Loenen (1969), as 418-DL-67, 380-DL-66, and 146-DL-62, respectively. Samples S2 and S3 from lateral 7, about 1,200 feet from the mouth of the Pole Canyon adit. Sample S3 contains fluorite, giving the high F content of 0.88 percent. Chemical analyses and powder density determinations by Elaine Munson. Semiquantitative spectrographic analyses by Chris Heropoulos. 0, below limit of detection. General limitations of method given in text]

| | Osceola Argillite | | | | | | Prospect Mountain Quartzite | | | | Pioche Shale | | | | | | | | |
|---|---|---|---|---|---|---|---|---|---|---|---|---|---|---|---|---|---|---|---|
| Sample No. | Ar1 | Ar2 | Ar3 | Ar4 | Ar5 | Ar6 | Q1 | Q2 | Q3 | Q4 | S1 | S2 | S3 | S4 | S5 | S6 | S7 | S8 | S9 |
| **Chemical analyses (weight percent)** | | | | | | | | | | | | | | | | | | | |
| $SiO_2$ | 60.49 | 63.87 | 64.04 | 59.43 | 58.45 | 67.88 | 92.38 | 85.74 | 90.74 | 96.53 | 70.08 | 73.03 | 40.62 | 64.61 | 55.59 | 58.12 | 57.07 | 52.46 | 69.22 |
| $Al_2O_3$ | 18.12 | 14.01 | 17.07 | 19.49 | 12.31 | 15.41 | 3.60 | 6.65 | 4.85 | 1.30 | 7.97 | 5.30 | 12.32 | 17.83 | 22.26 | 20.47 | 21.07 | 21.84 | 8.24 |
| $Fe_2O_3$ | 3.15 | 3.92 | 4.69 | 5.18 | 4.35 | 4.22 | .63 | 1.26 | .72 | .55 | 3.98 | 1.40 | 1.76 | 2.18 | 2.44 | 3.27 | 4.15 | 2.65 | 9.61 |
| FeO | 3.29 | .90 | 2.33 | 2.16 | .90 | 1.39 | .12 | .46 | .24 | .18 | .43 | 3.44 | 5.29 | 2.39 | 5.09 | 3.76 | 2.52 | 4.92 | 3.42 |
| MgO | 2.59 | 2.07 | 2.05 | 2.43 | 2.28 | 1.82 | .11 | .49 | .23 | 09 | .70 | 2.44 | 9.60 | 1.48 | 1.97 | 1.91 | 1.95 | 2.28 | 1.40 |
| CaO | 2.21 | 10.69 | .19 | .50 | 14.39 | .21 | .00 | .02 | .00 | .00 | 6.28 | 4.37 | 8.81 | .90 | .18 | .23 | .29 | .27 | 2.83 |
| $Na_2O$ | 2.86 | 1.38 | 1.05 | .98 | 1.41 | 1.45 | .18 | .17 | .08 | .08 | .16 | .10 | .19 | .38 | .40 | .50 | .65 | 2.24 | .11 |
| $K_2O$ | 3.17 | .41 | 4.26 | 5.27 | .93 | 4.04 | 2.17 | 3.62 | 2.25 | .41 | 2.98 | 1.73 | 4.37 | 4.74 | 7.05 | 7.12 | 6.88 | 9.53 | 1.39 |
| $H_2O(+)$ | 2.61 | 1.01 | 2.83 | 3.04 | .72 | 2.25 | .15 | .60 | .47 | .14 | 1.55 | 1.03 | 2.69 | 2.99 | 3.45 | 2.94 | 3.52 | 2.11 | 2.42 |
| $H_2O(-)$ | .08 | .12 | .11 | .07 | .17 | .08 | .00 | .02 | .03 | .02 | .11 | .01 | .06 | .12 | .08 | .12 | .29 | .08 | .21 |
| $TiO_2$ | .67 | .66 | .82 | .82 | .56 | .67 | .25 | .65 | .10 | .45 | .34 | .21 | .68 | .79 | .82 | .83 | .92 | .84 | .28 |
| $P_2O_5$ | .12 | .13 | .13 | .12 | .13 | .13 | .01 | .07 | .01 | .02 | .48 | .52 | .25 | .41 | .15 | .18 | .12 | .11 | .45 |
| MnO | .20 | .42 | .06 | .03 | .20 | .04 | .01 | .01 | .01 | .00 | .20 | .21 | 12 | .10 | .05 | .03 | .03 | .03 | .10 |
| $CO_2$ | .04 | .05 | .02 | .01 | 3.00 | .02 | 04 | .01 | .00 | .01 | 4.59 | 5.96 | 12.27 | .61 | .06 | .01 | .11 | .09 | .07 |
| Cl | .00 | .00 | .00 | .00 | .00 | .00 | .00 | .00 | .00 | .00 | .01 | .00 | .00 | .00 | .00 | .00 | .00 | .00 | .00 |
| F | .08 | .05 | .07 | .11 | .05 | .06 | .01 | .02 | .01 | .02 | .17 | .08 | .88 | .08 | .11 | .18 | .12 | .17 | .10 |
| | 99.68 | 99.69 | 99.72 | 99.64 | 99.85 | 99.67 | 99.66 | 99.79 | 99.74 | 99.80 | 100.03 | 99.83 | 99.91 | 99.61 | 99.70 | 99.67 | 99.69 | 99.62 | 99.85 |
| Less 0 | .03 | .02 | .03 | .05 | .02 | .03 | .00 | .01 | .00 | .01 | .07 | .03 | .37 | .03 | .05 | .08 | .05 | .07 | .04 |
| Total | 99.65 | 99.67 | 99.69 | 99.59 | 99.83 | 99.64 | 99.66 | 99.78 | 99.74 | 99.79 | 99.96 | 99.80 | 99.54 | 99.58 | 99.65 | 99.59 | 99.64 | 99.55 | 99.81 |
| **Powder density** | | | | | | | | | | | | | | | | | | | |
| | 2.81 | 2.97 | 2.82 | 2.86 | 2.94 | 2.79 | 2.68 | 2.70 | 2.68 | 2.69 | 2.76 | 2.78 | 2.87 | 2.80 | 2.86 | 2.85 | 2.81 | 2.79 | 2.88 |
| **Semiquantitative spectrographic analyses (parts per million)** | | | | | | | | | | | | | | | | | | | |
| Ag | 0 | 0 | 0 | 0 | 0 | 0 | 0 | 0 | 0 | 0 | 0 | 0 | 1 | 0 | 0 | 0 | 0 | 0 | 1 |
| B | 0 | 0 | 15 | 15 | 0 | 70 | 0 | 0 | 0 | 0 | 15 | 7 | 10 | 100 | 50 | 15 | 20 | 10 | 0 |
| Ba | 1,000 | 200 | 1,500 | 1,000 | 700 | 700 | 300 | 700 | 700 | 300 | 1,000 | 500 | 700 | 700 | 1,500 | 1,500 | 2,000 | 2,000 | 300 |
| Be | 3 | 5 | 5 | 5 | 3 | 3 | 0 | 0 | 0 | 0 | 7 | 2 | 5 | 5 | 5 | 7 | 5 | 3 | 2 |
| Ce | 0 | 0 | 150 | 200 | 0 | 0 | 0 | 0 | 0 | 0 | 0 | 0 | 0 | 200 | 150 | 200 | 150 | 150 | 150 |
| Co | 20 | 20 | 20 | 20 | 20 | 20 | 0 | 5 | 5 | 0 | 15 | 10 | 50 | 10 | 30 | 20 | 20 | 20 | 20 |
| Cr | 100 | 100 | 150 | 150 | 150 | 150 | 3 | 10 | 15 | 3 | 70 | 50 | 1,000 | 150 | 150 | 150 | 150 | 150 | 70 |
| Cu | 7 | 10 | 7 | 3 | 5 | 200 | 5 | 100 | 5 | 5 | 10 | 15 | 100 | 20 | 30 | 100 | 100 | 50 | 300 |
| Ga | 50 | 30 | 50 | 50 | 30 | 50 | 5 | 10 | 7 | 0 | 20 | 15 | 20 | 50 | 50 | 50 | 50 | 50 | 20 |
| La | 100 | 70 | 70 | 100 | 50 | 70 | 0 | 0 | 0 | 0 | 70 | 50 | 70 | 100 | 100 | 100 | 100 | 100 | 70 |
| Li | 0 | 0 | 0 | 0 | 0 | 0 | 0 | 0 | 0 | 0 | 0 | 0 | 700 | 0 | 0 | 0 | 0 | 0 | 0 |
| Mo | 0 | 0 | 0 | 0 | 0 | 0 | 0 | 0 | 0 | 5 | 0 | 0 | 0 | 0 | 0 | 7 | 0 | 0 | 0 |
| Nb | 15 | 20 | 30 | 20 | 15 | 20 | 0 | 0 | 0 | 0 | 15 | 15 | 10 | 30 | 20 | 30 | 20 | 20 | 15 |
| Ni | 100 | 70 | 70 | 70 | 70 | 70 | 7 | 10 | 7 | 0 | 50 | 30 | 300 | 30 | 70 | 50 | 70 | 70 | 30 |
| Pb | 150 | 70 | 30 | 20 | 100 | 50 | 0 | 15 | 0 | 0 | 0 | 20 | 50 | 30 | 100 | 15 | 100 | 100 | 30 |
| Sc | 20 | 20 | 20 | 30 | 20 | 20 | 0 | 5 | 0 | 0 | 20 | 15 | 50 | 20 | 30 | 30 | 30 | 30 | 20 |
| Sr | 700 | 500 | 100 | 50 | 300 | 70 | 15 | 30 | 15 | 0 | 100 | 200 | 1,000 | 150 | 70 | 50 | 100 | 300 | 200 |
| V | 100 | 150 | 150 | 150 | 150 | 150 | 10 | 70 | 0 | 10 | 100 | 70 | 300 | 150 | 150 | 150 | 200 | 200 | 100 |
| Y | 50 | 50 | 70 | 70 | 50 | 50 | 10 | 15 | 0 | 10 | 100 | 100 | 30 | 70 | 70 | 70 | 70 | 50 | 100 |
| Yb | 5 | 5 | 7 | 7 | 5 | 5 | 1 | 3 | 0 | 2 | 10 | 10 | 3 | 7 | 7 | 7 | 7 | 5 | 10 |
| Zr | 200 | 700 | 300 | 300 | 300 | 500 | 500 | 700 | 70 | 500 | 500 | 200 | 150 | 700 | 150 | 200 | 300 | 700 | 500 |

TABLE 2.—*Analytical data for Wheeler limestone (of local usage) and Pole Canyon Limestone*

[All samples were grab samples. Localities shown on plate 1; samples in each group are numbered from west to east. Approximate stratigraphic positions shown in figure 2. Samples WLS2–5 collected underground in the Mount Wheeler mine; WLS2 from lateral 1, about 200 feet from the mouth of the Pole Canyon adit; WLS3 and 4 from lateral 3, about 500 feet from the mouth of the Pole Canyon adit; WLS5 from lateral 4, about 600 feet from the mouth of the Pole Canyon adit; WLS6, from roof pendant (could possibly be Pole Canyon Limestone). Chemical analyses and powder density determinations by Elaine Munson. Semiquantitative spectrographic analyses by Chris Heropoulos. 0, below limit of detection. General limitations of method given in text]

| | Wheeler limestone | | | | | | Pole Canyon Limestone | | | | | | | | |
|---|---|---|---|---|---|---|---|---|---|---|---|---|---|---|---|
| Sample No. | WLS1 | WLS2 | WLS3 | WLS4 | WLS5 | WLS6 | P1 | P2 | P3 | P4 | P5 | P6 | P7 | P8 | P9 |
| **Chemical analyses (weight percent)** | | | | | | | | | | | | | | | |
| $SiO_2$ | 3.25 | 20.94 | 30.04 | 34.13 | 7.32 | 30.16 | 7.64 | 1.11 | 3.12 | .15 | 7.14 | 1.89 | .77 | .92 | .26 |
| $Al_2O_3$ | .48 | .47 | .40 | .50 | .23 | 9.39 | 2.12 | .43 | .28 | .08 | 1.37 | .89 | .15 | .18 | .13 |
| $Fe_2O_3$ | .57 | 1.13 | .77 | 1.03 | 2.00 | .99 | .64 | .14 | .13 | .06 | .10 | .11 | .05 | .38 | .11 |
| FeO | 5.43 | 2.52 | 4.41 | 3.31 | 3.29 | 2.01 | .23 | .14 | .12 | .05 | .30 | .24 | .10 | .10 | .04 |
| MgO | 13.90 | 12.87 | 10.18 | 10.00 | 14.33 | 4.58 | 1.19 | 1.12 | .55 | 2.78 | 1.20 | .99 | .76 | .54 | 1.14 |
| CaO | 31.61 | 24.86 | 21.45 | 20.09 | 28.84 | 31.40 | 47.96 | 53.61 | 53.04 | 52.61 | 49.41 | 52.98 | 54.66 | 54.40 | 54.37 |
| $Na_2O$ | .05 | .03 | .03 | .05 | .04 | .99 | .24 | .12 | .03 | .01 | .14 | .03 | .03 | .03 | .01 |
| $K_2O$ | .12 | .10 | .08 | .10 | .03 | 1.24 | .80 | .06 | .22 | .02 | .48 | .25 | .02 | .06 | .03 |
| $H_2O(+)$ | .02 | .00 | .03 | .01 | .01 | .59 | .06 | .01 | .00 | .03 | .10 | .00 | .00 | .02 | .03 |
| $H_2O(-)$ | .00 | .02 | .00 | .02 | .04 | .03 | .03 | .00 | .01 | .00 | .02 | .01 | .02 | .00 | .00 |
| $TiO_2$ | .02 | .03 | .04 | .05 | .01 | .38 | .09 | .02 | .03 | .01 | .04 | .03 | .01 | .02 | .01 |
| $P_2O_5$ | .16 | .27 | .24 | .48 | .13 | .07 | .05 | .01 | .05 | .01 | .02 | .01 | .01 | .02 | .01 |
| MnO | .90 | .82 | .87 | .83 | 1.71 | .05 | .04 | .01 | .03 | .01 | .03 | .06 | .03 | .07 | .01 |
| $CO_2$ | 43.34 | 35.50 | 31.02 | 28.63 | 41.53 | 17.74 | 38.26 | 43.11 | 42.00 | 44.13 | 39.06 | 41.98 | 43.23 | 43.03 | 43.74 |
| Cl | .02 | .02 | .01 | .01 | .02 | .00 | .00 | .00 | .00 | .00 | .01 | .00 | .01 | .00 | .00 |
| F | .08 | .04 | .04 | .07 | .03 | .07 | .05 | .01 | .01 | .01 | .03 | .03 | .02 | .01 | .01 |
| | 99.75 | 99.62 | 99.61 | 99.31 | 99.56 | 99.69 | 99.40 | 99.90 | 99.62 | 99.96 | 99.45 | 99.50 | 99.87 | 99.79 | 99.90 |
| Less 0 | .03 | .02 | .02 | .03 | .01 | .03 | .02 | .00 | .00 | .00 | .01 | .01 | .01 | .00 | .00 |
| Total | 99.72 | 99.60 | 99.59 | 99.28 | 99.55 | 99.66 | 99.38 | 99.90 | 99.62 | 99.96 | 99.44 | 99.49 | 99.86 | 99.79 | 99.90 |
| **Powder density** | | | | | | | | | | | | | | | |
| | 2.91 | 2.85 | 2.85 | 2.84 | 2.89 | 2.92 | 2.73 | 2.72 | 2.71 | 2.72 | 2.71 | 2.71 | 2.71 | 2.72 | 2.72 |
| **Semiquantitative spectrographic analyses (parts per million)** | | | | | | | | | | | | | | | |
| Ba | 20 | 50 | 20 | 50 | 30 | 30 | 200 | 20 | 100 | 5 | 1,500 | 50 | 7 | 20 | 10 |
| Co | 15 | 0 | 0 | 0 | 5 | 5 | 0 | 0 | 0 | 0 | 0 | 0 | 0 | 0 | 0 |
| Cr | 7 | 7 | 15 | 20 | 7 | 7 | 20 | 30 | 20 | 20 | 15 | 10 | 3 | 3 | 0 |
| Cu | 7 | 7 | 10 | 7 | 5 | 7 | 10 | 10 | 5 | 70 | 3 | 10 | 7 | 7 | 7 |
| Ga | 0 | 0 | 0 | 0 | 0 | 20 | 5 | 0 | 0 | 0 | 0 | 0 | 0 | 0 | 0 |
| Ni | 7 | 5 | 7 | 7 | 5 | 5 | 7 | 5 | 5 | 5 | 5 | 5 | 5 | 3 | 3 |
| Pb | 50 | 0 | 30 | 15 | 100 | 30 | 0 | 0 | 30 | 0 | 30 | 0 | 0 | 30 | 0 |
| Sr | 1,000 | 1,000 | 700 | 700 | 700 | 700 | 2,000 | 2,000 | 2,000 | 1,000 | 3,000 | 2,000 | 700 | 2,000 | 1,500 |
| V | 15 | 0 | 20 | 15 | 10 | 15 | 30 | 0 | 0 | 0 | 30 | 15 | 0 | 0 | 10 |
| Y | 30 | 20 | 30 | 30 | 15 | 20 | 15 | 0 | 10 | 0 | 0 | 10 | 0 | 0 | 0 |
| Yb | 3 | 2 | 3 | 3 | 2 | 2 | 2 | 0 | 1 | 0 | 0 | 0 | 0 | 0 | 0 |
| Zr | 20 | 30 | 50 | 100 | 15 | 100 | 70 | 15 | 50 | 0 | 15 | 15 | 0 | 0 | 0 |

phism. Where exposed in contact with the granitoid rocks described in this study, the Prospect Mountain Quartzite is a mature shelf sediment.

The Pioche Shale is probably 300–450 feet thick in the study area. Lithologic variations are pronounced, including some rather striking lateral changes of facies (Drewes, 1958; Whitebread and Lee, 1961). In general, the lower three-fourths of the formation is micaceous to silty shale with a limestone unit in the lower part, and the upper one-fourth is fine-grained calcareous quartzite with interbeds and lenses of limestone. The limestone unit in the lower part of the Pioche ranges in thickness from about 5 to 25 feet. It has all the known nonpegmatite beryllium in the Mount Wheeler mine area and is known locally as the Wheeler limestone. It might be equivalent to the Combined Metals Member of the Pioche (Stager, 1960; Palmer, 1958). An example of the lateral changes of facies noted above is near the Pole Canyon adit of the Mount Wheeler mine (pl. 1). There the Wheeler limestone is about 20 feet thick and 45–65 feet above the base of the Pioche, but on the crest of the range some 3 miles to the northeast the Wheeler comprises several beds and lenses of limestone and sandy limestone, each as much as 4 feet thick, within about 70 feet of the base of the Pioche (Whitebread and Lee, 1961).

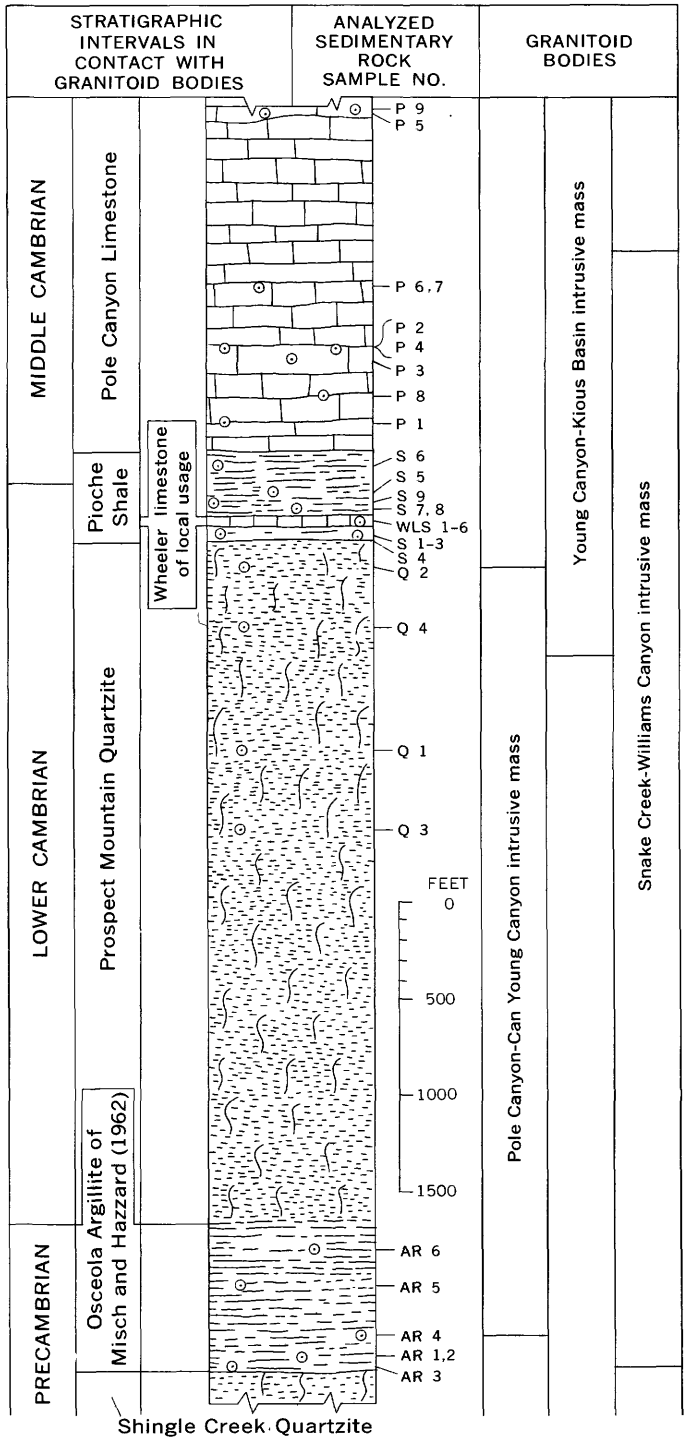


FIGURE 2.—Schematic upper Precambrian to Middle Cambrian stratigraphic column, modified from Drewes (1958, p. 224). Sample localities shown areally on plate 1 or indicated in tables 1 and 2. Analyses of rock samples given in tables 1 and 2.

The Cambrian Pole Canyon Limestone was defined and described by Drewes and Palmer (1957, p. 110–113). This limestone is massive and about 2,000 feet thick. Five members have been mapped in the Wheeler Peak quadrangle (Drewes, 1958; Whitebread and others, 1962), but in the Garrison quadrangle, just east of the Wheeler Peak quadrangle, the members are difficult to distinguish because of structural complexities. Except for a few 5- to 10-foot-thick beds of fine-grained calcareous quartzite in the basal member and some shaly partings in the other members, the Pole Canyon Limestone is a rather pure carbonate rock (table 2).

Analyses in tables 1 and 2 are discussed further in later sections (p. 36–37).

## CHEMISTRY AND MINERALOGY OF THE GRANITOID ROCKS

### TECHNIQUES OF THIS STUDY

Excluding aplites, 115 granitoid rock samples were analyzed for major and minor elements—87 from the Snake Creek-Williams Canyon area, nine from the Pole Canyon-Can Young Canyon area, and 19 from the Young Canyon-Kious Basin area. These analyses are grouped in three separate tables according to area. In these and other tables each sample is identified by a sample number corresponding to its locality number on plate 1. Field numbers were used in our previous publications on the Mount Wheeler mine area. (A given field number has been used to identify both the rock and each of the constituent mineral phases recovered from that rock.) As a cross reference to previous reports, table 3 lists field numbers of the analyzed samples and the corresponding sample (and locality) numbers used in the present report.

Minor elements were determined by semiquantitative spectrographic methods described by Myers, Havens, and Dunton (1961). The results of the spectrographic analyses were reported in geometric intervals having the boundaries 1200, 830, 560, 380, 260, 180, 120, and so on, in parts per million. The intervals are identified by the approximate geometric midpoints such as 1000, 700, 500, 300, 200, 150, 100. Thus, a reported value of 300 parts per million identifies the range from 260 to 380 parts per million as the analysts' best estimate of the concentration present in the analyzed sample. The precision of a reported value is approximately plus or minus one interval at 68 percent confidence, or plus or minus two intervals at 95 percent confidence. The 45 minor elements sought, together with limits of detection by the method used, are listed in table 4.

The modal analyses listed in tables 5–7 are based on calibrated X-ray diffraction patterns, following the general procedure given by Tatlock (1966). The present results were obtained by means of a Picker X-ray diffractometer equipped with a pulse-height analyzer,

TABLE 3.—*Field numbers of analyzed granitoid rock samples keyed to sample numbers*

[Asterisk indicates sample discussed (by field number) in one or more previous studies: Lee and Bastron (1962, 1967); Lee and Dodge (1964); Lee, Stern, Mays, and Van Loenen (1968); Lee, Mays, Van Loenen, and Rose (1969, 1971); Lee and Van Loenen (1969, 1970); Lee, Marvin, Stern, and Peterman (1970)]

| Field No. | Sample No. (pl. 1) |
|---|---|
| **–MW–60** | |
| 14* | 31 |
| 16* | 83 |
| 21A* | 69 |
| 24 | 4 |
| 28 | 10 |
| 38* | 55 |
| 40A* | 46 |
| 40B* | 71 |
| 62* | 131 |
| 63* | 3 |
| 71* | 28 |
| 119* | 124 |
| 120* | 93 |
| **–MW–61** | |
| 125 | 100 |
| 126* | 72 |
| 139 | 132 |
| 141 | 5 |
| 145 | 12 |
| 146 | 17 |
| 147* | 15 |
| 148 | 18 |
| 149 | 19 |
| 151* | 22 |
| 152* | 67 |
| 154 | 47 |
| 156 | 29 |
| 158 | 26 |
| 161 | 125 |
| 184* | 108 |
| 185 | 104 |
| 188* | 105 |
| 190* | 101 |
| 195 | 128 |
| 205* | 107 |
| 210 | 123 |
| 214 | 120 |
| 223 | 88 |
| 226* | 92 |
| 229* | 97 |
| 230* | 98 |
| 231 | 118 |
| 232 | 99 |
| 234* | 102 |
| 236 | 20 |
| 238* | 6 |
| **–DL–61** | |
| 1 | 32 |
| 3 | 30 |
| 4 | 33 |
| 8* | 39 |
| 11 | 48 |
| 12 | 34 |
| 19 | 79 |
| 21 | 80 |
| 22 | 68 |
| 25* | 66 |
| 27* | 81 |
| 28 | 56 |
| 30 | 35 |
| 31* | 49 |
| 35 | 36 |
| 37 | 58 |
| 38 | 57 |
| 41 | 50 |
| 43* | 78 |
| 49* | 1 |
| **–DL–62** | |
| 50 | 109 |
| 54 | 103 |
| 57 | 106 |
| 59 | 110 |
| 60 | 113 |
| 62 | 115 |
| 65 | 114 |
| 67 | 112 |
| 71 | 129 |
| 84 | 111 |
| 96 | 133 |
| 98* | 85 |
| 100 | 116 |
| 102 | 117 |
| 111 | 119 |
| 115 | 121 |
| 118 | 122 |
| 120 | 96 |
| 122* | 90 |
| 126 | 95 |
| 133 | 94 |
| 135* | 89 |
| 139 | 74 |
| 140 | 87 |
| 143 | 40 |
| 144 | 51 |
| 145 | 41 |
| 148 | 21 |
| 156 | 65 |
| 157 | 73 |
| 161 | 76 |
| 164 | 52 |
| 168 | 130 |
| 171 | 23 |
| 172 | 14 |
| 174 | 16 |
| 178 | 11 |
| 179 | 77 |
| 185 | 59 |
| 190* | 27 |
| 197 | 24 |
| 205 | 42 |
| **–DL–63** | |
| 228 | 86 |
| 229 | 84 |
| 236 | 43 |
| 237 | 25 |
| 238 | 63 |
| 241 | 13 |
| 246 | 91 |
| 247 | 44 |
| 248 | 53 |
| 255 | 37 |
| 258 | 45 |
| 259 | 70 |
| 260 | 64 |
| 261 | 60 |
| 262 | 2 |
| 264 | 9 |
| 265 | 8 |
| 270 | 38 |
| 271 | 54 |
| 273 | 75 |
| 276 | 82 |
| 278 | 61 |
| 279 | 62 |
| 280 | 126 |
| 284 | 127 |
| 286 | 7 |

TABLE 4.—*Limits of detection, by emission spectrography, for minor elements in sedimentary and granitoid rocks considered in this report*

[In the emission spectrographic method used, some unusual combinations of elements affect the limits of determination, and so the limits listed (in parts per million) are approximate]

| Element | Limit | Element | Limit | Element | Limit |
|---|---|---|---|---|---|
| Ag | 1 | Hf | 100 | Sc | 3 |
| As | 2, 000 | Hg | 10, 000 | Sm | 100 |
| Au | 20 | In | 10 | Sn | 10 |
| B | 7 | La | 30 | Sr | 5 |
| Ba | 2 | Li | 100 | Ta | 200 |
| Be | 1 | Mo | 2 | Te | 2, 000 |
| Bi | 10 | Nb | 3 | Th | 200 |
| Cd | 50 | Nd | 70 | Tl | 50 |
| Ce | 100 | Ni | 2 | U | 500 |
| Co | 3 | Pb | 10 | V | 7 |
| Cr | 1 | Pd | 2 | W | 100 |
| Cu | 1 | Pr | 100 | Y | 10 |
| Ga | 5 | Pt | 50 | Yb | 1 |
| Ge | 50 | Re | 50 | Zn | 200 |
| Gd | 50 | Sb | 200 | Zr | 10 |

using a Cu target, a Ni filter, 0.010 mm (millimeter) receiving slit, 30 counts per minute, and a 3-second time constant.

The general procedure used was as follows: Two splits of 2 grams each were taken from the crushed (−60 mesh) sample by means of a microsplitter. Each split was ground in a power mortar for about 30 minutes, producing powder mostly less than 20 microns in size. Then each ground sample was split into two parts, giving a total of four splits from each analyzed rock sample. Each of these four splits was firmly packed into a sample holder and scanned from 6° to 36° $2\theta$ at a speed of 2° per minute. Peak intensities taken from the four individual diffractograms were averaged to give a final value for each peak.

Because the amount of quartz present bears a straight-line relation to the intensity of the 4.26 A (20.85° $2\theta$) peak for that mineral, it is possible to read quartz content directly from peak height. A constant power supply was maintained by running quartz calibration standards periodically and adjusting the pulse-height analyzer as necessary.

Standard curves for plagioclase, microcline, biotite, and muscovite were prepared with minerals separated from the rocks under study. The peaks used for modal analysis were plagioclase, 3.20 A (27.9° $2\theta$); microcline, 3.25 A (27.4° $2\theta$); biotite plus muscovite, 10 A )8.9° $2\theta$), and muscovite alone, 5 A (17.8° $2\theta$).

Margins of error for values reported are about as follows: Quartz, ±2 percent; microcline, plagioclase, biotite, and muscovite, ±3 percent each. These are observed ranges of replicate determinations from their average. For example, if the value for plagioclase reads 31, then the actual value is probably between 28 and 34.

TABLE 5.—*Analytical and other data for granitoid rocks from the Snake Creek–Williams Canyon area*

[Samples arranged according to increasing CaO content. Sample localities shown on plate 1]

| Sample No. | 1 | 2 | 3 | 4 | 5 | 6 | 7 | 8 | 9 | 10 | 11 | 12 | 13 | 14 | 15 |
|---|---|---|---|---|---|---|---|---|---|---|---|---|---|---|---|
| **Chemical analyses (weight percent)[1]** | | | | | | | | | | | | | | | |
| $SiO_2$ | 75.9 | 76.2 | 76.0 | 75.2 | 75.7 | 74.9 | 76.1 | 76.4 | 74.7 | 75.3 | 76.5 | 75.4 | 73.4 | 74.7 | 73.4 |
| $Al_2O_3$ | 13.4 | 13.2 | 12.9 | 14.0 | 13.7 | 13.7 | 13.5 | 12.9 | 14.0 | 13.6 | 13.3 | 13.6 | 14.1 | 13.4 | 14.1 |
| $Fe_2O_3$ | .33 | .60 | .42 | .27 | .38 | .41 | .46 | .69 | .74 | .57 | .42 | .66 | .54 | .91 | .68 |
| FeO | .23 | .24 | .21 | .44 | .44 | .52 | .16 | .24 | .42 | .36 | .44 | .40 | .30 | .72 | .95 |
| MgO | .17 | .12 | .21 | .32 | .10 | .16 | .15 | .10 | .15 | .25 | .17 | .62 | .25 | .22 | .83 |
| CaO | .47 | .52 | .55 | .61 | .64 | .78 | .78 | .83 | .85 | 1.1 | 1.1 | 1.2 | 1.2 | 1.4 | 1.5 |
| $Na_2O$ | 3.7 | 5.2 | 3.7 | 4.1 | 3.9 | 3.7 | 3.7 | 3.5 | 3.7 | 3.4 | 3.5 | 3.3 | 4.8 | 3.2 | 3.6 |
| $K_2O$ | 4.4 | 4.1 | 4.3 | 4.2 | 4.3 | 4.4 | 4.4 | 4.4 | 4.5 | 4.4 | 4.2 | 4.5 | 4.5 | 4.2 | 4.0 |
| $H_2O(+)$ | .84 | .19 | .85 | .54 | .16 | .87 | .36 | .45 | .48 | .22 | .39 | .14 | .65 | .18 | .72 |
| $H_2O(-)$ | .08 | .10 | .04 | .09 | .06 | .11 | .24 | .18 | .11 | .08 | .24 | .11 | .08 | .28 | .16 |
| $TiO_2$ | .08 | .06 | .08 | .10 | .11 | .11 | .08 | .06 | .08 | .11 | .09 | .13 | .04 | .18 | .19 |
| $P_2O_5$ | .01 | .00 | .01 | .02 | .02 | .01 | .00 | .01 | .02 | .03 | .02 | .04 | .00 | .05 | .06 |
| MnO | .02 | .07 | .03 | .04 | .06 | .03 | .05 | .07 | .05 | .06 | .05 | .06 | .03 | .05 | .04 |
| $CO_2$ | <.05 | <.05 | <.05 | <.05 | <.05 | <.05 | <.05 | <.05 | <.05 | <.05 | <.05 | <.05 | <.05 | <.05 | <.05 |
| Cl | | .01 | | | .00 | | .00 | | | .00 | | .00 | | .00 | |
| F | | .03 | | | .03 | | .04 | | | .02 | | .03 | | .04 | |
| Total | 100 | 101 | 99 | 100 | 100 | 100 | 100 | 100 | 100 | 100 | 100 | 100 | 100 | 100 | 100 |
| **Powder density[2]** | | | | | | | | | | | | | | | |
| | 2.64 | 2.64 | 2.60 | | 2.64 | | 2.63 | | | 2.64 | | 2.65 | | 2.66 | 2.67 |
| **Rittmann *s*[3]** | | | | | | | | | | | | | | | |
| | 1.99 | 2.60 | 1.94 | 2.14 | 2.06 | 2.06 | 1.98 | 1.87 | 2.12 | 1.88 | 1.77 | 1.88 | 2.85 | 1.73 | 1.90 |
| **CIPW norms[4]** | | | | | | | | | | | | | | | |
| Quartz | 36.4 | 29.2 | 36.8 | 33.3 | 34.9 | 34.5 | 35.6 | 37.4 | 34.0 | 36.1 | 37.2 | 35.3 | 25.8 | 36.7 | 32.2 |
| Corundum | 1.7 | | 1.2 | 1.6 | 1.5 | 1.4 | 1.2 | .88 | 1.5 | 1.3 | 1.0 | 1.1 | | 1.1 | 1.1 |
| Zircon | | | | | .02 | | | | | | .02 | | | .03 | |
| Orthoclase | 26.1 | 24.0 | 25.6 | 24.8 | 25.4 | 26.1 | 26.0 | 26.0 | 26.6 | 26.1 | 24.7 | 26.4 | 26.6 | 24.9 | 23.5 |
| Albite | 31.4 | 43.6 | 31.5 | 34.7 | 33.0 | 31.4 | 31.2 | 29.7 | 31.3 | 28.8 | 29.5 | 27.7 | 40.6 | 27.2 | 30.3 |
| Anorthite | 2.4 | .57 | 2.8 | 3.0 | 3.1 | 3.9 | 4.0 | 4.1 | 4.3 | 5.4 | 5.4 | 5.8 | 3.7 | 6.9 | 7.4 |
| Wollastonite | | .85 | | | | | | | | | | | 1.0 | | |
| Enstatite | .43 | .30 | .53 | .80 | .25 | .40 | .25 | .25 | .25 | .62 | .42 | 1.5 | .62 | .55 | 2.1 |
| Ferrosilite | .06 | | | .49 | .42 | .49 | | | .12 | .12 | .40 | .09 | .10 | .37 | .94 |
| Magnetite | .48 | .82 | .55 | .39 | .55 | .60 | .45 | .83 | 1.1 | .83 | .63 | .95 | .78 | 1.3 | .98 |
| Hematite | | .03 | .05 | | | | .15 | .12 | | | | | | | |
| Ilmenite | .15 | .11 | .15 | .19 | .21 | .21 | .15 | .11 | .15 | .21 | .17 | .25 | .08 | .34 | .36 |
| Apatite | .02 | | .02 | .05 | .05 | .02 | | .02 | .05 | .07 | .05 | .09 | | .12 | .14 |
| Calcite | | | | | | | | | | | | | | | |
| $H_2O+F+Cl$ | .92 | .33 | .89 | .63 | .25 | .98 | .64 | .63 | .59 | .32 | .63 | .28 | .73 | .47 | .88 |
| Total | 100 | 100 | 100 | 100 | 100 | 100 | 100 | 100 | 100 | 100 | 100 | 100 | 100 | 100 | 100 |
| **Partial modal analyses[5]** | | | | | | | | | | | | | | | |
| Quartz | 33 | 37 | 40 | 34 | 37 | 42 | 35 | 37 | 37 | 35 | 38 | 33 | 37 | 34 | 34 |
| Microcline | 25 | 23 | 20 | 23 | 22 | 23 | 25 | 23 | 23 | 23 | 23 | 27 | 27 | 20 | 18 |
| Plagioclase | 35 | 37 | 34 | 38 | 35 | 32 | 35 | 35 | 34 | 35 | 34 | 36 | 34 | 38 | 38 |
| Biotite | P | 3 | P | 3 | P | 5 | P | 4 | P | 3 | 5 | 5 | 4 | 6 | 10 |
| **Semiquantitative spectrographic analyses (parts per million)[6]** | | | | | | | | | | | | | | | |
| Ag | 0 | 0 | 0 | 0 | 0 | 0 | 0 | 1.5 | 0 | 0 | 0 | 0 | 0 | 0 | 0 |
| B | 0 | 7 | 0 | 0 | 0 | 0 | 0 | 7 | 7 | 0 | 0 | 0 | 10 | 0 | 0 |
| Ba | 500 | 300 | 700 | 500 | 500 | 500 | 500 | 300 | 1,000 | 500 | 500 | 1,000 | 1,000 | 1,500 | 2,000 |
| Be | 5 | 5 | 3 | 7 | 3 | 3 | 5 | 3 | 5 | 5 | 3 | 3 | 7 | 5 | 3 |
| Ce | 0 | 0 | 0 | 0 | 0 | 0 | 0 | 0 | 0 | 0 | 0 | 0 | 0 | 0 | 0 |
| Co | 0 | 0 | 3 | 0 | 0 | 0 | 0 | 0 | 0 | 0 | 0 | 0 | 0 | 3 | 5 |
| Cr | 15 | 20 | 5 | 10 | 7 | 10 | 7 | 15 | 20 | 10 | 15 | 10 | 30 | 20 | 5 |
| Cu | 20 | 3 | 5 | 20 | 20 | 7 | 15 | 3 | 5 | .7 | 1 | .7 | 15 | 1 | 7 |
| Ga | 30 | 30 | 30 | 30 | 20 | 20 | 30 | 30 | 30 | 30 | 30 | 20 | 30 | 30 | 20 |
| La | 0 | 0 | 0 | 0 | 0 | 0 | 0 | 0 | 30 | 0 | 0 | 0 | 0 | 0 | 0 |
| Li | 0 | 0 | 0 | 0 | 0 | 0 | 0 | 0 | 0 | 0 | 0 | 0 | 0 | 0 | 0 |
| Mo | 3 | 0 | 0 | 0 | 0 | 0 | 2 | 0 | 0 | 0 | 0 | 0 | 0 | 0 | 0 |
| Nb | 10 | 50 | 30 | 30 | 50 | 50 | 30 | 30 | 20 | 20 | 20 | 10 | 30 | 20 | 10 |
| Nd | 0 | 0 | 0 | 0 | 0 | 0 | 0 | 0 | 0 | 0 | 0 | 0 | 0 | 0 | 0 |
| Ni | 0 | 7 | 0 | 0 | 2 | 0 | 5 | 7 | 7 | 7 | 3 | 2 | 15 | 5 | 0 |
| Pb | 70 | 70 | 70 | 70 | 70 | 50 | 70 | 70 | 50 | 70 | 70 | 30 | 70 | 50 | 50 |
| Sc | 3 | 5 | 5 | 5 | 5 | 5 | 5 | 5 | 5 | 5 | 3 | 3 | 3 | 5 | 3 |
| Sr | 100 | 100 | 300 | 200 | 200 | 300 | 150 | 100 | 300 | 200 | 200 | 300 | 500 | 700 | 1,500 |
| V | 10 | 10 | 10 | 0 | 15 | 15 | 10 | 10 | 20 | 20 | 20 | 15 | 15 | 30 | 20 |
| Y | 20 | 50 | 70 | 30 | 50 | 30 | 30 | 30 | 20 | 20 | 20 | 10 | 50 | 20 | 15 |
| Yb | 2 | 5 | 7 | 3 | 5 | 5 | 3 | 3 | 2 | 2 | 2 | 1 | 5 | 2 | 1 |
| Zr | 70 | 70 | 70 | 70 | 100 | 50 | 50 | 50 | 70 | 50 | 100 | 70 | 70 | 150 | 70 |

See footnotes at end of table.

TABLE 5.—*Analytical and other data for granitoid rocks from the Snake Creek–Williams Canyon area*—Continued

| Sample No. | 16 | 17 | 18 | 19 | 20 | 21 | 22 | 23 | 24 | 25 | 26 | 27 | 28 | 29 | 30 |
|---|---|---|---|---|---|---|---|---|---|---|---|---|---|---|---|
| **Chemical analyses (weight percent)** [1] | | | | | | | | | | | | | | | |
| $SiO_2$ | 73.7 | 73.9 | 74.0 | 72.9 | 73.5 | 73.3 | 73.2 | 74.0 | 71.0 | 73.5 | 73.0 | 71.4 | 71.4 | 71.6 | 71.7 |
| $Al_2O_3$ | 14.5 | 14.3 | 14.4 | 14.2 | 13.8 | 14.0 | 14.3 | 13.7 | 15.1 | 14.1 | 14.0 | 15.4 | 14.8 | 15.4 | 14.5 |
| $Fe_2O_3$ | .83 | .88 | .75 | .50 | 1.1 | .88 | .68 | .81 | 1.1 | .80 | .85 | .79 | 1.1 | 1.1 | 1.1 |
| FeO | .70 | .84 | .86 | .82 | .44 | .84 | .78 | .90 | 1.2 | .70 | .90 | 1.1 | 1.0 | .96 | 1.2 |
| MgO | .33 | .23 | .50 | .56 | .85 | .61 | 1.2 | .39 | .79 | .43 | .58 | .80 | .82 | .53 | .73 |
| CaO | 1.6 | 1.7 | 1.7 | 1.7 | 1.7 | 1.7 | 1.8 | 1.8 | 1.8 | 1.8 | 1.9 | 2.0 | 2.1 | 2.1 | 2.2 |
| $Na_2O$ | 3.4 | 3.4 | 3.3 | 3.5 | 3.8 | 3.4 | 3.6 | 3.4 | 3.6 | 3.6 | 3.4 | 3.8 | 3.5 | 3.2 | 3.6 |
| $K_2O$ | 4.0 | 3.7 | 3.9 | 3.8 | 3.7 | 3.8 | 3.6 | 3.7 | 3.8 | 4.1 | 4.1 | 3.6 | 3.8 | 3.8 | 3.7 |
| $H_2O(+)$ | .52 | .43 | .26 | .59 | .58 | .55 | .79 | .46 | .84 | .24 | .34 | .39 | .66 | .68 | .54 |
| $H_2O(-)$ | .11 | .09 | .19 | .09 | .09 | .29 | .07 | .09 | .16 | .04 | .06 | .12 | .18 | .11 | .07 |
| $TiO_2$ | .16 | .20 | .18 | .15 | .27 | .22 | .19 | .21 | .28 | .18 | .24 | .25 | .20 | .25 | .30 |
| $P_2O_5$ | .06 | .07 | .06 | .06 | .06 | .06 | .06 | .06 | .09 | .07 | .07 | .10 | .06 | .10 | .09 |
| MnO | .05 | .06 | .06 | .05 | .06 | .06 | .04 | .06 | .05 | .05 | .05 | .06 | .10 | .06 | .05 |
| $CO_2$ | <.05 | <.05 | <.05 | <.05 | <.05 | <.05 | <.05 | <.05 | <.05 | <.05 | <.05 | <.05 | <.05 | <.05 | <.05 |
| Cl | | | .00 | | | | | | | .00 | .00 | .01 | | .01 | .01 |
| F | | | .03 | | | | | | | .03 | .04 | .05 | | .05 | .05 |
| Total | 100 | 100 | 100 | 99 | 100 | 100 | 100 | 100 | 100 | 100 | 100 | 100 | 100 | 100 | 100 |
| **Powder density** [2] | | | | | | | | | | | | | | | |
| | | | 2.65 | | | | 2.65 | | | 2.67 | 2.68 | 2.68 | | | 2.69 |
| **Rittmann s** [3] | | | | | | | | | | | | | | | |
| | 1.78 | 1.63 | 1.67 | 1.78 | 1.84 | 1.71 | 1.72 | 1.63 | 1.96 | 1.83 | 1.92 | 1.93 | 1.88 | 1.71 | 1.63 |
| **CIP W norms** [4] | | | | | | | | | | | | | | | |
| Quartz | 34.7 | 36.0 | 35.2 | 33.4 | 32.4 | 34.3 | 32.6 | 35.8 | 30.2 | 32.0 | 32.1 | 29.8 | 30.7 | 33.0 | 29.83 |
| Corundum | 1.8 | 1.8 | 1.8 | 1.1 | .50 | 1.3 | 1.3 | .88 | 1.9 | 1.0 | 1.0 | 1.9 | 1.2 | 2.3 | 1.4 |
| Zircon | | | .02 | .03 | .05 | .02 | .02 | .02 | .03 | .03 | .02 | | .03 | .03 | .0 |
| Orthoclase | 23.7 | 21.9 | 23.0 | 22.5 | 21.8 | 22.5 | 21.2 | 22.0 | 22.5 | 24.2 | 24.2 | 21.2 | 22.3 | 22.4 | 22.0 |
| Albite | 28.8 | 28.8 | 27.9 | 29.6 | 32.1 | 28.8 | 30.4 | 28.9 | 30.5 | 30.5 | 28.7 | 32.1 | 29.5 | 27.0 | 30.6 |
| Anorthite | 7.6 | 8.0 | 8.0 | 8.7 | 8.3 | 8.3 | 8.5 | 8.9 | 8.6 | 8.7 | 9.0 | 9.3 | 10.2 | 10.1 | 10.1 |
| Wollastonite | | | | | | | | | | | | | | | |
| Enstatite | .82 | .57 | 1.2 | 1.4 | 2.1 | 1.5 | 3.0 | .85 | 2.0 | 1.1 | 1.5 | 2.0 | 2.0 | 1.3 | 2.0 |
| Ferrosilite | .43 | .60 | .77 | | | .56 | .63 | .75 | .93 | .40 | .73 | 1.1 | | .52 | .93 |
| Magnetite | 1.2 | 1.3 | 1.1 | .14 | .83 | 1.3 | .98 | 1.2 | 1.6 | 1.2 | 1.2 | 1.1 | 1.2 | 1.6 | 1.6 |
| Hematite | | | | .41 | .53 | | | | | | .68 | | .29 | | |
| Ilmenite | .30 | .38 | .34 | 1.9 | .51 | .42 | .36 | .40 | .53 | .34 | .47 | .47 | 1.6 | .47 | .55 |
| Apatite | .14 | .17 | .14 | | .14 | .14 | .14 | .14 | .21 | .17 | .17 | .24 | .14 | .24 | .21 |
| Calcite | | | | | | | | | | | | | | | |
| $H_2O+F+Cl$ | .63 | .52 | .48 | .68 | .67 | .84 | .86 | .54 | 1.0 | .31 | .44 | .57 | .84 | .79 | .67 |
| Total | 100 | 100 | 100 | 100 | 100 | 100 | 100 | 100 | 100 | 100 | 100 | 100 | 100 | 100 | 100 |
| **Partial modal analyses** [5] | | | | | | | | | | | | | | | |
| Quartz | 32 | 32 | 33 | 35 | 34 | 33 | 37 | 33 | 30 | 32 | 32 | 32 | 32 | 33 | 32 |
| Microcline | 21 | 19 | 20 | 20 | 17 | 19 | 17 | 17 | 16 | 20 | 24 | 14 | 15 | 22 | 15 |
| Plagioclase | 38 | 40 | 41 | 39 | 40 | 38 | 40 | 40 | 40 | 38 | 37 | 41 | 41 | 40 | 39 |
| Biotite | 5 | 8 | 7 | 6 | 8 | 6 | 7 | 7 | 11 | 7 | 8 | 14 | 12 | 5 | 12 |
| **Semiquantitative spectrographic analyses (parts per million)** [6] | | | | | | | | | | | | | | | |
| Ag | 0 | 0 | 0 | 0 | 0 | 0 | 0 | 0 | 0 | 0 | 0 | 0 | 0 | 0 | 0 |
| B | 0 | 0 | 0 | 0 | 0 | 0 | 0 | 0 | 10 | 0 | 0 | 0 | 0 | 0 | 0 |
| Ba | 1,500 | 1,000 | 1,500 | 1,500 | 1,500 | 1,500 | 1,500 | 1,500 | 1,500 | 1,500 | 1,500 | 700 | 1,500 | 2,000 | 2,000 |
| Be | 3 | 5 | 5 | 5 | 5 | 5 | 2 | 5 | 7 | 3 | 5 | 5 | 5 | 3 | 3 |
| Ce | 0 | 0 | 0 | 0 | 0 | 0 | 0 | 0 | 0 | 0 | 0 | 0 | 0 | 150 | 0 |
| Co | 0 | 3 | 3 | 3 | 2 | 3 | 5 | 3 | 5 | 0 | 3 | 0 | 7 | 5 | 5 |
| Cr | 20 | 20 | 15 | 20 | 7 | 15 | 10 | 15 | 70 | 30 | 50 | 7 | 50 | 20 | 15 |
| Cu | 1 | 1.5 | 1 | 3 | 15 | 1 | 10 | 0.7 | 20 | 3 | 20 | 2 | 10 | 5 | 15 |
| Ga | 20 | 30 | 20 | 30 | 30 | 30 | 20 | 30 | 30 | 30 | 30 | 15 | 30 | 30 | 20 |
| La | 30 | 30 | 30 | 50 | 50 | 30 | 0 | 30 | 50 | 50 | 30 | 0 | 30 | 50 | 30 |
| Li | 0 | 0 | 0 | 0 | <200 | 0 | 0 | 0 | 0 | 0 | 0 | 0 | 0 | 0 | 0 |
| Mo | 0 | 0 | 0 | 0 | 0 | 0 | 0 | 0 | 0 | 0 | 0 | 0 | 0 | 0 | 0 |
| Nb | 15 | 20 | 15 | 20 | 15 | 20 | 3 | 10 | 20 | 15 | 20 | 0 | 20 | 7 | 15 |
| Nd | 0 | 0 | 0 | 0 | 0 | 0 | 0 | 0 | 0 | 0 | 0 | 0 | 0 | 0 | 0 |
| Ni | 10 | 7 | 5 | 15 | 5 | 7 | 0 | 5 | 20 | 20 | 15 | 7 | 20 | 10 | 5 |
| Pb | 50 | 50 | 30 | 50 | 50 | 50 | 50 | 50 | 70 | 50 | 50 | 50 | 50 | 70 | 30 |
| Sc | 5 | 5 | 5 | 5 | 5 | 5 | 3 | 5 | 10 | 5 | 5 | 5 | 7 | 7 | 3 |
| Sr | 700 | 700 | 500 | 700 | 700 | 700 | 1,000 | 1,000 | 1,000 | 1,000 | 700 | 500 | 1,000 | 1,000 | 1,000 |
| V | 30 | 50 | 30 | 50 | 30 | 30 | 30 | 50 | 70 | 50 | 50 | 30 | 70 | 50 | 50 |
| Y | 20 | 15 | 15 | 15 | 15 | 15 | 10 | 20 | 30 | 15 | 10 | 20 | 20 | 10 | 15 |
| Yb | 2 | 1.5 | 1.5 | 1.5 | 1.5 | 1.5 | 1 | 2 | 3 | 1.5 | 1 | 2 | 2 | 1 | 2 |
| Zr | 50 | 50 | 100 | 150 | 100 | 100 | 100 | 100 | 200 | 200 | 100 | 70 | 150 | 150 | 150 |

See footnotes at end of table.

TABLE 5.—*Analytical and other data for granitoid rocks from the Snake Creek–Williams Canyon area*—Continued

| Sample No. | 31 | 32 | 33 | 34 | 35 | 36 | 37 | 38 | 39 | 40 | 41 | 42 | 43 | 44 | 45 |
|---|---|---|---|---|---|---|---|---|---|---|---|---|---|---|---|
| **Chemical analyses (weight percent)** [1] | | | | | | | | | | | | | | | |
| $SiO_2$ | 71.2 | 72.0 | 71.4 | 70.9 | 70.2 | 71.7 | 70.7 | 71.1 | 70.9 | 70.2 | 71.1 | 71.5 | 70.7 | 71.2 | 71.5 |
| $Al_2O_3$ | 14.5 | 13.8 | 14.8 | 15.2 | 15.2 | 14.5 | 14.8 | 14.3 | 14.6 | 15.0 | 15.0 | 15.8 | 15.4 | 15.2 | 15.0 |
| $Fe_2O_3$ | 1.4 | 1.1 | 1.5 | 1.5 | 1.3 | 1.3 | 1.7 | 1.6 | 1.2 | 1.4 | 1.4 | 1.2 | 1.8 | 1.0 | 1.4 |
| FeO | .80 | 1.0 | 1.0 | .98 | 1.2 | .90 | .72 | .64 | 1.1 | 1.1 | 1.1 | 1.1 | .86 | 1.0 | 1.0 |
| MgO | .70 | 1.2 | .84 | .97 | .94 | .90 | 1.0 | 1.0 | .88 | 1.9 | .91 | .67 | 1.0 | .85 | .93 |
| CaO | 2.2 | 2.2 | 2.2 | 2.2 | 2.2 | 2.2 | 2.2 | 2.2 | 2.3 | 2.3 | 2.3 | 2.3 | 2.3 | 2.3 | 2.3 |
| $Na_2O$ | 3.6 | 3.7 | 3.5 | 3.6 | 3.6 | 3.3 | 4.0 | 4.2 | 3.6 | 3.6 | 3.6 | 3.1 | 3.4 | 4.2 | 3.7 |
| $K_2O$ | 3.5 | 3.6 | 3.6 | 3.4 | 3.6 | 3.7 | 3.3 | 3.3 | 3.2 | 3.0 | 3.2 | 3.5 | 3.0 | 3.2 | 2.9 |
| $H_2O(+)$ | .93 | .81 | .59 | .66 | .85 | .89 | .95 | .50 | 1.1 | .87 | .53 | .84 | .94 | .39 | .54 |
| $H_2O(-)$ | .16 | .16 | .16 | .17 | .15 | .11 | .14 | .12 | .06 | .10 | .09 | .16 | .16 | .10 | .13 |
| $TiO_2$ | .33 | .36 | .37 | .42 | .33 | .28 | .28 | .32 | .33 | .34 | .34 | .27 | .32 | .25 | .29 |
| $P_2O_5$ | .11 | .09 | .11 | .05 | .06 | .05 | .05 | .10 | .10 | .06 | .06 | .13 | .06 | .03 | .07 |
| MnO | .04 | .06 | .08 | .07 | .01 | .02 | .02 | .06 | .05 | .03 | .03 | .05 | .02 | .02 | .04 |
| $CO_2$ | <.05 | <.05 | <.05 | <.05 | .19 | .12 | <.05 | <.05 | <.05 | <.05 | <.05 | <.05 | <.05 | <.05 | .11 |
| Cl | | | | .01 | | | | | | | .01 | | | .01 | |
| F | | | | .05 | | | | | | | .05 | | | .05 | |
| Total | 99 | 100 | 100 | 100 | 100 | 100 | 100 | 99 | 99 | 100 | 100 | 101 | 100 | 100 | 100 |
| **Powder density** [2] | | | | | | | | | | | | | | | |
| | | | | 2.68 | | | | | 2.67 | | 2.71 | | | 2.70 | |
| **Rittmann *s*** [3] | | | | | | | | | | | | | | | |
| | 1.79 | 1.84 | 1.78 | 1.76 | 1.91 | 1.71 | 1.92 | 2.02 | 1.66 | 1.60 | 1.65 | 1.53 | 1.48 | 1.94 | 1.53 |
| **CIPW norms** [4] | | | | | | | | | | | | | | | |
| Quartz | 31.0 | 30.1 | 31.3 | 30.7 | 29.6 | 32.5 | 29.0 | 28.3 | 31.5 | 29.8 | 31.4 | 34.6 | 33.0 | 28.2 | 32.8 |
| Corundum | .93 | | 1.3 | 1.6 | 1.8 | 1.3 | | .06 | 1.2 | 1.7 | 1.4 | 2.9 | 2.4 | .72 | 1.9 |
| Zircon | .02 | .03 | .03 | .03 | .03 | .03 | .03 | .03 | .03 | .03 | .05 | .02 | .03 | .03 | .03 |
| Orthoclase | 20.8 | 21.2 | 21.2 | 20.0 | 21.3 | 21.8 | 19.8 | 19.6 | 19.0 | 17.7 | 18.9 | 20.6 | 17.7 | 19.0 | 17.1 |
| Albite | 30.7 | 31.2 | 29.5 | 30.4 | 30.5 | 27.9 | 33.7 | 35.7 | 30.6 | 30.4 | 30.4 | 26.1 | 28.7 | 35.6 | 31.3 |
| Anorthite | 10.6 | 10.4 | 10.5 | 10.9 | 9.7 | 10.2 | 11.0 | 10.3 | 11.2 | 11.4 | 11.4 | 10.8 | 11.4 | 11.2 | 10.6 |
| Wollastonite | | .11 | | | | | .02 | | | | | | | | |
| Enstatite | 1.8 | 3.0 | 2.1 | 2.4 | 2.3 | 2.2 | 2.5 | 2.5 | 2.2 | 4.8 | 2.3 | .60 | 2.5 | 2.1 | 2.3 |
| Ferrosilite | | .44 | .13 | | .60 | .15 | | | .58 | .36 | .36 | .67 | | .64 | .28 |
| Magnetite | 1.8 | 1.6 | 2.2 | 2.2 | 1.9 | 1.9 | 1.6 | 1.3 | 1.8 | 2.0 | 2.0 | 1.7 | 1.9 | 1.5 | 2.0 |
| Hematite | .19 | | | | | | .61 | .69 | | | | | .48 | | |
| Ilmenite | .63 | .68 | .70 | .80 | .63 | .53 | .53 | .61 | .63 | .65 | .65 | .51 | .61 | .48 | .55 |
| Apatite | .26 | .21 | .26 | .12 | .14 | .12 | .12 | .24 | .24 | .14 | .14 | .31 | .14 | .07 | .17 |
| Calcite | | | | | .43 | .27 | | | | | | | | | .25 |
| $H_2O+F+Cl$ | 1.1 | .97 | .75 | .83 | 1.0 | 1.0 | 1.1 | .62 | 1.2 | .97 | .68 | 1.0 | 1.1 | .55 | .67 |
| Total | 100 | 100 | 100 | 100 | 100 | 100 | 100 | 100 | 100 | 100 | 100 | 100 | 100 | 100 | 100 |
| **Partial modal analyses** [5] | | | | | | | | | | | | | | | |
| Quartz | 28 | 34 | 35 | 31 | 31 | 32 | 30 | 33 | 36 | 31 | 32 | 31 | 32 | 32 | 32 |
| Microcline | 22 | 18 | 17 | 14 | 15 | 16 | 15 | 17 | 14 | 15 | 14 | 17 | 15 | 19 | 17 |
| Plagioclase | 42 | 40 | 39 | 41 | 42 | 40 | 42 | 41 | 43 | 42 | 43 | 43 | 40 | 40 | 44 |
| Biotite | 5 | 7 | 9 | 10 | 11 | 10 | 10 | 8 | 8 | 9 | 8 | 10 | 11 | 7 | 4 |
| **Semiquantitative spectrographic analyses (parts per million)** [6] | | | | | | | | | | | | | | | |
| Ag | 0 | 0 | 0 | 0 | 0 | 0 | 0 | 0 | <0.7 | 0 | 0 | 0 | 0 | 0 | 0 |
| B | 7 | 0 | 10 | 0 | 10 | 10 | 10 | 0 | 0 | 0 | 10 | 0 | 15 | 0 | 0 |
| Ba | 2,000 | 2,000 | 2,000 | 2,000 | 2,000 | 2,000 | 2,000 | 1,500 | 2,000 | 2,000 | 2,000 | 1,500 | 2,000 | 2,000 | 2,000 |
| Be | 3 | 3 | 3 | 3 | 3 | 3 | 2 | 2 | 3 | 3 | 3 | 3 | 3 | 3 | 3 |
| Ce | 0 | 0 | 0 | 0 | 0 | 0 | 0 | 0 | 100 | 0 | 0 | 150 | 0 | 0 | 0 |
| Co | 7 | 5 | 5 | 7 | 7 | 7 | 7 | 7 | 7 | 7 | 7 | 7 | 7 | 5 | 5 |
| Cr | 15 | 15 | 70 | 50 | 70 | 70 | 50 | 20 | 5 | 20 | 70 | 30 | 70 | 50 | 30 |
| Cu | 30 | 30 | 7 | 10 | 7 | 7 | 7 | 7 | 7 | 5 | 15 | 2 | 10 | 5 | 20 |
| Ga | 30 | 20 | 30 | 30 | 30 | 30 | 30 | 30 | 20 | 20 | 30 | 30 | 30 | 30 | 30 |
| La | 70 | 50 | 50 | 50 | 50 | 50 | 70 | 70 | 50 | 70 | 50 | 70 | 70 | 50 | 50 |
| Li | 0 | 0 | 0 | 0 | 0 | 0 | 0 | 0 | 0 | 0 | 0 | 0 | 0 | 0 | 0 |
| Mo | 0 | 0 | 3 | 0 | 0 | 0 | 0 | 0 | 0 | 0 | 0 | 0 | 3 | 3 | 0 |
| Nb | 10 | 15 | 15 | 15 | 15 | 15 | 15 | 10 | 5 | 15 | 15 | 15 | 15 | 20 | 15 |
| Nd | 0 | 0 | 0 | 0 | 0 | 0 | 0 | 0 | 0 | 0 | 0 | 0 | 0 | 0 | 0 |
| Ni | 7 | 10 | 20 | 20 | 20 | 20 | 20 | 15 | 0 | 10 | 30 | 15 | 50 | 15 | 15 |
| Pb | 50 | 30 | 30 | 30 | 50 | 50 | 50 | 30 | 30 | 30 | 50 | 50 | 70 | 50 | 50 |
| Sc | 7 | 5 | 7 | 7 | 7 | 7 | 5 | 5 | 2 | 7 | 7 | 7 | 5 | 7 | 7 |
| Sr | 1,000 | 1,000 | 1,000 | 1,000 | 1,000 | 1,500 | 1,500 | 1,000 | 700 | 1,500 | 1,500 | 1,000 | 1,500 | 1,500 | 1,500 |
| V | 70 | 70 | 70 | 70 | 70 | 70 | 70 | 50 | 30 | 70 | 70 | 70 | 70 | 70 | 70 |
| Y | 20 | 20 | 15 | 15 | 20 | 20 | 15 | 20 | 20 | 15 | 20 | 30 | 20 | 20 | 20 |
| Yb | 2 | 2 | 1.5 | 1.5 | 2 | 2 | 1.5 | 2 | 1.5 | 1.5 | 2 | 3 | 2 | 2 | 2 |
| Zr | 100 | 150 | 200 | 150 | 200 | 150 | 200 | 200 | 150 | 200 | 300 | 100 | 200 | 150 | 150 |

See footnotes at end of table.

TABLE 5.—*Analytical and other data for granitoid rocks from the Snake Creek–Williams Canyon area*—Continued

| Sample No. | 46 | 47 | 48 | 49 | 50 | 51 | 52 | 53 | 54 | 55 | 56 | 57 | 58 | 59 | 60 |
|---|---|---|---|---|---|---|---|---|---|---|---|---|---|---|---|
| **Chemical analyses (weight percent)[1]** | | | | | | | | | | | | | | | |
| $SiO_2$ | 71.8 | 72.2 | 70.3 | 70.9 | 70.3 | 71.6 | 72.1 | 71.7 | 71.4 | 71.5 | 70.0 | 71.6 | 71.0 | 70.2 | 70.1 |
| $Al_2O_3$ | 14.3 | 14.6 | 14.9 | 15.0 | 14.7 | 14.8 | 14.6 | 14.9 | 14.7 | 14.2 | 15.2 | 13.9 | 15.6 | 14.6 | 15.5 |
| $Fe_2O_3$ | 1.2 | 1.5 | 1.6 | 1.2 | 1.5 | 1.1 | 1.3 | 1.6 | 1.2 | 1.1 | .29 | 1.3 | 1.1 | 1.0 | 1.3 |
| FeO | .90 | .88 | .84 | 1.1 | 1.0 | 1.1 | 1.0 | .62 | 1.0 | 1.2 | 2.1 | 1.2 | 1.4 | 1.3 | 1.4 |
| MgO | .85 | .90 | 1.2 | .98 | 1.3 | 1.1 | .64 | .70 | 1.1 | .91 | 1.1 | .92 | .95 | .86 | 1.0 |
| CaO | 2.4 | 2.4 | 2.4 | 2.4 | 2.4 | 2.4 | 2.4 | 2.4 | 2.4 | 2.5 | 2.5 | 2.5 | 2.6 | 2.6 | 2.7 |
| $Na_2O$ | 3.4 | 3.2 | 3.7 | 3.5 | 3.7 | 3.5 | 3.5 | 3.3 | 3.6 | 3.4 | 3.6 | 4.0 | 3.6 | 3.3 | 3.9 |
| $K_2O$ | 3.8 | 3.4 | 3.3 | 3.3 | 3.1 | 3.3 | 3.1 | 3.7 | 3.4 | 3.8 | 3.3 | 3.4 | 1.8 | 3.5 | 2.5 |
| $H_2O(+)$ | .23 | .81 | .84 | .87 | .63 | .45 | .66 | .66 | .51 | .31 | .87 | .78 | .37 | .53 | .94 |
| $H_2O(-)$ | .09 | .10 | .15 | .08 | .18 | .17 | .18 | .12 | .20 | .12 | .13 | .16 | .17 | .19 | .16 |
| $TiO_2$ | .29 | .28 | .39 | .34 | .40 | .30 | .30 | .28 | .30 | .31 | .45 | .32 | .35 | .34 | .33 |
| $P_2O_5$ | .09 | .10 | .12 | .10 | .12 | .10 | .09 | .09 | .11 | .11 | .07 | .06 | .06 | .12 | .07 |
| MnO | .05 | .05 | .06 | .04 | .05 | .06 | .04 | .05 | .04 | .07 | .07 | .04 | .02 | .07 | .03 |
| $CO_2$ | <.05 | <.05 | <.05 | <.05 | <.05 | <.05 | <.05 | <.05 | <.05 | <.05 | .12 | .08 | .12 | .48 | <.05 |
| Cl | .01 | .01 | | | | | | | | .00 | | | .01 | .01 | |
| F | .04 | .04 | | | | | | | | .05 | | | .05 | .09 | |
| Total | 99 | 100 | 100 | 100 | 99 | 100 | 100 | 100 | 100 | 100 | 100 | 100 | 99 | 99 | 100 |
| **Powder density[2]** | | | | | | | | | | | | | | | |
| | 2.68 | | | 2.70 | | | | | | 2.68 | | | 2.69 | 2.70 | |
| **Rittmann *s*[3]** | | | | | | | | | | | | | | | |
| | 1.80 | 1.49 | 1.79 | 1.66 | 1.69 | 1.62 | 1.50 | 1.50 | 1.73 | 1.82 | 1.76 | 1.91 | 1.04 | 1.70 | 1.51 |
| **CIPW norms[1]** | | | | | | | | | | | | | | | |
| Quartz | 31.0 | 34.2 | 29.4 | 31.2 | 30.1 | 31.8 | 33.7 | 32.9 | 30.6 | 30.3 | 28.4 | 29.8 | 36.1 | 32.0 | 30.2 |
| Corundum | .32 | 1.5 | 1.0 | 1.4 | 1.1 | 1.4 | 1.2 | 1.2 | .87 | .12 | 1.5 | | 3.3 | 2.0 | 1.5 |
| Zircon | .03 | .03 | .03 | .03 | .03 | .03 | .03 | .02 | .03 | .03 | .03 | .03 | .03 | .02 | .02 |
| Orthoclase | 22.4 | 20.0 | 19.5 | 19.5 | 18.4 | 19.5 | 18.3 | 21.9 | 20.1 | 22.5 | 19.5 | 20.0 | 10.7 | 20.8 | 14.8 |
| Albite | 28.7 | 27.0 | 31.3 | 29.6 | 31.4 | 29.6 | 29.6 | 27.9 | 30.4 | 28.8 | 30.4 | 33.7 | 30.5 | 28.0 | 33.0 |
| Anorthite | 11.7 | 11.2 | 11.5 | 11.6 | 11.5 | 11.3 | 11.7 | 11.7 | 11.5 | 12.0 | 11.5 | 8.1 | 12.1 | 9.2 | 13.2 |
| Wollastonite | | | | | | | | | | | | 1.5 | | | |
| Enstatite | 2.1 | 2.2 | 3.0 | 2.4 | 3.3 | 2.7 | 1.6 | .70 | 2.7 | 2.3 | 2.7 | 2.3 | 2.4 | 2.2 | 2.5 |
| Ferrosilite | .28 | .01 | | .54 | .03 | .73 | .34 | | .42 | .91 | .85 | .67 | .67 | 1.1 | 1.0 |
| Magnetite | 1.7 | 2.2 | 1.8 | 1.7 | 2.2 | 1.6 | 1.9 | 1.4 | 1.7 | 1.6 | .42 | 1.9 | 1.6 | 1.5 | 1.9 |
| Hematite | | | .38 | | | | | .67 | | | | | | | |
| Ilmenite | .55 | .53 | .74 | .65 | .76 | .57 | .57 | .53 | .57 | .59 | .85 | .61 | .67 | .65 | .63 |
| Apatite | .21 | .24 | .28 | .24 | .29 | .24 | .21 | .21 | .26 | .26 | .17 | .14 | .14 | .29 | .17 |
| Calcite | | | | | | | | | | | .27 | .18 | .27 | 1.1 | |
| $H_2O+F+Cl$ | .37 | .91 | .99 | .95 | .81 | .62 | .84 | .78 | .71 | .48 | 1.0 | .94 | .60 | .82 | 1.1 |
| Total | 100 | 100 | 100 | 100 | 100 | 100 | 100 | 100 | 100 | 100 | 100 | 100 | 100 | 100 | 100 |
| **Partial modal analyses[5]** | | | | | | | | | | | | | | | |
| Quartz | 30 | 33 | 34 | 31 | 30 | 31 | 32 | 35 | 31 | 32 | 32 | 28 | 29 | 33 | 32 |
| Microcline | 17 | 17 | 15 | 15 | 12 | 15 | 16 | 19 | 16 | 16 | 13 | 13 | 14 | 15 | 17 |
| Plagioclase | 42 | 42 | 40 | 43 | 42 | 40 | 44 | 40 | 42 | 41 | 43 | 44 | 43 | 44 | 44 |
| Biotite | 10 | 8 | 10 | 10 | 12 | 11 | 8 | 7 | 9 | 11 | 11 | 13 | 9 | 8 | 5 |
| **Semiquantitative spectrographic analyses (parts per million)[6]** | | | | | | | | | | | | | | | |
| Ag | 0 | 0 | 0 | 0 | 0 | 0 | 0 | 0 | 0 | 0 | 0 | 0 | 0 | 0 | 0 |
| B | 0 | 0 | 0 | 0 | 0 | 0 | 0 | 0 | 0 | 0 | 0 | 15 | 0 | 0 | 0 |
| Ba | 2,000 | 3,000 | 2,000 | 2,000 | 2,000 | 2,000 | 2,000 | 2,000 | 2,000 | 1,500 | 2,000 | 2,000 | 2,000 | 700 | 1,500 |
| Be | 3 | 3 | 3 | 2 | 2 | 3 | 3 | 2 | 3 | 3 | 3 | 3 | 3 | 5 | 3 |
| Ce | 0 | 150 | 0 | 100 | 0 | 0 | 0 | 0 | 0 | 0 | 0 | 0 | 0 | 0 | 0 |
| Co | 5 | 5 | 7 | 5 | 7 | 7 | 5 | 5 | 5 | 5 | 7 | 7 | 7 | 5 | 10 |
| Cr | 20 | 20 | 10 | 10 | 15 | 15 | 15 | 30 | 15 | 15 | 50 | 50 | 50 | 7 | 5 |
| Cu | 1.5 | 1.5 | 15 | 20 | 20 | 15 | 20 | 2 | 10 | 1.5 | 20 | 15 | 7 | 7 | 10 |
| Ga | 20 | 30 | 20 | 20 | 20 | 20 | 30 | 20 | 20 | 30 | 30 | 30 | 30 | 20 | 30 |
| La | 50 | 70 | 70 | 30 | 70 | 30 | 50 | 50 | 50 | 50 | 50 | 50 | 50 | 30 | 70 |
| Li | 0 | 0 | 0 | 0 | 0 | 0 | 0 | 0 | 0 | 0 | 0 | 0 | 0 | 0 | 0 |
| Mo | 0 | 0 | 0 | 0 | 0 | 0 | 0 | 0 | 3 | 0 | 0 | 0 | 0 | 0 | 0 |
| Nb | 15 | 10 | 15 | 5 | 10 | 0 | 0 | 15 | 15 | 10 | 15 | 20 | 10 | 0 | 15 |
| Nd | 0 | 0 | 0 | 0 | 0 | 0 | 0 | 0 | 0 | 0 | 0 | 0 | 0 | 0 | 0 |
| Ni | 5 | 7 | 5 | 0 | 10 | 7 | 10 | 5 | 7 | 7 | 15 | 20 | 20 | 5 | 20 |
| Pb | 30 | 30 | 30 | 30 | 30 | 30 | 50 | 30 | 100 | 50 | 30 | 50 | 50 | 50 | 30 |
| Sc | 5 | 5 | 5 | 3 | 5 | 5 | 7 | 5 | 5 | 5 | 7 | 7 | 7 | 5 | 7 |
| Sr | 1,000 | 1,000 | 1,000 | 700 | 1,000 | 1,000 | 1,000 | 700 | 1,000 | 1,000 | 1,500 | 1,500 | 1,500 | 300 | 1,500 |
| V | 50 | 50 | 70 | 50 | 70 | 70 | 70 | 50 | 70 | 50 | 100 | 70 | 70 | 50 | 70 |
| Y | 20 | 10 | 20 | 7 | 15 | 20 | 10 | 20 | 15 | 15 | 20 | 15 | 15 | 20 | 15 |
| Yb | 2 | 1 | 2 | 1 | 1.5 | 2 | 1 | 2 | 1.5 | 1.5 | 2 | 2 | 2 | 3 | 1.5 |
| Zr | 200 | 150 | 150 | 150 | 150 | 150 | 150 | 100 | 150 | 150 | 200 | 150 | 150 | 100 | 200 |

See footnotes at end of table.

TABLE 5.—*Analytical and other data for granitoid rocks from the Snake Creek–Williams Canyon area*—Continued

| Sample No. | 61 | 62 | 63 | 64 | 65 | 66 | 67 | 68 | 69 | 70 | [7] 71 | [7] 72 | 73 | 74 | 75 |
|---|---|---|---|---|---|---|---|---|---|---|---|---|---|---|---|
| **Chemical analyses (weight percent) [1]** | | | | | | | | | | | | | | | |
| $SiO_2$ | 68.7 | 70.5 | 70.2 | 70.0 | 70.0 | 70.3 | 71.1 | 68.5 | 62.0 | 67.8 | 65.8 | 62.1 | 67.2 | 67.6 | 68.0 |
| $Al_2O_3$ | 15.9 | 15.3 | 15.3 | 15.4 | 15.2 | 15.5 | 15.0 | 15.1 | 16.4 | 14.8 | 16.3 | 16.6 | 16.5 | 16.2 | 16.0 |
| $Fe_2O_3$ | 2.0 | 1.5 | 1.2 | 1.5 | 1.2 | .85 | 1.0 | 1.5 | 1.1 | 1.4 | 2.9 | 2.5 | 1.5 | 1.7 | 1.8 |
| FeO | 1.3 | 1.1 | 1.4 | 1.5 | 1.7 | 1.5 | 1.2 | 1.8 | 3.2 | 2.0 | 1.7 | 3.6 | 2.2 | 1.7 | 1.6 |
| MgO | 1.9 | .91 | .95 | 1.3 | 1.2 | .90 | .38 | 1.3 | 1.9 | 1.9 | .92 | 2.1 | 1.4 | 1.5 | 1.7 |
| CaO | 2.7 | 2.7 | 2.9 | 2.9 | 3.0 | 3.1 | 3.2 | 3.3 | 3.4 | 3.4 | 3.5 | 3.5 | 3.5 | 3.6 | 3.6 |
| $Na_2O$ | 3.8 | 3.3 | 3.7 | 3.7 | 4.3 | 3.8 | 3.8 | 3.8 | 4.0 | 3.6 | 4.2 | 4.2 | 3.6 | 3.7 | 3.6 |
| $K_2O$ | 2.1 | 3.2 | 2.6 | 2.3 | 2.2 | 2.3 | 2.5 | 2.7 | 3.3 | 2.7 | 2.8 | 2.1 | 2.4 | 2.2 | 2.3 |
| $H_2O(+)$ | .63 | .74 | .90 | .43 | .60 | .91 | .96 | .54 | 2.2 | .67 | .56 | 1.3 | .65 | .75 | .88 |
| $H_2O(-)$ | .14 | .12 | .12 | .14 | .16 | .06 | .08 | .15 | .09 | .22 | .07 | .24 | .14 | .16 | .12 |
| $TiO_2$ | .47 | .35 | .34 | .39 | .43 | .34 | .30 | .53 | .64 | .52 | .60 | .77 | .54 | .51 | .50 |
| $P_2O_5$ | .13 | .12 | .07 | .09 | .17 | .12 | .10 | .17 | .23 | .20 | .22 | .33 | .19 | .14 | .19 |
| MnO | .03 | .07 | .03 | .02 | .07 | .04 | .04 | .07 | .05 | .05 | .10 | .17 | .07 | .04 | .05 |
| $CO_2$ | <.05 | <0.5 | .09 | <.05 | <.05 | <.05 | <.05 | <.05 | <.05 | <.05 | <.05 | <.05 | <.05 | <.05 | <.05 |
| Cl | .00 | | .00 | .01 | .00 | | | .01 | | .01 | .01 | | .01 | .01 | |
| F | .06 | | .04 | .05 | .06 | | | .07 | | .06 | .07 | | .06 | .05 | |
| Total | 100 | 100 | 100 | 100 | 100 | 100 | 100 | 100 | 99 | 99 | 100 | 100 | 100 | 100 | 100 |
| **Powder density [2]** | | | | | | | | | | | | | | | |
| | 2.75 | | | 2.72 | 2.72 | 2.72 | | 2.73 | 2.73 | 2.74 | 2.74 | 2.75 | 2.74 | 2.74 | |
| **Rittmann *s* [3]** | | | | | | | | | | | | | | | |
| | 1.38 | 1.54 | 1.46 | 1.33 | 1.56 | 1.36 | 1.41 | 1.66 | 2.80 | 1.60 | 2.15 | 2.08 | 1.49 | 1.42 | 1.39 |
| **CIPW norms [4]** | | | | | | | | | | | | | | | |
| Quartz | 30.3 | 31.9 | 30.8 | 31.3 | 28.1 | 31.0 | 31.8 | 26.8 | 14.9 | 26.5 | 22.3 | 18.3 | 26.9 | 27.5 | 27.9 |
| Corundum | 2.8 | 1.7 | 1.4 | 1.7 | .70 | 1.4 | .34 | .21 | .53 | | .43 | 1.8 | 2.0 | 1.4 | 1.4 |
| Zircon | .03 | .03 | .03 | .03 | .03 | .03 | .03 | .03 | .05 | .03 | .05 | .10 | .03 | .03 | .03 |
| Orthoclase | 12.4 | 18.9 | 15.3 | 13.6 | 13.0 | 13.6 | 14.8 | 15.9 | 19.8 | 16.1 | 16.5 | 12.5 | 14.1 | 13.0 | 13.6 |
| Albite | 32.2 | 27.9 | 31.2 | 31.3 | 36.3 | 32.2 | 32.2 | 32.1 | 34.3 | 30.8 | 35.5 | 35.6 | 30.4 | 31.2 | 30.4 |
| Anorthite | 12.6 | 13.0 | 13.7 | 14.1 | 13.7 | 14.8 | 15.6 | 15.6 | 15.8 | 15.1 | 16.2 | 15.4 | 16.4 | 17.2 | 16.8 |
| Wollastonite | | | | | | | | | | .40 | | | | | |
| Enstatite | 4.7 | 2.3 | 2.4 | 3.2 | 3.0 | 2.2 | .95 | 3.2 | 4.8 | 4.8 | 2.3 | 5.3 | 3.5 | 3.7 | 4.2 |
| Ferrosilite | .02 | .33 | 1.1 | .91 | 1.5 | 1.6 | .96 | 1.3 | 4.1 | 1.8 | | 3.6 | 2.0 | .95 | 1.1 |
| Magnetite | 2.9 | 2.2 | 1.7 | 2.2 | 1.7 | 1.2 | 1.5 | 2.2 | 1.6 | 2.1 | 4.1 | 3.6 | 2.2 | 2.5 | 2.6 |
| Hematite | | | | | | | | | | | .10 | | | | |
| Ilmenite | .89 | .66 | .64 | .74 | .82 | .65 | .57 | 1.0 | 1.2 | 1.0 | 1.1 | 1.5 | 1.0 | 1.0 | .53 |
| Apatite | .31 | .28 | .17 | .21 | .40 | .29 | .24 | .40 | .55 | .48 | .52 | .78 | .45 | .33 | .45 |
| Calcite | | | .20 | | | | | | | | | | | | |
| $H_2O+F+Cl$ | .83 | .86 | 1.0 | .83 | .82 | .97 | 1.0 | .77 | 2.3 | .96 | .71 | 1.5 | .86 | .97 | 1.0 |
| Total | 100 | 100 | 100 | 100 | 100 | 100 | 100 | 100 | 100 | 100 | 100 | 100 | 100 | 100 | 100 |
| **Partial modal analyses [5]** | | | | | | | | | | | | | | | |
| Quartz | 31 | 29 | 32 | 29 | 29 | 31 | 29 | 29 | 22 | 26 | 22 | 20 | 23 | 23 | 27 |
| Microcline | 4 | 15 | 13 | 10 | 5 | 10 | 7 | 10 | P | 7 | 5 | | 6 | 3 | 6 |
| Plagioclase | 45 | 43 | 44 | 46 | 47 | 45 | 44 | 46 | 40 | 46 | 47 | 55 | 48 | 50 | 46 |
| Biotite | 16 | 8 | 7 | 11 | 16 | 10 | 14 | 14 | 26 | 18 | 22 | 23 | 18 | 18 | 15 |
| **Semiquantitative spectrographic analyses (parts per million) [6]** | | | | | | | | | | | | | | | |
| Ag | 0 | 0 | 0 | 0 | 0 | 0 | 0 | 0 | 0 | 0 | 0 | <0.7 | 0 | 0 | 0 |
| B | 0 | 0 | 0 | 0 | 0 | 0 | 0 | 0 | 0 | 0 | 0 | 0 | 0 | 0 | 0 |
| Ba | 1,500 | 2,000 | 2,000 | 1,500 | 1,500 | 1,000 | 2,000 | 2,000 | 1,500 | 1,500 | 1,500 | 700 | 1,500 | 1,500 | 1,500 |
| Be | 3 | 2 | 5 | 3 | 3 | 2 | 3 | 2 | 3 | 3 | 5 | 5 | 3 | 2 | 2 |
| Ce | 0 | 0 | 0 | 0 | 0 | 100 | 200 | 200 | 200 | 0 | 150 | 150 | 150 | 0 | 0 |
| Co | 10 | 7 | 10 | 10 | 7 | 3 | 7 | 10 | 15 | 10 | 7 | 20 | 10 | 15 | 10 |
| Cr | 70 | 20 | 70 | 70 | 20 | 10 | 15 | 50 | 30 | 20 | 10 | 20 | 30 | 70 | 50 |
| Cu | 30 | 20 | 20 | 10 | 5 | 7 | 15 | 20 | 15 | 20 | 15 | 30 | 10 | 7 | 20 |
| Ga | 100 | 50 | 30 | 30 | 30 | 20 | 15 | 30 | 20 | 30 | 30 | 30 | 30 | 30 | 30 |
| La | 100 | 50 | 70 | 70 | 70 | 30 | 200 | 100 | 150 | 70 | 70 | 50 | 70 | 100 | 50 |
| Li | 0 | 0 | 0 | 0 | 0 | 0 | 0 | 0 | 0 | 0 | 0 | 0 | 0 | 0 | 0 |
| Mo | 0 | 0 | 0 | 0 | 0 | 0 | 0 | 0 | 0 | 5 | 0 | 3 | 0 | 0 | 0 |
| Nb | 15 | 15 | 0 | 15 | 10 | 5 | 3 | 15 | 5 | 15 | 30 | 15 | 10 | 15 | 15 |
| Nd | 0 | 0 | 0 | 0 | 0 | 0 | 0 | 0 | 0 | 0 | 100 | 0 | 0 | 0 | 0 |
| Ni | 20 | 15 | 20 | 20 | 10 | 0 | 0 | 10 | 50 | 10 | 5 | 50 | 15 | 20 | 30 |
| Pb | 20 | 30 | 50 | 50 | 20 | 20 | 30 | 20 | 10 | 30 | 30 | 20 | 30 | 30 | 30 |
| Sc | 7 | 7 | 5 | 7 | 7 | 2 | 7 | 10 | 5 | 10 | 10 | 20 | 10 | 10 | 7 |
| Sr | 1,500 | 1,000 | 1,500 | 1,500 | 1,500 | 1,000 | 1,500 | 2,000 | 1,500 | 1,500 | 1,000 | 1,000 | 1,500 | 2,000 | 1,000 |
| V | 100 | 70 | 70 | 100 | 100 | 50 | 50 | 150 | 100 | 150 | 100 | 150 | 150 | 150 | 100 |
| Y | 15 | 20 | 15 | 20 | 15 | 3 | 10 | 30 | 10 | 20 | 70 | 30 | 20 | 20 | 15 |
| Yb | 1 | 1 | 1.5 | 2 | 1.5 | 0 | 1 | 3 | 1 | 2 | 7 | 3 | 2 | 2 | 1.5 |
| Zr | 200 | 150 | 200 | 150 | 150 | 150 | 200 | 200 | 300 | 200 | 300 | 700 | 200 | 150 | 200 |

See footnotes at end of table.

TABLE 5.—*Analytical and other data for granitoid rocks from the Snake Creek–Williams Canyon area*—Continued

| Sample No. | 76 | [7] 77 | 78 | 79 | 80 | [7] 81 | 82 | 83 | 84 | [7] 85 | 86 | [7] 87 |
|---|---|---|---|---|---|---|---|---|---|---|---|---|
| **Chemical analyses** [1] | | | | | | | | | | | | |
| $SiO_2$ | 65.4 | 65.9 | 66.3 | 63.5 | 65.2 | 66.2 | 67.1 | 63.7 | 61.9 | 57.4 | 62.8 | 60.2 |
| $Al_2O_3$ | 16.9 | 15.6 | 16.5 | 17.3 | 16.4 | 15.6 | 16.0 | 17.1 | 17.9 | 18.3 | 17.2 | 19.6 |
| $Fe_2O_3$ | 1.7 | 1.9 | 1.7 | 1.7 | 2.0 | 1.6 | 2.2 | 2.5 | 2.5 | 3.5 | 1.9 | 2.1 |
| FeO | 2.3 | 2.5 | 1.9 | 2.7 | 2.0 | 2.6 | 1.3 | 2.3 | 2.5 | 3.9 | 3.0 | 3.8 |
| MgO | 1.7 | 2.0 | 1.6 | 2.1 | 2.2 | 2.7 | 1.4 | 2.2 | 2.1 | 2.8 | 2.1 | 3.3 |
| CaO | 3.8 | 3.8 | 3.9 | 4.0 | 4.1 | 4.1 | 4.2 | 4.3 | 4.3 | 4.5 | 4.5 | 5.7 |
| $Na_2O$ | 3.8 | 3.8 | 4.0 | 3.8 | 3.7 | 3.7 | 4.0 | 3.4 | 3.7 | 4.0 | 3.8 | 3.8 |
| $K_2O$ | 2.3 | 1.9 | 1.8 | 2.5 | 2.2 | 1.8 | 2.0 | 2.7 | 2.3 | 2.6 | 2.2 | 1.6 |
| $H_2O(+)$ | .62 | .97 | 1.4 | .77 | .69 | .97 | .63 | 1.15 | 1.30 | 1.05 | .87 | 1.4 |
| $H_2O(-)$ | .15 | .33 | .12 | .16 | .17 | .13 | .07 | .09 | .15 | .21 | .19 | .20 |
| $TiO_2$ | .59 | .72 | .55 | .76 | .65 | .52 | .53 | .73 | .77 | 1.0 | .79 | .88 |
| $P_2O_5$ | .14 | .27 | .19 | .19 | .22 | .17 | .22 | .23 | .22 | .56 | .21 | .24 |
| MnO | .04 | .18 | .05 | .07 | .06 | .12 | .05 | .08 | .05 | .14 | .05 | .11 |
| $CO_2$ | <.05 | <.05 | <.05 | .08 | <.05 | <.05 | <.05 | .03 | <.05 | <.05 | <.05 | <.05 |
| Cl | .01 | .01 | ---- | .01 | .01 | ---- | .01 | .01 | .01 | .01 | .01 | ---- |
| F | .06 | .26 | ---- | .07 | .06 | ---- | .06 | .13 | .07 | .25 | .07 | ---- |
| Total | 99 | 100 | 100 | 100 | 100 | 100 | 100 | 101 | 100 | 100 | 100 | 101 |
| **Powder density** [2] | | | | | | | | | | | | |
| | 2.73 | 2.76 | 2.74 | 2.75 | 2.77 | 2.78 | 2.76 | 2.80 | 2.78 | 2.80 | 2.75 | 2.85 |
| **Rittmann *s*** [3] | | | | | | | | | | | | |
| | 1.66 | 1.42 | 1.44 | 1.94 | 2.57 | 1.31 | 1.49 | 1.80 | 1.90 | 3.03 | 1.81 | 1.70 |
| **CIPW norms** [4] | | | | | | | | | | | | |
| Quartz | 23.2 | 25.1 | 25.2 | 19.8 | 23.4 | 24.0 | 25.8 | 21.2 | 19.1 | 10.6 | 18.8 | 14.4 |
| Corundum | 1.5 | 1.0 | 1.2 | 1.7 | 1.0 | .45 | .15 | 1.4 | 1.9 | 2.0 | .80 | ---- |
| Zircon | .05 | .03 | .03 | .05 | .05 | .02 | .03 | .04 | .05 | .03 | .03 | .02 |
| Orthoclase | 13.6 | 11.2 | 10.6 | 14.8 | 13.0 | 10.6 | 11.9 | 15.9 | 13.6 | 15.3 | 13.0 | 9.5 |
| Albite | 32.1 | 32.1 | 33.8 | 32.3 | 31.4 | 31.2 | 33.9 | 28.6 | 31.2 | 33.7 | 32.2 | 32.1 |
| Anorthite | 18.2 | 17.2 | 18.4 | 18.2 | 19.0 | 19.3 | 19.5 | 19.5 | 20.1 | 18.7 | 21.3 | 23.5 |
| Wollastonite | ---- | ---- | ---- | ---- | ---- | ---- | ---- | ---- | ---- | ---- | ---- | 1.4 |
| Enstatite | 4.2 | 5.0 | 4.0 | 5.3 | 5.5 | 6.7 | 3.5 | 5.5 | 5.2 | 6.9 | 5.2 | 8.2 |
| Ferrosilite | 1.9 | 2.2 | 1.3 | 2.4 | 1.1 | 2.9 | ---- | 1.1 | 1.3 | 2.9 | 2.7 | 4.0 |
| Magnetite | 2.5 | 2.8 | 2.5 | 2.5 | 2.9 | 2.3 | 2.8 | 3.6 | 3.6 | 5.1 | 3.0 | 3.0 |
| Hematite | ---- | ---- | ---- | ---- | ---- | ---- | .26 | ---- | ---- | ---- | ---- | ---- |
| Ilmenite | 1.1 | 1.4 | 1.0 | 1.5 | 1.2 | .98 | 1.0 | 1.4 | 1.5 | 1.9 | 1.5 | 1.7 |
| Apatite | .33 | .64 | .45 | .45 | .52 | .40 | .52 | .54 | .52 | 1.3 | .50 | .57 |
| Calcite | ---- | ---- | ---- | .18 | ---- | ---- | ---- | .07 | ---- | ---- | ---- | ---- |
| $H_2O+F+Cl$ | .74 | 1.6 | 1.5 | 1.0 | .93 | 1.1 | .77 | 1.4 | 1.5 | 1.5 | 1.1 | 1.6 |
| Total | 99 | 100 | 100 | 100 | 100 | 100 | 100 | 100 | 100 | 100 | 100 | 100 |
| **Partial modal analyses** [5] | | | | | | | | | | | | |
| Quartz | 25 | 27 | 26 | 23 | 25 | 24 | 25 | 20 | 21 | 12 | 21 | 20 |
| Microcline | 4 | 0 | P | 3 | 3 | 5 | P | 3 | 0 | 0 | P | 0 |
| Plagioclase | 47 | 45 | 49 | 48 | 46 | 43 | 49 | 48 | 47 | 54 | 48 | 48 |
| Biotite | 20 | 22 | 19 | 21 | 21 | 25 | 21 | 25 | 26 | 32 | 26 | 30 |
| **Semiquantitative spectrographic analyses (parts per million)** [6] | | | | | | | | | | | | |
| Ag | 0 | 0 | 0 | 0 | 0 | 0 | 0 | 0 | 0 | 0 | 0 | 0 |
| B | 0 | 0 | 0 | 0 | 0 | 0 | 0 | 0 | 0 | 0 | 0 | 0 |
| Ba | 1,500 | 1,000 | 2,000 | 1,500 | 1,500 | 1,000 | 1,500 | 1,500 | 1,500 | 300 | 1,500 | 702 |
| Be | 2 | 3 | 2 | 3 | 2 | 1.5 | 2 | 7 | 3 | 2 | 3 | 0 |
| Ce | 0 | 0 | 100 | 0 | 0 | 0 | 0 | 150 | 0 | 0 | 0 | 0 |
| Co | 15 | 15 | 20 | 15 | 15 | 15 | 10 | 15 | 15 | 15 | 15 | 30 |
| Cr | 70 | 30 | 30 | 50 | 20 | 100 | 50 | 100 | 70 | 10 | 70 | 70 |
| Cu | 7 | 15 | 15 | 15 | 30 | 30 | 15 | 70 | 50 | 30 | 15 | 50 |
| Ga | 30 | 30 | 20 | 30 | 30 | 15 | 30 | 50 | 30 | 70 | 30 | 20 |
| La | 100 | 30 | 50 | 70 | 70 | 30 | 50 | 70 | 70 | 70 | 70 | 0 |
| Li | 0 | 0 | 0 | 0 | 0 | 0 | 0 | 0 | 0 | 0 | 0 | 0 |
| Mo | 0 | 0 | 0 | 0 | 0 | 0 | 0 | 0 | 5 | 0 | 0 | 0 |
| Nb | 15 | 20 | 5 | 15 | 10 | 0 | 15 | 15 | 20 | 0 | 0 | 0 |
| Nd | 0 | 0 | 0 | 0 | 0 | 0 | 0 | 0 | ---- | 0 | 0 | 0 |
| Ni | 20 | 30 | 30 | 20 | 15 | 50 | 30 | 50 | 30 | 10 | 50 | 50 |
| Pb | 20 | 15 | 15 | 30 | 20 | 15 | 30 | 30 | 30 | 15 | 30 | 10 |
| Sc | 10 | 15 | 10 | 15 | 7 | 0 | 10 | 15 | 15 | 15 | 10 | 20 |
| Sr | 2,000 | 1,000 | 1,500 | 2,000 | 1,500 | 500 | 1,500 | 1,500 | 2,000 | 500 | 2,000 | 700 |
| V | 150 | 150 | 70 | 150 | 150 | 100 | 150 | 200 | 150 | 150 | 200 | 150 |
| Y | 15 | 30 | 15 | 20 | 15 | 20 | 20 | 30 | 30 | 15 | 20 | 30 |
| Yb | 1.5 | 3 | 1.5 | 2 | 1.5 | 1.5 | 2 | 3 | 3 | 1.5 | 2 | 3 |
| Zr | 300 | 150 | 200 | 300 | 300 | 70 | 150 | 300 | 300 | 150 | 200 | 70 |

[1] Cl and F determinations by Vertie C. Smith. --, no data. Where values for Cl and F are listed, $H_2O$ also determined by Vertie C. Smith. Other $H_2O$ figures, as well as all other determinations, by Paul Elmore, Samuel Botts, Gillison Chloe, Lowell Artis, and H. Smith, using methods similar to those developed by Shapiro and Brannock (1956).

[2] Determinations by Vertie C. Smith. --, no data.

[3] Rittmann $s = \frac{(Na_2O+K_2O)^2}{SiO_2-43}$.

[4] Normative halite and fluorite excluded from calculations for consistency.

[5] Based mainly on calibrated X-ray diffraction patterns. --, not found; P, present, probably less than 2 percent. Biotite figures for samples 81 and 87 include some amphibole, and biotite figure for sample 69 includes much chlorite.

[6] Analyses by Chris Heropoulos and R. E. Mays. 0, below limit of detection. Table 4 lists the 45 minor elements sought, together with limits of detection. General limitations of method are given in text.

[7] Xenoliths of Pioche Shale. Samples 72 and 85 collected from Young Canyon area.

TABLE 6.—*Analytical and other data for granitoid rocks from the Pole Canyon–Can Young Canyon area*

[Samples arranged according to increasing CaO content. Sample localities shown on plate 1]

| Sample No. | 88 | 89 | 90 | 91 | 92 | 93 | 94 | 95 | 96 |
|---|---|---|---|---|---|---|---|---|---|
| **Chemical analyses (weight percent)** [1] | | | | | | | | | |
| $SiO_2$ | 73.8 | 72.3 | 73.0 | 73.8 | 73.9 | 71.6 | 74.9 | 72.5 | 71.1 |
| $Al_2O_3$ | 15.1 | 14.9 | 15.0 | 14.0 | 14.7 | 15.5 | 14.5 | 15.1 | 15.0 |
| $Fe_2O_3$ | .72 | 1.2 | .54 | .68 | .78 | .88 | .48 | .85 | 2.2 |
| FeO | .24 | .77 | .95 | .38 | .38 | .38 | .40 | .32 | .20 |
| MgO | .27 | .58 | .12 | .24 | .36 | .45 | .18 | .12 | .64 |
| CaO | .87 | .98 | 1.1 | 1.2 | 1.3 | 1.3 | 1.4 | 1.6 | 1.8 |
| $Na_2O$ | 3.6 | 3.2 | 3.4 | 3.1 | 3.4 | 3.9 | 3.4 | 3.8 | 3.4 |
| $K_2O$ | 3.9 | 4.0 | 3.9 | 4.5 | 3.8 | 4.2 | 3.8 | 4.0 | 4.1 |
| $H_2O(+)$ | 1.0 | .83 | .45 | .95 | .51 | .32 | .71 | .67 | .56 |
| $H_2O(-)$ | .21 | .23 | .15 | .15 | .10 | .17 | .11 | .19 | .16 |
| $TiO_2$ | .12 | .24 | .18 | .01 | .12 | .86 | .08 | .11 | .32 |
| $P_2O_5$ | .06 | .07 | .10 | .00 | .06 | .01 | .06 | .06 | .08 |
| MnO | .02 | .02 | .05 | .00 | .04 | .08 | .02 | .02 | .03 |
| $CO_2$ | <.05 | <.05 | <.05 | .86 | <.05 | <.05 | <.05 | <.05 | <.05 |
| Cl | ---- | .01 | .01 | ---- | .01 | .00 | ---- | ---- | .00 |
| F | ---- | .08 | .08 | ---- | .05 | .07 | ---- | ---- | .09 |
| Total | 100 | 100 | 100 | 100 | 100 | 100 | 100 | 100 | 100 |
| **Powder density** [2] | | | | | | | | | |
| | ---- | 2.67 | 2.66 | ---- | 2.65 | 2.65 | ---- | ---- | 2.66 |
| **CIPW norms** [3] | | | | | | | | | |
| Quartz | 35.8 | 35.7 | 36.0 | 37.9 | 36.5 | 29.4 | 37.3 | 31.8 | 30.9 |
| Corundum | 3.5 | 3.7 | 3.4 | 3.8 | 2.8 | 2.1 | 2.3 | 1.7 | 1.8 |
| Zircon | .02 | .02 | ---- | .02 | ---- | .02 | .02 | .02 | .03 |
| Orthoclase | 23.0 | 23.7 | 23.1 | 26.5 | 22.5 | 24.8 | 22.4 | 23.8 | 24.2 |
| Albite | 30.4 | 27.1 | 28.8 | 26.2 | 28.9 | 33.0 | 28.7 | 32.4 | 28.7 |
| Anorthite | 4.1 | 4.5 | 4.9 | .70 | 6.2 | 6.6 | 6.7 | 7.8 | 8.7 |
| Enstatite | .67 | 1.5 | .30 | .60 | .90 | 1.7 | .45 | .30 | 1.6 |
| Ferrosilite | ---- | .06 | 1.1 | .12 | ---- | ---- | .24 | ---- | ---- |
| Magnetite | .49 | 1.7 | .78 | .99 | 1.1 | ---- | .70 | .78 | ---- |
| Hematite | ---- | ---- | ---- | ---- | .09 | .88 | ---- | .32 | 2.2 |
| Ilmenite | .23 | .46 | .34 | .02 | .23 | .98 | .15 | .21 | .49 |
| Rutile | ---- | ---- | ---- | ---- | ---- | .35 | ---- | ---- | .06 |
| Apatite | .14 | .17 | .24 | ---- | .14 | .02 | .14 | .14 | .19 |
| Calcite | ---- | ---- | ---- | 2.0 | ---- | ---- | ---- | ---- | ---- |
| $H_2O+F+Cl$ | 1.2 | 1.2 | .68 | 1.1 | .67 | .56 | .82 | .86 | .81 |
| Total | 100 | 100 | 100 | 100 | 100 | 100 | 100 | 100 | 100 |
| **Partial modal analyses** [4] | | | | | | | | | |
| Quartz | 35 | 31 | 33 | 39 | 38 | 31 | 37 | 32 | 28 |
| Orthoclase | 20 | 19 | 17 | 20 | 19 | 19 | 20 | 19 | 17 |
| Plagioclase | 33 | 35 | 36 | 27 | 36 | 40 | 34 | 38 | 38 |
| Biotite | P | 6 | 5 | P | 4 | 4 | ---- | P | 10 |
| Muscovite | 8 | 6 | 9 | 12 | 4 | 5 | 9 | 10 | 6 |
| **Semiquantitative spectrographic analyses (parts per million)** [5] | | | | | | | | | |
| B | 7 | 0 | 0 | 15 | 0 | 0 | 0 | 0 | 0 |
| Ba | 1,000 | 500 | 500 | 1,000 | 500 | 1,000 | 1,000 | 1,000 | 1,500 |
| Be | 5 | 3 | 3 | 7 | 5 | 7 | 5 | 5 | 3 |
| Co | 0 | 0 | 0 | 0 | 0 | 0 | 0 | 0 | 3 |
| Cr | 3 | 7 | 7 | 20 | 3 | 7 | 7 | 7 | 7 |
| Cu | 50 | 2 | 2 | 100 | 2 | 50 | 10 | 30 | 5 |
| Ga | 50 | 30 | 30 | 50 | 30 | 30 | 50 | 30 | 30 |
| La | 0 | 0 | 0 | 0 | 0 | 0 | 0 | 0 | 30 |
| Mo | 0 | 0 | 0 | 100 | 0 | 0 | 0 | 3 | 0 |
| Nb | 0 | 0 | 0 | 10 | 0 | 10 | 0 | 0 | 0 |
| Ni | 2 | 2 | 2 | 15 | 0 | 5 | 3 | 3 | 3 |
| Pb | 50 | 50 | 50 | 70 | 30 | 50 | 50 | 70 | 50 |
| Sr | 700 | 300 | 300 | 300 | 300 | 700 | 500 | 700 | 1,000 |
| V | 10 | 20 | 15 | 15 | 0 | 15 | 10 | 20 | 30 |
| Y | 7 | 7 | 20 | 10 | 7 | 10 | 10 | 10 | 7 |
| Yb | 0 | 0 | 0 | 1 | 0 | 0 | 0 | 0 | 0 |
| Zr | 70 | 70 | 50 | 70 | 50 | 70 | 70 | 100 | 150 |

[1] Cl and F determinations by Vertie C. Smith. Dashed entries mean "no data". Where values for Cl and F are listed, $H_2O$ also determined by Vertie C. Smith. Other $H_2O$ figures, as well as all other determinations, by Paul Elmore, Samuel Botts, Gillison Chloe, Lowell Artis, and H. Smith, using methods similar to those developed by Shapiro and Brannock (1956).

[2] Determinations by Vertie C. Smith. ———, no data.

[3] Normative halite and fluorite excluded from calculations for consistency.

[4] Based mainly on calibrated X-ray diffraction patterns. ------, not found; P, present, probably less than 2 percent.

[5] Analyses by Chris Heropoulos and R. E. Mays. 0, below limit of detection. Table 4 lists the 45 minor elements sought, together with limits of detection. General limitations of method are given in text.

TABLE 7.—*Analytical and other data for granitoid rocks from the Young Canyon–Kious Basin area*

[Samples 97–102 from undeformed rocks; samples 103–115 from part of intrusive brecciated by décollement. Sample localities shown on plate 1]

| Sample No. | 97 | 98 | 99 | 100 | 101 | 102 | 103 | 104 | 105 | 106 | 107 | 108 | 109 | 110 | 111 | 112 | 113 | 114 | 115 |
|---|---|---|---|---|---|---|---|---|---|---|---|---|---|---|---|---|---|---|---|
| **Chemical analyses (weight percent)** [1] | | | | | | | | | | | | | | | | | | | |
| $SiO_2$ | 75.6 | 76.4 | 74.7 | 75.4 | 74.5 | 72.8 | 71.9 | 73.7 | 79.3 | 73.3 | 74.6 | 74.8 | 69.5 | 70.2 | 72.2 | 70.3 | 70.9 | 69.9 | 68.1 |
| $Al_2O_3$ | 13.4 | 13.0 | 13.8 | 13.1 | 13.5 | 14.3 | 13.4 | 14.0 | 10.7 | 13.6 | 13.3 | 13.2 | 14.8 | 14.6 | 14.2 | 14.1 | 14.2 | 14.5 | 15.2 |
| $Fe_2O_3$ | .44 | .48 | .55 | .63 | .72 | .70 | .85 | .96 | .85 | 1.0 | .65 | .74 | 1.2 | 1.4 | 1.1 | 1.0 | 1.3 | 1.1 | 1.3 |
| FeO | .18 | .31 | .22 | .34 | .38 | 1.2 | 1.5 | .40 | .19 | .68 | .49 | .42 | 1.5 | 1.4 | 1.1 | 1.3 | 1.2 | 1.6 | 2.0 |
| MgO | .11 | .13 | .29 | .34 | .20 | .34 | .67 | .65 | .16 | .81 | .24 | .33 | 1.8 | 1.0 | .45 | .91 | .74 | 1.4 | 1.9 |
| CaO | .68 | .75 | .96 | 1.1 | 1.2 | 1.6 | 1.0 | 1.1 | 1.1 | 1.3 | 1.4 | 1.6 | 2.0 | 2.1 | 2.1 | 2.2 | 2.3 | 2.6 | 2.9 |
| $Na_2O$ | 3.5 | 3.4 | 3.3 | 2.8 | 3.2 | 3.5 | 2.7 | 3.4 | 1.5 | 2.7 | 3.3 | 3.2 | 3.4 | 3.0 | 3.4 | 3.2 | 2.6 | 2.9 | 3.0 |
| $K_2O$ | 4.5 | 4.3 | 5.3 | 5.1 | 4.5 | 4.1 | 5.3 | 4.4 | 3.5 | 5.1 | 4.5 | 4.2 | 3.8 | 4.3 | 4.3 | 4.0 | 4.6 | 4.1 | 3.7 |
| $H_2O(+)$ | .92 | .66 | .40 | .32 | .85 | .90 | 1.1 | .95 | 1.0 | .91 | .87 | .90 | 1.0 | 1.0 | .58 | 1.1 | 1.1 | 1.0 | 1.2 |
| $H_2O(-)$ | .13 | .08 | .14 | .16 | .15 | .15 | .18 | .15 | .11 | .19 | .04 | .08 | .21 | .14 | .05 | .16 | .08 | .15 | .11 |
| $TiO_2$ | .07 | .09 | .19 | .30 | .14 | .21 | .42 | .21 | .12 | .28 | .15 | .16 | .46 | .47 | .38 | .40 | .36 | .48 | .44 |
| $P_2O_5$ | .01 | .01 | .00 | .00 | .02 | .06 | .13 | .07 | .01 | .07 | .02 | .08 | .19 | .15 | .10 | .13 | .12 | .16 | .18 |
| MnO | .03 | .03 | .05 | .10 | .05 | .05 | .05 | .06 | .03 | .04 | .04 | .04 | .05 | .05 | .07 | .05 | .06 | .06 | .05 |
| $CO_2$ | <.05 | <.05 | <.05 | <.05 | <.05 | <.05 | .30 | <.05 | <.05 | <.05 | <.05 | <.05 | <.05 | <.05 | <.05 | .36 | .12 | <.05 | <.05 |
| Total | 100 | 100 | 100 | 100 | 99 | 100 | 100 | 100 | 99 | 100 | 100 | 100 | 100 | 100 | 100 | 99 | 100 | 100 | 100 |
| **Powder density** [2] | | | | | | | | | | | | | | | | | | | |
| | 2.63 | 2.62 | ..... | | 2.65 | 2.67 | ..... | | 2.75 | ..... | 2.66 | ..... | | | | | 2.58 | ..... | |
| **CIPW norms** | | | | | | | | | | | | | | | | | | | |
| Quartz | 36.7 | 38.5 | 32.9 | 36.6 | 36.0 | 32.3 | 33.8 | 33.9 | 55.4 | 34.2 | 34.9 | 36.5 | 28.1 | 30.2 | 30.7 | 31.3 | 32.5 | 29.4 | 26.9 |
| Corundum | 1.5 | 1.4 | .99 | .93 | 1.2 | 1.3 | 2.3 | 1.8 | 2.5 | 1.4 | .49 | .64 | 1.8 | 1.4 | .31 | 1.6 | 1.3 | .85 | 1.3 |
| Zircon | .02 | .02 | .02 | .02 | .02 | .03 | .03 | .03 | .02 | .03 | .03 | .02 | .03 | .05 | .05 | .03 | .03 | .05 | .05 |
| Orthoclase | 26.7 | 25.5 | 31.3 | 30.2 | 26.7 | 24.2 | 31.5 | 26.0 | 21.0 | 30.1 | 26.7 | 24.9 | 22.4 | 25.4 | 25.4 | 23.8 | 27.2 | 24.2 | 21.8 |
| Albite | 29.6 | 28.9 | 27.9 | 23.7 | 27.2 | 29.6 | 23.0 | 28.7 | 12.9 | 22.8 | 28.0 | 27.1 | 28.7 | 25.4 | 28.7 | 27.2 | 22.0 | 24.5 | 25.3 |
| Anorthite | 3.3 | 3.7 | 4.5 | 5.9 | 5.9 | 7.6 | 2.5 | 5.1 | 5.5 | 6.2 | 6.9 | 7.5 | 8.9 | 9.8 | 9.9 | 8.1 | 10.1 | 12.1 | 13.5 |
| Wollastonite | ..... | | | | | | | | | | | | | | | | | | |
| Enstatite | .27 | .33 | .72 | .85 | .50 | .85 | 1.0 | 1.6 | .40 | 2.0 | .60 | .83 | 4.5 | 2.5 | 1.1 | 2.3 | 1.9 | 3.5 | 4.7 |
| Ferrosilite | ..... | .08 | ..... | | | 1.4 | 1.5 | ..... | | .04 | .19 | ..... | 1.1 | .73 | .61 | 1.0 | .65 | 1.4 | 2.0 |
| Magnetite | .63 | .70 | .32 | ..... | .99 | 1.0 | 1.2 | .88 | .37 | 1.5 | .95 | 1.0 | 1.7 | 2.0 | 1.6 | 1.5 | 1.9 | 1.6 | 1.9 |
| Hematite | ..... | | .33 | .63 | .04 | ..... | | .36 | .61 | ..... | | .04 | ..... | | | | | | |
| Ilmenite | .13 | .17 | .36 | .57 | .27 | .40 | .80 | .40 | .23 | .53 | .29 | .30 | .87 | .89 | .72 | .76 | .69 | .91 | .83 |
| Apatite | .02 | .02 | ..... | | .04 | .14 | .31 | .17 | .02 | .17 | .05 | .19 | .45 | .36 | .24 | .31 | .29 | .38 | .43 |
| Calcite | ..... | | | | | | .69 | ..... | | | | | | | | .82 | .27 | ..... | |
| $H_2O$ | 1.1 | .74 | .54 | .40 | 1.0 | 1.1 | 1.3 | 1.1 | 1.1 | 1.1 | .91 | .98 | 1.2 | 1.1 | .63 | 1.3 | 1.2 | 1.2 | 1.3 |
| Total | 100 | 100 | 100 | 100 | 100 | 100 | 100 | 100 | 100 | 100 | 100 | 100 | 100 | 100 | 100 | 100 | 100 | 100 | 100 |
| **Partial modal anaylses** [3] | | | | | | | | | | | | | | | | | | | |
| Quartz | 37 | 39 | 37 | 37 | 33 | 32 | 34 | 36 | 58 | 37 | 36 | 43 | 28 | 31 | 33 | 31 | 37 | 30 | 27 |
| Orthoclase | 23 | 21 | 27 | 25 | 23 | 22 | 29 | 25 | 15 | 12 | 22 | 18 | 15 | 23 | 20 | 23 | 12 | 18 | 16 |
| Plagioclase | 35 | 34 | 32 | 30 | 35 | 35 | 26 | 32 | 19 | 20 | 33 | 35 | 38 | 30 | 35 | 35 | 23 | 35 | 39 |
| Biotite | P | 6 | 4 | 6 | 5 | 8 | P | P | ..... | | 4 | ..... | | | 8 | ..... | | | P |
| Muscovite | 4 | P | P | P | 3 | P | 6 | 4 | 6 | 4 | P | 4 | 15 | 10 | P | 10 | P | 12 | 13 |
| **Semiquantitative spectrographic analyses (parts per million)** [4] | | | | | | | | | | | | | | | | | | | |
| B | 0 | 0 | 10 | 15 | 0 | 0 | 0 | 0 | 0 | 0 | 0 | 0 | 0 | 0 | 0 | 0 | 0 | 0 | 0 |
| Ba | 200 | 150 | 300 | 700 | 300 | 500 | 1,500 | 700 | 200 | 1,000 | 300 | 500 | 1,500 | 2,000 | 1,000 | 1,500 | 1,000 | 1,500 | 1,500 |
| Be | 3 | 3 | 5 | 3 | 3 | 5 | 2 | 3 | 2 | 3 | 3 | 2 | 3 | 2 | 3 | 2 | 1 | 2 | 2 |
| Ce | 0 | 0 | 0 | 0 | 100 | 100 | 0 | 0 | 100 | 0 | 200 | 0 | 200 | 0 | 0 | 0 | 0 | 0 | 0 |
| Co | 0 | 0 | 0 | 0 | 0 | 5 | 5 | 0 | 0 | 2 | 0 | 0 | 5 | 7 | 3 | 5 | 0 | 5 | 7 |
| Cr | 10 | 3 | 50 | 70 | 3 | 10 | 10 | 7 | 5 | 7 | 5 | 7 | 10 | 7 | 7 | 10 | 10 | 10 | 10 |
| Cu | 2 | 2 | 2 | 2 | 10 | 5 | 20 | 20 | 5 | 10 | 7 | 7 | 5 | 20 | 30 | 10 | 2 | 30 | 20 |
| Ga | 30 | 30 | 30 | 30 | 20 | 30 | 30 | 30 | 20 | 30 | 20 | 20 | 30 | 30 | 30 | 30 | 15 | 30 | 30 |
| La | 0 | 0 | 0 | 0 | 0 | 0 | 50 | 50 | 0 | 0 | 150 | 0 | 100 | 50 | 50 | 50 | 0 | 70 | 70 |
| Nb | 10 | 10 | 10 | 15 | 10 | 7 | 15 | 20 | 7 | 10 | 7 | 0 | 15 | 15 | 10 | 10 | 0 | 10 | 15 |
| Nd | 0 | 0 | 0 | 0 | 0 | 0 | 0 | 0 | 0 | 0 | 150 | 0 | 0 | 0 | 0 | 0 | 0 | 0 | 0 |
| Ni | 0 | 0 | 15 | 20 | 0 | 0 | 5 | 3 | 0 | 3 | 0 | 3 | 3 | 3 | 3 | 3 | 0 | 5 | 3 |
| Pb | 70 | 70 | 70 | 70 | 50 | 50 | 50 | 50 | 20 | 50 | 70 | 70 | 50 | 50 | 50 | 50 | 20 | 50 | 30 |
| Sc | 5 | 5 | 0 | 3 | 5 | 7 | 7 | 7 | 5 | 5 | 7 | 0 | 5 | 5 | 7 | 3 | 0 | 5 | 7 |
| Sr | 100 | 100 | 200 | 300 | 300 | 500 | 500 | 300 | 200 | 500 | 500 | 200 | 700 | 700 | 500 | 700 | 500 | 700 | 1,000 |
| V | 7 | 7 | 10 | 30 | 15 | 20 | 70 | 20 | 20 | 50 | 20 | 15 | 70 | 70 | 50 | 50 | 50 | 70 | 100 |
| Y | 0 | 15 | 10 | 0 | 10 | 15 | 20 | 20 | 20 | 15 | 30 | 10 | 30 | 20 | 10 | 15 | 15 | 15 | 20 |
| Yb | 0 | 1.5 | 1.5 | 0 | 1 | 1 | 2 | 2 | 2 | 2 | 3 | 1 | 2 | 2 | 1 | 1.5 | 1.5 | 1.5 | 2 |
| Zr | 70 | 100 | 100 | 100 | 70 | 200 | 200 | 150 | 100 | 150 | 150 | 70 | 200 | 300 | 300 | 200 | 200 | 300 | 300 |

[1] Analyses by Paul Elmore, Samuel Botts, Gillison Chloe, Lowell Artis, and H. Smith, using methods similar to those developed by Shapiro and Brannock (1956).

[2] Determinations by Vertie C. Smith. ....., no data.

[3] Based mainly on calibrated X-ray diffraction patterns. ....., not found; P, present, probably less than 2 percent. Muscovite figures for brecciated samples (103–115) include any chlorite present.

[4] Analyses by Chris Heropoulos and R. E. Mays. 0, below limit of detection. Table 4 lists the 45 minor elements sought, together with limits of detection. General limitations of method are given in text.

Modal analyses determined in this manner are not likely to total exactly 100 weight percent, except where there are compensating errors. Therefore, the modal analyses in tables 5–7 are presented as partial analyses, including only the essential (as opposed to accessory) minerals present in the rock.

Taken as a whole, the major- and minor-element analyses listed in tables 5–7 define chemical gradients that appear to be related to type of country rock, whatever way we interpret the trends. The areal distribution of CaO values is considered first. Then, by comparing other chemical variables with CaO, we are able to show indirectly the relation between country rock and the other variables. The only two xenoliths of Pioche Shale (samples 72 and 85) recovered from the Young Canyon area are somewhat arbitrarily included in table 5 with the rocks of the Snake Creek-Williams Canyon area, where such xenoliths are very common.

Earlier we noted that influence of host-rock type on the nature of the intrusive is most apparent in the Snake Creek-Williams Canyon area. Thus, isopleths based on analytical results for rocks whose positions are indicated on plate 1 show CaO values increasing from less than 1.0 percent where the intrusive is in contact with quartzite near the crest of the range to more than 4.0 percent where the eastern part of the intrusive is in contact with limestone and shale.

We cannot be sure where to project the western edge (Pioche Shale) of the main syncline across the igneous outcrop; but were it not for the intrusive, the Pioche Shale probably would crop out on the present erosion surface somewhere between or near the 2.0- and 2.5-percent-CaO contours on plate 1. This deduction is based partly on the fact that Pioche Shale abuts the intrusive in this position and partly on the fact that the intrusive is almost devoid of (Pioche Shale) xenoliths west of the 2.0-percent-CaO contour, whereas these xenoliths are common to abundant east of this contour. Whatever the structural interpretation, it is clear that lower CaO contents in the granitoid rock are near the quartzite country rock, and higher CaO contents are near the shale and limestone.

In the extreme western part of this same continuous igneous outcrop, where granitoid rock is in contact with the Osceola Argillite, CaO content again increases and is 2.0 percent or more locally (samples 27, 28, 42, 59). However, because most of the intrusive in this area is badly altered, no attempt was made to contour CaO values there.

In the Pole Canyon-Can Young Canyon area, nine analyses of the main (not aplitic) intrusive phase show CaO values ranging from 0.87 percent to 1.8 percent (table 6). As noted earlier, we interpret the distinctive nature of the granitoid rock in this area to result from assimilation of the Osceola Argillite. The relatively minor differences in the nine analyses probably are due to compositional differences within the argillite, which are shown in table 1.

In the Young Canyon-Kious Basin area, 19 analyses show CaO values ranging from 0.68 to 2.9 percent (table 7). Lowest CaO contents are found in the undeformed part of the intrusive, where the host rock is quartzite. Higher CaO contents are found where the host rock is limestone, but this is the same part of the igneous body that has been brecciated and mylonitized by thrust faulting. The cataclasis has obscured the original mineralogy of the granitoid rock and to some extent, probably, the original chemistry, too; and we have not tried to contour CaO values in this area.

## CHEMISTRY

### MAJOR ELEMENTS

We will first describe the relations of other major oxides to CaO in rocks from the three areas discussed above. The eight diagrams in figure 3 (based on tables 5–7) support the field evidence and indicate that these areas do indeed represent three separate situations. Moreover, these plots show that each of the other major oxides varies rather systematically one way or another with CaO, particularly for rocks from the Snake Creek-Williams Canyon area, where host-rock control of CaO content of the granitoid rock is best defined (pl. 1). In order to place the Snake Creek-Williams Canyon area in a more familiar frame of reference, we drew a line through the center of each of the "fields" shown for this area in figure 3 and brought these lines together in figure 4, a more conventional (Harker) diagram where other oxides are plotted against $SiO_2$. For comparison, figure 4 also shows Daly's average andesite-dacite-rhyolite as shown by Barth (1962, p. 164). Except for the $Al_2O_3$ plot, the two sets of lines in figure 4 practically coincide; assimilation has produced a rock series very similar to the normal differentiation sequence from andesite to rhyolite. A plot of powder density versus CaO (fig. 5) also shows the relation expectable in a normal differentiation sequence. These major-element oxides are discussed further in the sections on mineralogy and petrology.

### MINOR ELEMENTS

Most of the 22 minor elements listed in table 5 also vary rather systematically with CaO. The distribution of some of these minor elements has already been cited (Lee and Bastron, 1967) as evidence that the chemical processes once operative in these rocks might be similar to processes that contribute to the formation of alkalic

rocks and carbonatites. The much more complete data in table 5 are consistent with the earlier results.

Predominance of the most basic (lightest) rare-earth elements in alkalic rocks was noticed first by Goldschmidt, Hauptmann, and Peters (1933) and later by Haberlandt (1947). Murata, Rose, Carron, and Glass (1957) emphasized that cerium-earth minerals from both alkalic rocks and carbonatites are rich in the most basic rare earths. Figure 6 shows the trend toward increasing La : Y ratio—that is, toward a more basic rare-earth assemblage—with increasing CaO content of the rocks (table 5). This is contrary to what is expected in a normal sequence of differentiated rocks. In such a sequence, Y is enriched compared with La in the more basic rocks because the ionic radius of $Y^{3+}$ is closer to that of $Ca^{2+}$ than is that of $La^{3+}$. (See Rankama and Sahama, 1950, p. 527–528.)

Pecora (1956, p. 1544) emphasized that the rare earths and Zr, P, Ti, Ba, Sr, and Nb often are found in alkalic rocks and carbonatites in amounts that well exceed average abundance figures for igneous rocks. Let us consider the relationship between CaO and these rare constituents. The concentrations of the spectrographically determinable rare-earth elements—La, Ce, Y, and Yb—presented in table 5 indicate covariation of total rare earths and CaO. Earlier studies (Lee and Dodge, 1964; Lee and others, 1968) found that weight percentages of zircon and CaO vary directly in these rocks. The same trend (for Zr) is suggested by figure 6*B*. The striking covariance between CaO and both $TiO_2$ and $P_2O_5$ already has been illustrated in figure 3*G* and *H*. Although the trend for Ba is not as well defined, figure 6*C* suggests its sympathetic increase with CaO. This also is contrary to what one would expect in differentiated rocks, where barium increases toward the granitic end of the sequence. (See Rankama and Sahama, 1950, p. 475.)

In a comprehensive study, Turekian and Kulp (1956) found that for granitic rocks there is an increase in strontium content with an increase in calcium, not only for samples from a single batholith, but also for universal sampling. The same relation is evident in our samples (fig. 6*D*). A scatter diagram of Nb versus CaO for these rocks shows, if anything, an antipathetic relationship between the two. This departure from the trend expectable in alkalic rocks and carbonatites possibly resulted from contribution of niobium to the calcium-poor granitoid rocks by the quartzite country rock, as outlined by Lee and Bastron (1967).

Another element that may be concentrated in alkalic rocks and carbonatites is F (Pecora, 1956, p. 1544). This element was determined for 43 of the rocks listed in tables 5 and 6. Although amounts found are not large, F clearly tends to increase with CaO in these rocks (fig. 7). This relationship is especially evident when we consider only those rocks from the Snake Creek-Williams Canyon area. On page 37, we comment further on the general increase in volatiles with increasing CaO content of these hybrid rocks.

## CONCLUSIONS ON CHEMISTRY OF GRANITOID ROCKS

In addition to the relations discussed above, it is evident from tables 5, 6, and 7 that a number of other elements listed tend to vary either directly or inversely with CaO content of these rocks. Thus, Ni, Cr, and Co each show positive covariance with CaO, while Be and Pb show the opposite trend. In order to summarize the relations of the various other elements and oxides to each other as well as to CaO, we present in table 8 product moment correlation coefficiencies based on logarithmic concentrations to supplement relations already described graphically. Table 8 is based only on data from the Snake Creek-Williams Cayon area, where the composition of the intrusive is most obviously related to the chemistry of the host rock. Table 8 touches on problems of petrogenesis beyond the scope of this report. For example, $K_2O$ shows positive correlations only with MnO, Be, Nb, Pb, and Yb—components that are notably concentrated in fluorine-rich alkali rhyolites (Shawe, 1966).

## MINERALOGY

The chemical trends described for these granitoid rocks are attended by systematic changes in mineralogy. The influence of calcium content of granitic rocks on the species of heavy accessory minerals developed was outlined by Lee and Dodge (1964) and discussed in more detail by Lee and Bastron (1967), Lee, Stern, Mays, and Van Loenen (1968), and Lee, Mays, Van Loenen, and Rose (1969). These writers showed that a typical calcium-rich rock (CaO>1.8 percent) from the area has relatively large amounts of allanite, apatite, sphene, epidote, magnetite, and zircon. In a calcium-poor rock (CaO<0.7 percent), on the other hand, these minerals either are absent or are present in very sparse amounts, and monazite, ilmenite, and garnet are found. The latter suite also contains a few scattered grains of blue anatase.

Amounts of essential minerals in these granitoid rocks also are in accord with the chemical trends described. Relations are most clearly defined in the Snake Creek-Williams Canyon area where, as already emphasized, influence of host rock on chemistry of the intrusive also is most clearly shown. Thus, most of this section on mineralogy applies specifically to the Snake Creek-Williams Canyon area, and it is convenient to include

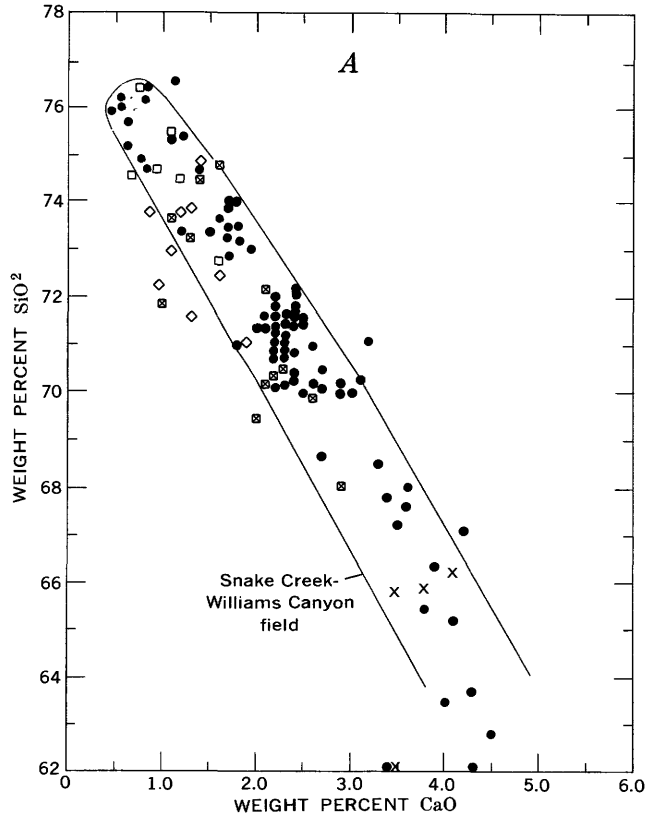
A
WEIGHT PERCENT $SiO^2$
WEIGHT PERCENT CaO
Snake Creek-
Williams Canyon
field

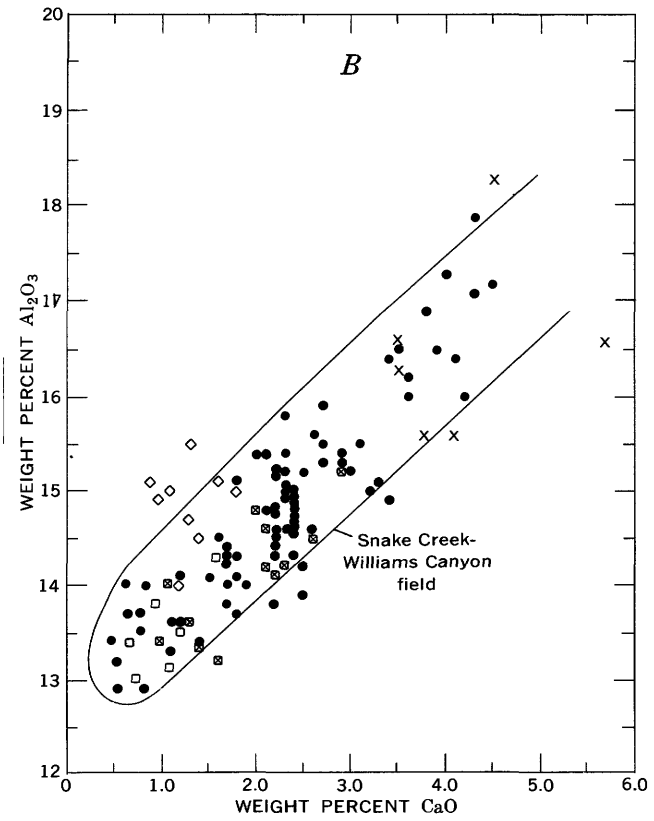
B
WEIGHT PERCENT $Al_2O_3$
WEIGHT PERCENT CaO
Snake Creek-
Williams Canyon
field

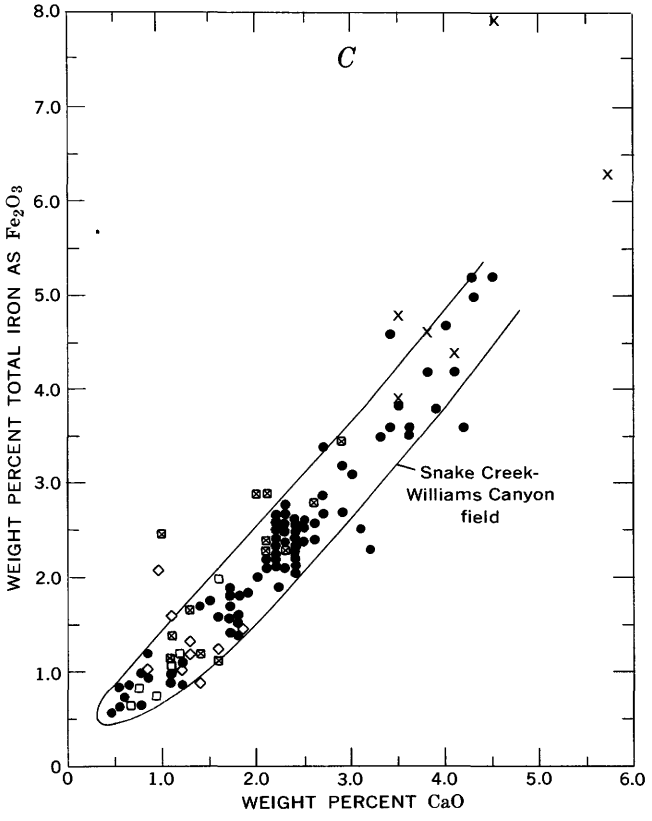
C
WEIGHT PERCENT TOTAL IRON AS $Fe_2O_3$
WEIGHT PERCENT CaO
Snake Creek-
Williams Canyon
field

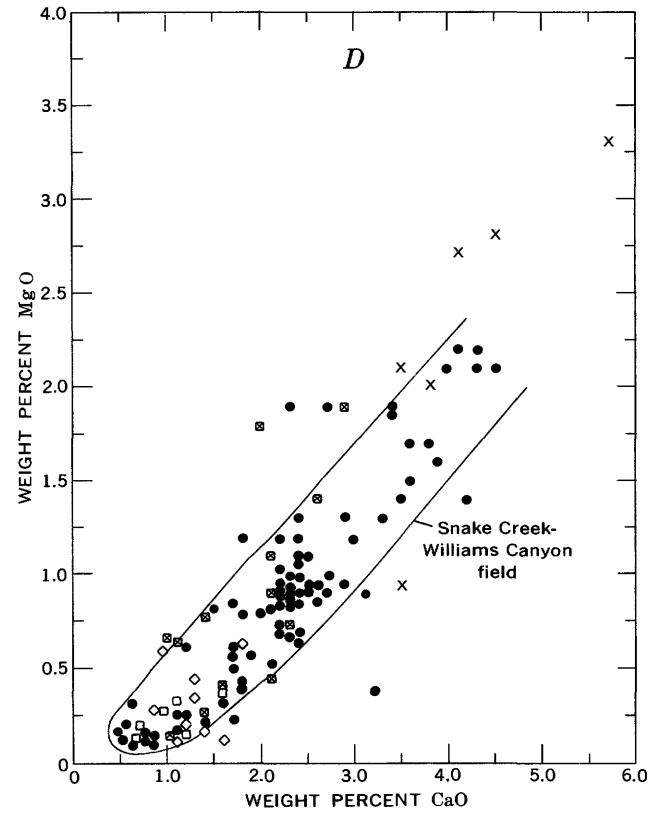
D
WEIGHT PERCENT MgO
WEIGHT PERCENT CaO
Snake Creek-
Williams Canyon
field

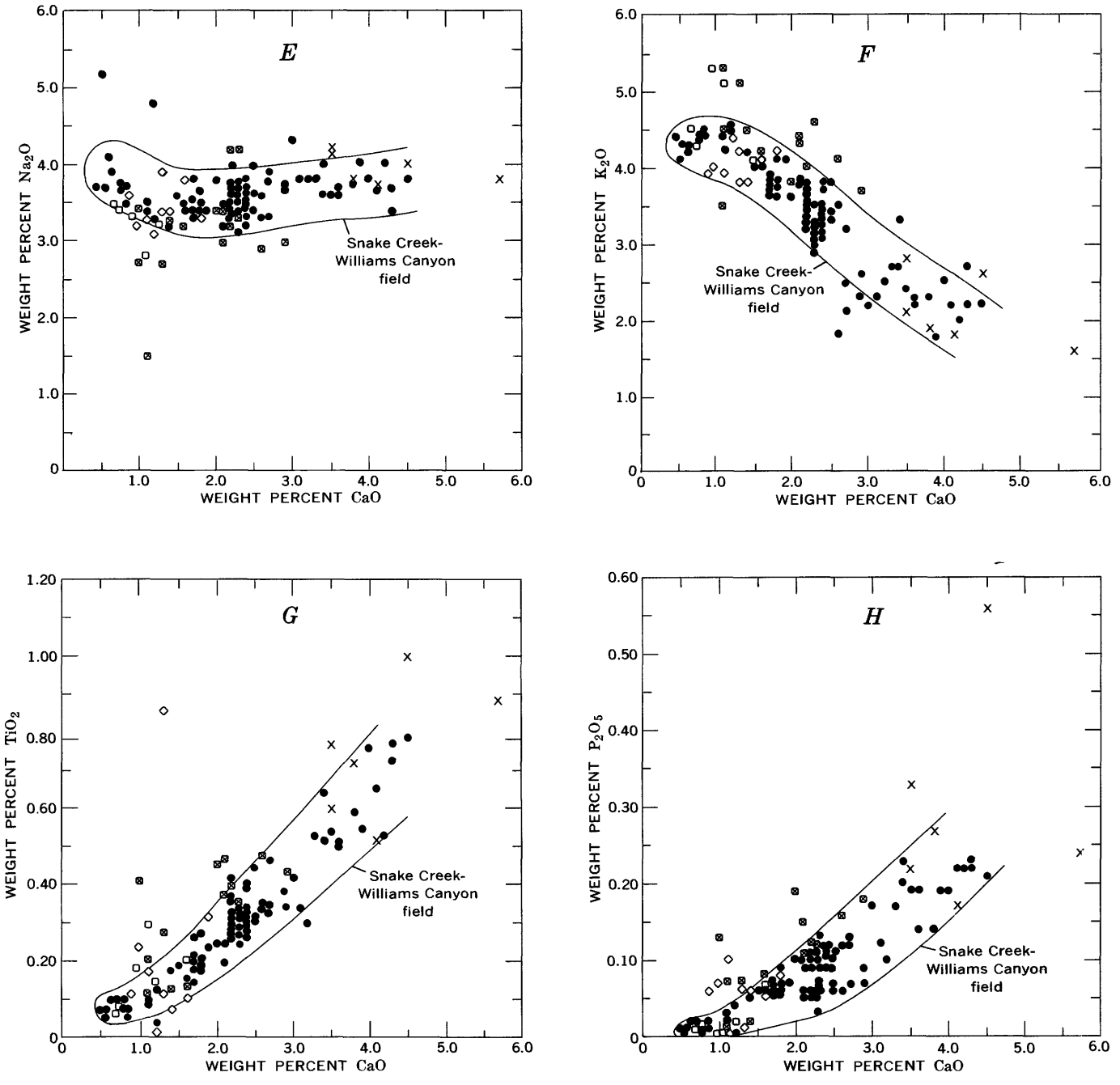


FIGURE 3.—Relation between CaO content and contents of other major-element oxides in granitoid rocks. Symbols: ●, sample from Snake Creek-Williams Canyon area; ◇, sample from Pole Canyon-Can Young Canyon area; ×, xenolith; □, sample from undeformed rocks, Young Canyon-Kious Basin area; ⊠, sample from deformed rocks, Young Canyon-Kious Basin area. *A*, $SiO_2$; *B*, $Al_2O_3$; *C*, total iron (as $Fe_2O_3$); *D*, MgO; *E*, $Na_2O$; *F*, $K_2O$; *G*, $TiO_2$; *H*, $P_2O_5$.

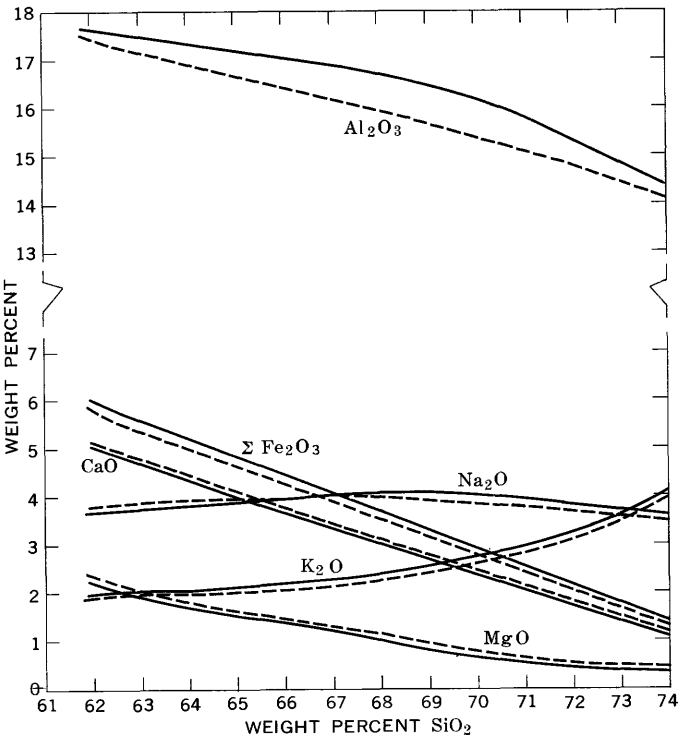


FIGURE 4.—Variation diagram comparing Daly's average andesite-dacite-rhyolite (solid lines; Barth, 1962, p. 164) with granitoid rocks of the Snake Creek-Williams Canyon area (dashed lines; derivation explained in text).

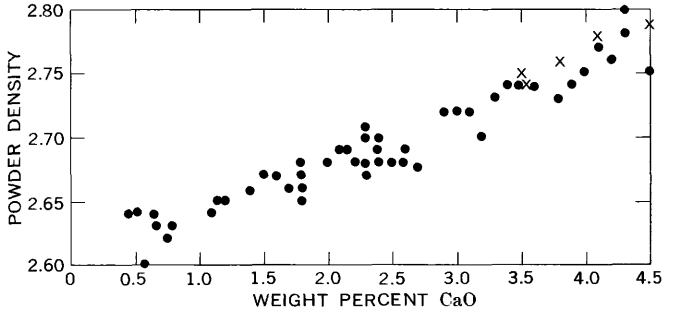


FIGURE 5.—Relation between CaO content and powder density in granitoid rocks of the Snake Creek-Williams Canyon area (table 5). ●, sample from main intrusive phase; ×, xenolith.

some of the similar information on the Pole Canyon-Can Young Canyon and the Young Canyon-Kious Basin areas in the discussion of their petrology.

Amounts of modal quartz range for the most part from 20 to 40 weight percent of the rock and tend to decrease as CaO content of the rock increases (fig. 8*A*). One of the xenoliths analyzed contains 4.5 percent CaO and only 12 percent modal quartz.

All the potassium-feldspar present is maximum microcline. (This applies to all the intrusive rocks included in this study.) The amount of modal microcline is inversely related to CaO content of the rock (table 5; fig. 8*B*), and the most calcium-rich rocks are practically devoid of this mineral. The trend for biotite is the opposite of that for microcline (fig. 8*C*). Five of the most calcium-poor rocks contain so little biotite that we were unable to detect any peaks for the mineral in our diffractometer work. However, inasmuch as thin sections show small amounts of biotite, we arbitrarily set the amount at 0.5 percent for each of the five rocks (fig. 8*C*). Some samples contain more than 25 percent biotite. In an extreme case, a xenolith is about one-third biotite. Because muscovite is hardly more than a minor accessory mineral in any of the Snake Creek-Williams Canyon specimens (table 5), it is clear from this and the preceding paragraph that the potassium economy of these rocks consists simply of a regular shift of that element from microcline to biotite as CaO content of the rock increases.

Modal plagioclase ranges from slightly less than 35 percent to approximately 50 percent and increases with CaO content of the rock (fig. 8*D*). The plagioclase also shows a range of An content (fig. 9) much as we would expect if these were normally differentiated rocks instead of a hybrid sequence.

The mineralogy of these rocks can be summarized diagrammatically. General relations between amounts of CaO and accessory minerals in rocks from the Snake Creek-Williams Canyon area are shown in figure 10, which is based upon results of systematic mineral-separation work on about 30 rock samples. The total mineralogy of these hybrid rocks is outlined in figure 11, which clearly has much in common with similar diagrams published elsewhere, to illustrate the variations and relative proportions of minerals composing major rock types as they result from magmatic differentiation. (See Pirsson, 1947, p. 117.) Information from several of the preceding diagrams is used in figure 12 to outline the calcium economy of these rocks. As CaO of the rock rises above 2.0 percent, about 40 percent of the increase is used to form apatite, allanite, epidote, and sphene. Prince (1943, p. 1) stated that "accessory minerals usually represent a small proportion of the rock concerned, yet this is no criterion of their importance."

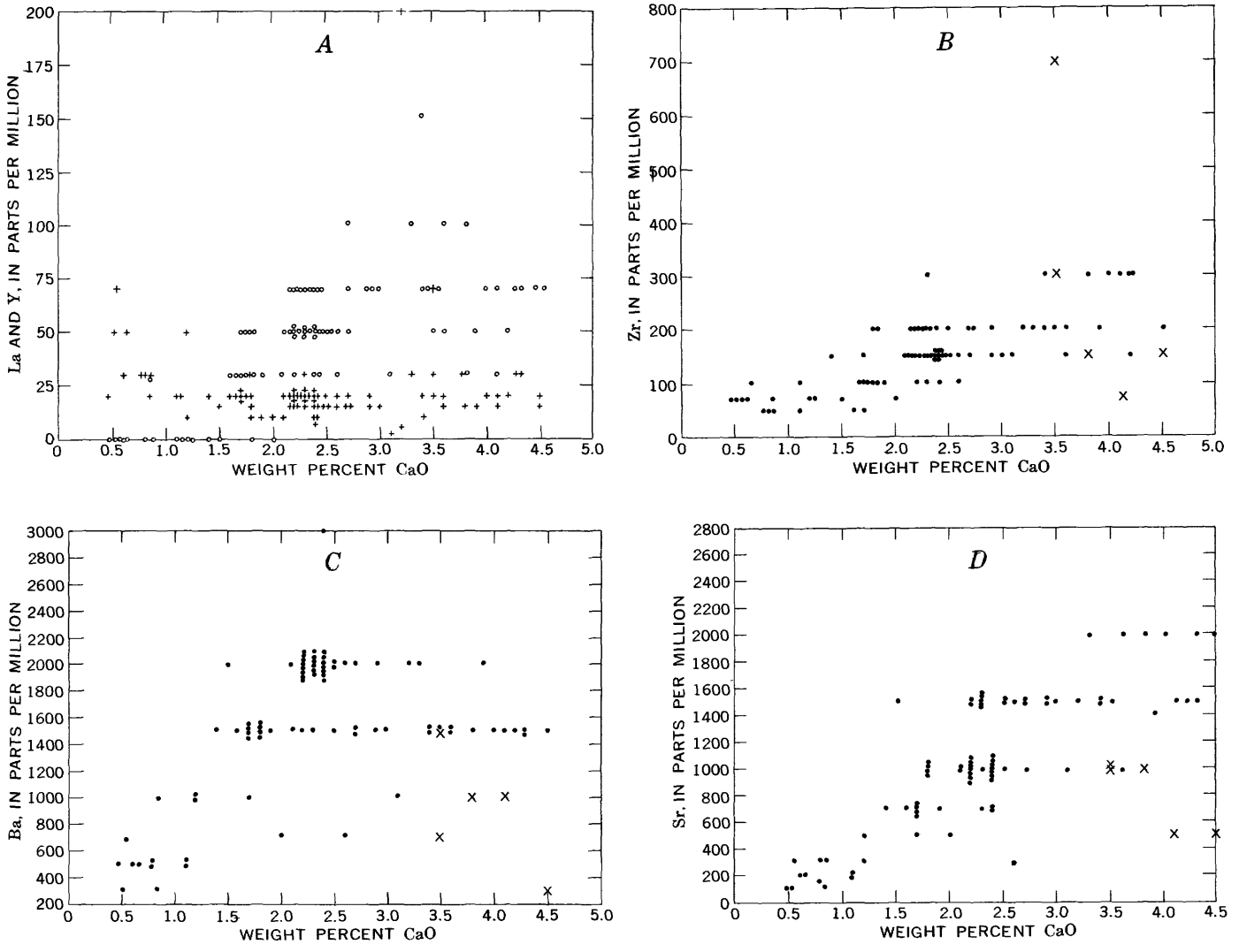


FIGURE 6.—Relation between CaO content and La, Y, Zr, Ba, and Sr contents in granitoid rocks of the Snake Creek-Williams Canyon area. ○, La content; +, Y content; ●, sample from main intrusive phase; ×, xenolith.

TABLE 8.—*Correlation coefficients for 87 granitoid rocks of the Snake Creek-Williams Canyon area (table 5)*

| | $SiO_2$ | $Al_2O_3$ | $Fe_2O_3$ | FeO | MgO* | CaO | $Na_2O$ | $K_2O$ | $H_2O(-)$ | $H_2O(+)$ | $TiO_2$ | $P_2O_5$ | MnO | Zr | Ba | Be | Cr | Ga | Nb | Ni | Pb | Sc | Sr | V | Yb | La | Co |
|---|---|---|---|---|---|---|---|---|---|---|---|---|---|---|---|---|---|---|---|---|---|---|---|---|---|---|---|
| $SiO_2$ | | −0.919 | −0.779 | −0.921 | −0.895 | −0.936 | −0.117 | 0.801 | −0.266 | −0.629 | −0.766 | −0.887 | −0.030 | −0.814 | −0.389 | 0.320 | −0.542 | −0.157 | 0.430 | −0.688 | 0.530 | −0.712 | −0.805 | −0.889 | 0.265 | −0.652 | 0.913 |
| $Al_2O_3$ | | | .740 | .845 | .794 | .875 | −.005 | −.796 | .215 | .549 | .688 | .805 | −.001 | .740 | .354 | −.284 | .580 | .157 | −.416 | .668 | −.445 | .702 | .746 | .815 | −.275 | .572 | .885 |
| $Fe_2O_3$ | | | | .549 | .723 | .802 | −.005 | −.726 | .321 | .355 | .567 | .729 | −.009 | .688 | .529 | −.385 | .595 | .241 | −.351 | .636 | −.460 | .641 | .717 | .767 | −.273 | .555 | .767 |
| FeO | | | | | .843 | .874 | −.020 | −.741 | .216 | .590 | .724 | .835 | −.096 | .751 | .283 | −.249 | .457 | .140 | −.418 | .592 | −.490 | .668 | .751 | .848 | −.257 | .596 | .849 |
| MgO | | | | | | .855 | .009 | −.771 | .284 | .508 | .705 | .803 | −.010 | .756 | .354 | −.321 | .466 | .105 | −.400 | .572 | −.488 | .630 | .761 | .844 | −.282 | .525 | .855 |
| CaO | | | | | | | .034 | −.887 | .285 | .505 | .728 | .894 | −.035 | .754 | .471 | −.403 | .503 | .129 | −.527 | .588 | −.546 | .682 | .821 | .887 | −.368 | .659 | .894 |
| $Na_2O$ | | | | | | | | −.159 | −.090 | −.081 | −.045 | −.028 | −.031 | .039 | −.085 | −.069 | −.032 | .111 | .172 | .058 | −.061 | .014 | .103 | .026 | .176 | .059 | −.446 |
| $K_2O$ | | | | | | | | | −.176 | −.489 | −.584 | −.742 | .155 | −.658 | −.425 | .456 | −.427 | −.107 | .463 | −.491 | .484 | −.581 | −.806 | −.772 | .336 | −.634 | −.817 |
| $H_2O(-)$ | | | | | | | | | | −.073 | .233 | .248 | .030 | .236 | .263 | −.063 | .231 | .024 | −.140 | .169 | −.107 | .280 | .280 | .322 | −.099 | .145 | .254 |
| $H_2O(+)$ | | | | | | | | | | | .376 | .696 | −.271 | .493 | .221 | −.320 | .231 | −.227 | −.301 | .415 | −.379 | .259 | .490 | .364 | −.129 | .528 | .615 |
| $TiO_2$ | | | | | | | | | | | | .606 | .420 | .644 | .333 | −.135 | .490 | .208 | −.301 | .548 | −.403 | .596 | .620 | .744 | −.291 | .489 | .704 |
| $P_2O_5$ | | | | | | | | | | | | | .138 | .662 | .309 | −.354 | .318 | .082 | −.471 | .495 | −.539 | .629 | .638 | .823 | −.266 | .568 | .806 |
| MnO | | | | | | | | | | | | | | −.029 | −.130 | .214 | −.111 | .137 | .052 | −.058 | −.177 | .100 | −.196 | .069 | −.067 | −.099 | −.059 |
| Zr | | | | | | | | | | | | | | | .473 | −.302 | .559 | .235 | −.329 | .634 | −.417 | .619 | .761 | .741 | −.278 | .660 | .781 |
| Ba | | | | | | | | | | | | | | | | −.424 | .287 | −.064 | −.521 | .253 | −.296 | .174 | .618 | .333 | −.519 | .482 | .403 |
| Be | | | | | | | | | | | | | | | | | −.003 | .293 | .267 | −.059 | .434 | −.052 | −.433 | −.269 | .283 | −.333 | −.376 |
| Cr | | | | | | | | | | | | | | | | | | .479 | −.051 | .744 | −.131 | .642 | .585 | .632 | −.012 | .338 | .556 |
| Ga | | | | | | | | | | | | | | | | | | | .182 | .423 | .116 | .464 | .180 | .374 | .141 | −.245 | .186 |
| Nb | | | | | | | | | | | | | | | | | | | | −.160 | .353 | −.035 | −.417 | −.307 | .723 | −.386 | −.382 |
| Ni | | | | | | | | | | | | | | | | | | | | | −.209 | .571 | .585 | .649 | −.094 | .429 | .660 |
| Pb | | | | | | | | | | | | | | | | | | | | | | −.266 | −.409 | −.436 | .364 | −.437 | −.506 |
| Sc | | | | | | | | | | | | | | | | | | | | | | | .655 | .811 | .067 | .448 | .718 |
| Sr | | | | | | | | | | | | | | | | | | | | | | | | .811 | −.333 | .694 | .816 |
| V | | | | | | | | | | | | | | | | | | | | | | | | | −.175 | .590 | .843 |
| Yb | | | | | | | | | | | | | | | | | | | | | | | | | | −.336 | −.214 |
| La | | | | | | | | | | | | | | | | | | | | | | | | | | | .647 |
| Co | | | | | | | | | | | | | | | | | | | | | | | | | | | |

NOTE.—For calculation of correlation coefficients, 0.005 percent was arbitrarily used for MgO, MnO, and $P_2O_5$ where values listed in table 5 are 0.00 percent. Where amount of a minor element in table 5 is below the limit of detection (table 4), the following figures (in parts per million) were used: Yb, 0.5; Co, Nb, Ni, and Sc, 1; V, 5; La and Pb, 10.

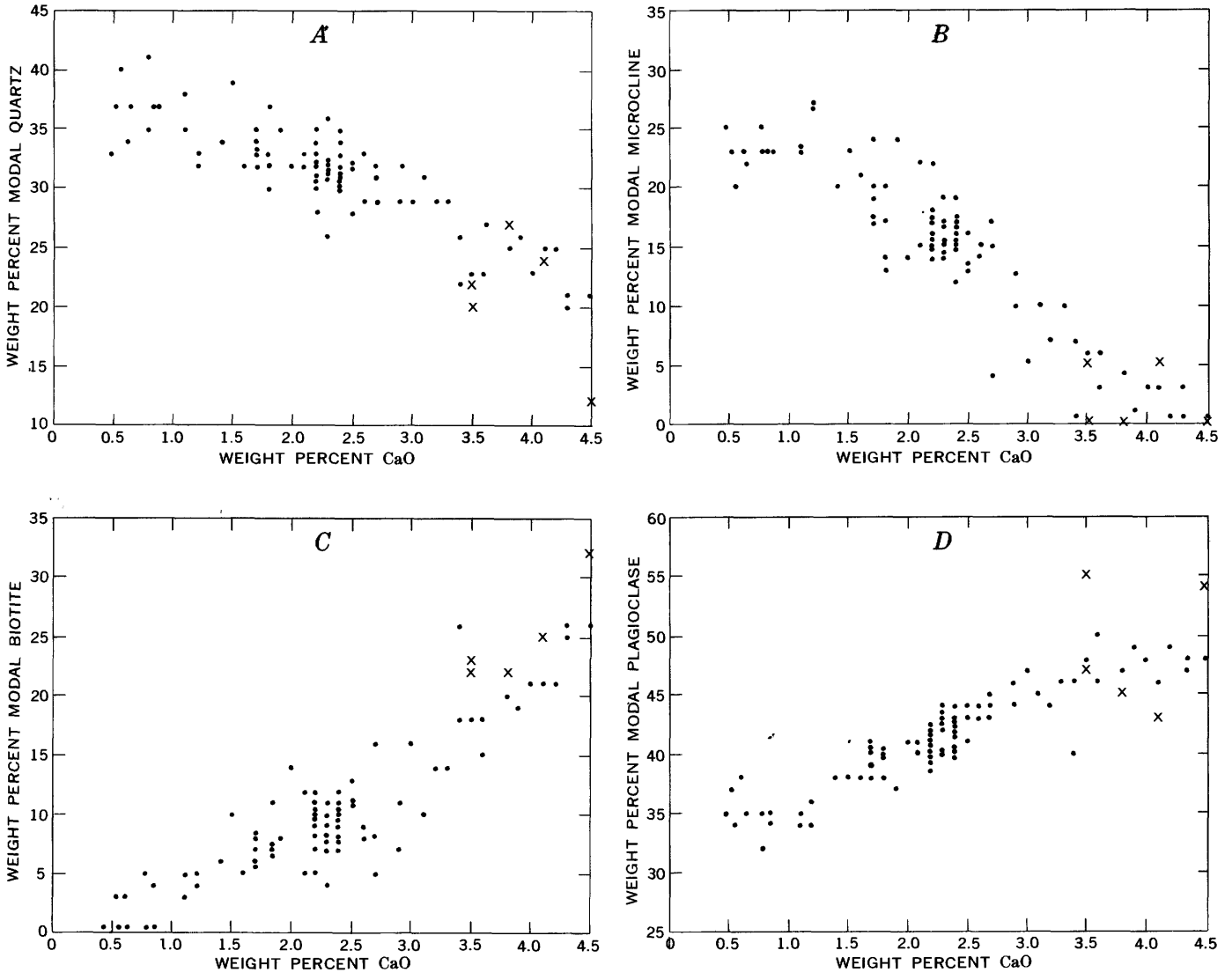


FIGURE 8.—Relation between CaO content and contents of modal quartz, microcline, biotite, and plagioclase in granitoid rocks of the Snake Creek-Williams Canyon area. ●, sample from main intrusive phase; ×, xenolith. *A*, modal quartz; *B*, modal microcline; *C*, modal biotie; *D*, modal plagioclase.

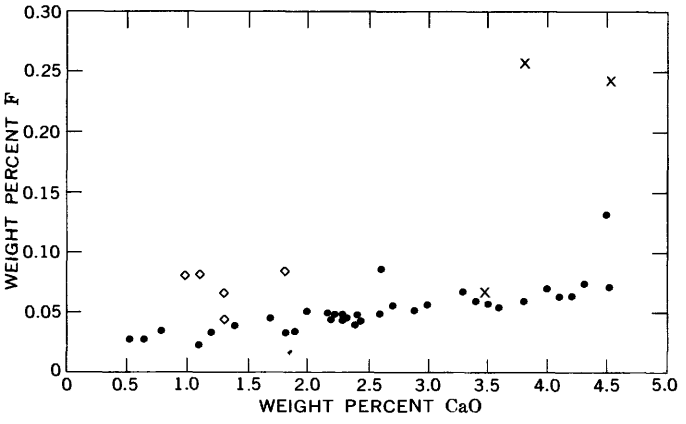


FIGURE 7.—Relation between CaO content and F content in selected granitoid rocks. ●, sample from Snake Creek-Williams Canyon area (table 5; ×, xenolith (table 5); ◇, sample from Pole Canyon-Can Young Canyon area (table 6).

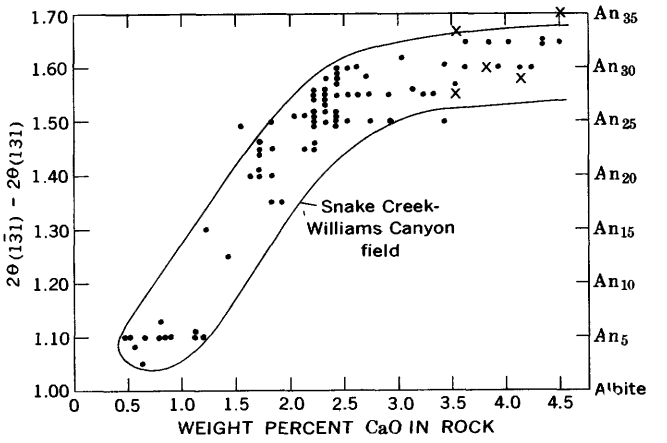


FIGURE 9.—Relation between CaO content of rock and angular difference between $2\theta_{(1\bar{3}1)}$ and $2\theta_{(131)}$ X-ray reflections of constituent plagioclase, Snake Creek-Williams Canyon area. Equivalent low-temperature plagioclase compositions (right ordinate) from Tuttle and Bowen (1958). ●, sample from main intrusive phase; ×, xenolith.

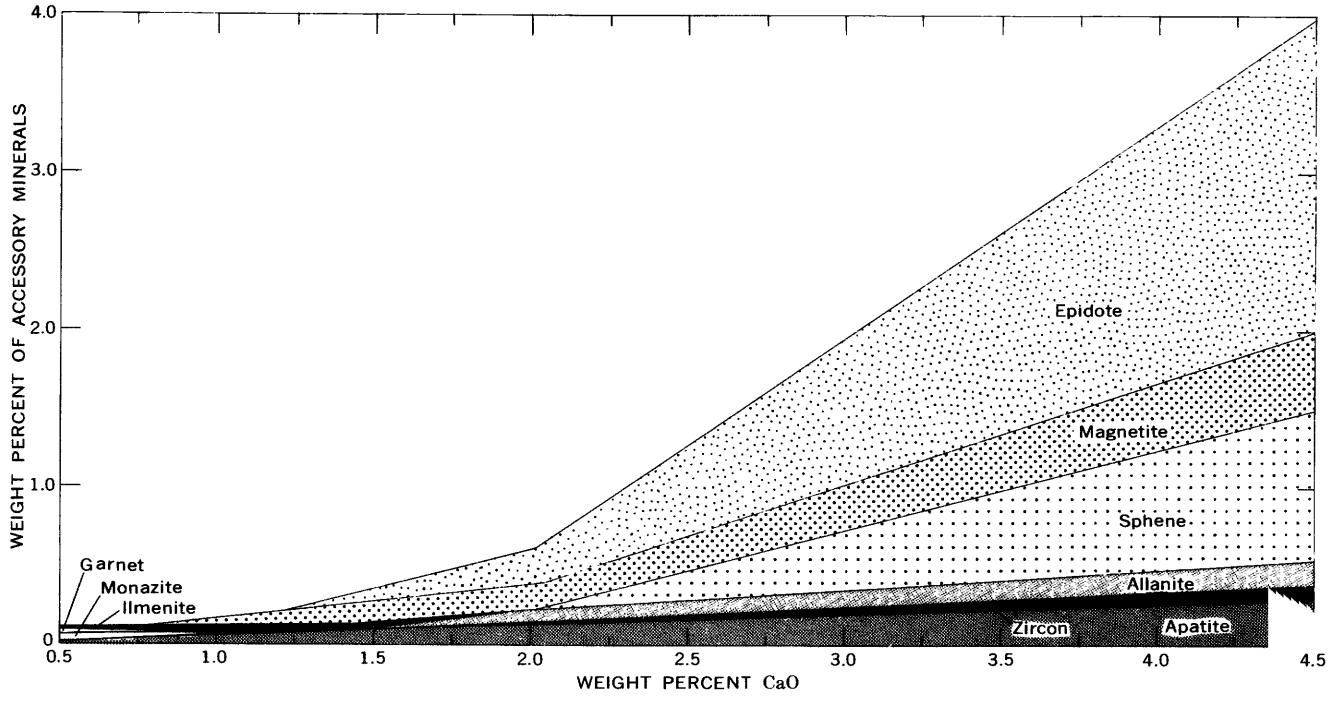


FIGURE 10.—General relations between CaO content and accessory mineral contents for granitoid rocks of the Snake Creek-Williams Canyon area.

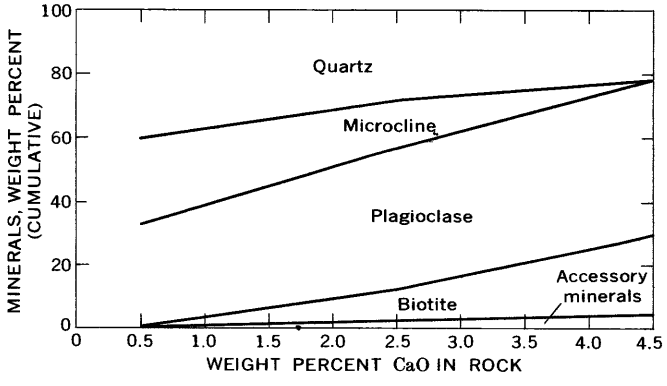


FIGURE 11.—General relations between CaO content and mineralogy, for granitoid rocks of the Snake Creek-Williams Canyon area.

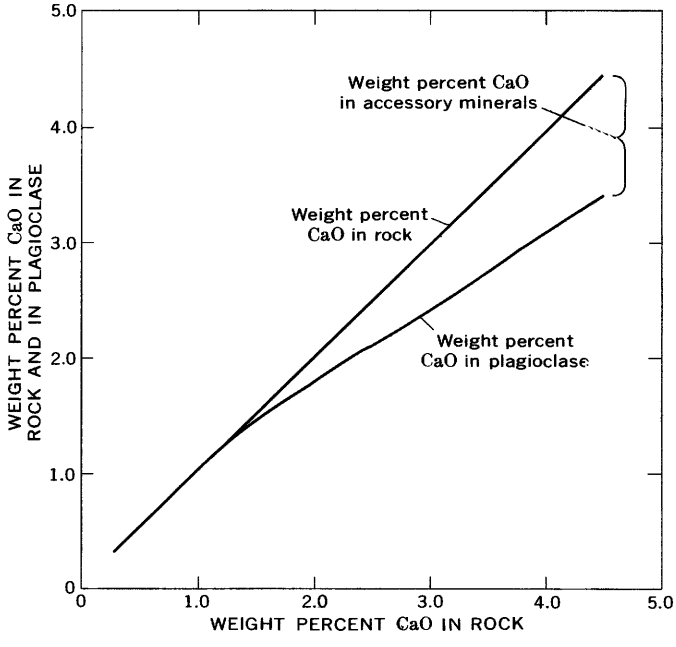


FIGURE 12.—Distribution of CaO in granitoid rocks of the Snake Creek-Williams Canyon area. As the CaO content rises above 2.0 percent, about 40 percent of the increase contributes to the formation of accessory minerals.

# PETROGRAPHY AND PETROLOGY OF THE GRANITOID ROCKS

## SNAKE CREEK-WILLIAMS CANYON AREA

### PETROGRAPHY

Petrographically, as well as chemically and mineralogically, there is nothing especially remarkable about any one sample from the Snake Creek-Williams Canyon area. It is the areal trends that are of interest. The appearance of a lime-poor rock in thin section is strikingly different from that of a lime-rich rock, but there are all gradations between the two. We will describe five representative rocks—three samples (6, 34, 79) of the main intrusive phase and two xenoliths (81, 71). Abundance figures used in these descriptions are from table 5, and statements on plagioclase compositions are based on the information in figure 9 and on preliminary analytical data for plagioclase.

Sample 6 contains 0.78 percent CaO. In hand specimen, the rock is rather coarse grained, with crystals of microcline and quartz commonly as much as 1 cm (centimeter) across. Few plagioclase crystals are this large. There is a complete size gradation between these larger mineral grains and the smaller grains that are less than 1 mm across. The freshly broken rock has a dense appearance because it is 95 percent quartz and feldspar and displays no directional element. The rather large and abundant quartz grains are smoky on a fresh surface. The weathered rock is much lighter in color than the fresh because the smoky nature of the quartz is obscured and the feldspars contain more clay minerals where weathered.

Sample 6 is hypidiomorphic granular. The plagioclase tends to be euhedral, although most of the microcline is subhedral and quartz is anhedral. This microcline is perthitic and covered with alteration products, giving the mineral a milky appearance in reflected light. The quartz is strained, but the intensity of this varies from grain to grain, and a much strained grain may be near one almost unstrained. The plagioclase is near $An_5$. Polysynthetic twinning is well developed. Some of the plagioclase is zoned, but the zoning is typically more gradational than sharp and steplike. A few grains are coated with clear albite. The sparse biotite is pleochroic from buff to reddish brown. The minor amounts of garnet and ilmenite present are associated with the biotite, which also contains tiny grains of a mineral that is almost certainly monazite. Each grain is surrounded by a halo that is dark but not pleochroic. Some muscovite is secondary after biotite.

Sample 34 has a CaO content of 2.2 percent. In grain size it is much the same as sample 6: on a polished and stained surface most of the larger grains are, however, seen to be plagioclase. Because of its higher biotite content and the fact that the quartz crystals do not appear as smoky, this rock seems less dense in hand specimen. The rock is darker where weathered than where fresh.

Sample 34 is hypidiomorphic granular. The plagioclase is euhedral to subhedral, and the microcline, subhedral to anhedral; quartz tends to fill the irregular interspaces. The microcline is perthitic but appears to carry somewhat less exsolved plagioclase and also less clay than the microcline in the lime-poor rock just described. The plagioclase is $An_{20-25}$, and it shows the effects of widespread sericitic alteration, despite the relatively fresh appearance of the coexisting microcline. Its degree of zoning varies. Where well developed, the zoning may be gradational, but more commonly it appears as a series of concentric layers. In general, the outer layers appear to be more calcic, but a diagnostic Becke line is difficult to detect between many adjacent zones. Where the plagioclase is relatively unzoned, it is included in quartz or, where next to microcline, it has armored itself against attack by development of an outer layer composed of myrmekite or of a clear and usually untwinned albite. Rarely, the plagioclase is coated by both kinds of layers. These plagioclase features appear identical with those found in two different contaminated granites by Nockolds (1932, p. 436). The quartz is strained, and the intensity of strain varies from grain to grain. Biotite, pleochroic from straw-colored to dark olive green, makes up about 10 percent of the rock. All the accessory minerals present (allanite, epidote, sphene, apatite, zircon, and magnetite) tend to be closely associated with this biotite. Some, especially apatite, may be included within the biotite. However, inclusions within the biotite are not especially abundant, and even where present, they totally lack the dark halos so common in biotite from the lime-poor rocks.

Sample 79 has a CaO content of 4.0 percent. In hand specimen, it looks like sample 34, except that sample 79 is darker because of its higher (21 percent) biotite content.

In thin section, the rock betrays its hybrid nature. Perthitic microcline remnants are altered to plagioclase and are usually bounded by arcuate areas of myrmekite convex inward. A narrow zone of quartz tends to develop where biotite and microcline are in contact. Myrmekitic intergrowths of biotite and quartz suggest replacement of microcline even where none remains. Borders between quartz and microcline are commonly sutured. Quartz alone also tends to develop a sutured texture. Almost all the quartz shows pronounced strain. The plagioclase has a composition near $An_{30}$. All this

plagioclase shows zoning, usually repeated; and each successive zone is rather consistently more calcic than the previous, although this is often difficult to determine because the Becke line between adjacent zones is commonly indistinct. Many grains are surrounded by a well-defined zone that is more sodic than the interior zones of the crystal. In contrast to the two more felsic rocks already described, not all the plagioclase with this albitic coating has a common border with microcline, but it is possible that all formed in this position, inasmuch as so little microcline remains. All plagioclase grains carry some sericitic alteration, and in some grains the distribution of the sericite conforms to the zonal structure. Some of the plagioclase also carries fine-grained zoisite. Accessory minerals are so abundant in this rock that all—even the tiny acicular euhedra of zircon—are easily found in thin section. Usually the accessories allanite, epidote, sphene, apatite, zircon, and magnetite are associated with each other and with biotite. None of the inclusions in the biotite is surrounded by a halo. Many acicular crystals of zircon and (especially) apatite are included in quartz. As in sample 34, biotite is pleochroic from straw-colored to dark olive green.

Sample 81 resembles a rather dense medium-grained diorite. It represents a large xenolithic mass having a volume of hundreds of cubic yards. It has a CaO content of 4.1 percent and lies within a host having a CaO content of about 2.7 percent.

In thin section, much of sample 81 has a texture that looks ophitic but involves different sets of minerals from place to place. Hornblende euhedra are enclosed in quartz, microcline, and plagioclase but most commonly in quartz. As many as 20 crystals of hornblende are included in a single grain of quartz. Plagioclase laths are enclosed in quartz and in microcline. The relatively small amounts of microcline present in the rock are perthitic and carry very few clay alteration products. The plagioclase displays polysynthetic twinning and is near $An_{30}$. Variation in composition, although apparently not great, is common in single grains. The most common type of compositional variation is a gradual concentric zonation. A few grains have a series of more abrupt, but rather poorly defined, zones superimposed on the more transitional change. Apparently, the outer parts of the grains are slightly more calcium rich. Some grains also show random and subtle zonation that probably formed rather late. Those plagioclase grains enclosed in microcline are surrounded by a cover of late albitic material. The quartz has undulose extinction, and in some grains this effect is pronounced. Hornblende and biotite are present in subequal amounts that together make up about 25 percent of the rock. Although there are good examples of biotite replacing hornblende, there also are many grains of each that show no relation to the other. The biotite is similar to that just described for the three more mafic rocks, except that some flakes contain groups of minute and transparent inclusions. These inclusions are distributed chiefly along one or more crystallographic directions. Some and possibly all of these inclusions are sphene, and they may have been left over after conversion of amphibole to biotite. We have repeatedly emphasized the abundance of accessory minerals in the lime-rich members of this rock series. However, regarding large masses of xenolithic material where much hornblende remains because assimilation was incipient, this generalization does not apply. The rock we are describing contains relatively small amounts of zircon, epidote, allanite, sphene, and magnetite when compared with its high lime content. Apatite is more abundant, and it occurs as extremely elongated crystals included within quartz, plagioclase, microcline, and biotite.

Megascopically, sample 71 is a rather friable fine- to medium-grained granodiorite. It is part of an ellipsoidal xenolith about 1 foot long that contains 3.5 percent CaO. The surrounding intrusive contains about 2.5 percent CaO.

Petrographic study shows that all the hornblende has been replaced by biotite, as is typical for xenoliths this size or smaller. Partly as a result of this replacement, the texture of the rock does not present the ophitic appearance just described for the much larger xenolithic mass (sample 81); biotite does not tend to be included in quartz and feldspar as does the hornblende it replaces. The biotite is similar to that already described for the more mafic rocks. It carries very few of the tiny oriented sphene inclusions present in the biotite of the much larger xenolithic mass (sample 81). The little microcline that remains is very similar in its appearance and paragenetic relations to microcline in the most mafic example of the main intrusive phase (sample 79). The plagioclase is $An_{25-30}$. Some grains are partly altered to zoisite and sericite. Zoning is similar to that of the plagioclase of the larger xenolithic mass (sample 81), though not as pronounced. Most of the quartz shows undulatory extinction. Zircon, epidote, magnetite, and sphene tend to be associated with biotite. Acicular apatite is included in biotite, quartz, and feldspar.

The petrographic evidence provided by these five representative rocks from the Snake Creek-Williams Canyon area is summarized as follows:

1. Zoning of the plagioclase becomes more widespread and more complex in the progression from the most felsic rocks (near $An_5$) to the most mafic ($An_{35}$). The outer zones generally appear to be more calcic than the inner, but in many grains

this is difficult to determine. Even where zoning is most complex, the compositional extremes within a single grain probably do not represent a range of anorthite content of much more than 5 molecular percent.

2. Some plagioclase crystals in all the rocks have a thin outer zone more albite rich than the interior of the grain. At least in the more felsic rocks, this outer zone must be near end-member albite. Some of these late albite-rich zones are very irregular in form. The albite-rich phase usually occurs where the plagioclase borders or is enclosed by microcline and may have developed from perthitic albite in the microcline. Where the albite-rich zone is not related to any microcline, it might represent introduction of sodium.
3. Plagioclase from the more mafic rocks tends to be more altered to sericite, and in the most mafic rocks zoisite also is present.
4. In contrast to the plagioclase, microcline in the most felsic rocks carries more fine-grained clay than does microcline in the mafic rocks.
5. All the microcline is perthitic. Textures show that the small amounts of microcline present in the mafic rocks are remnants of larger grains that have been partly replaced.
6. Biotite in the most felsic rocks is pleochroic from buff to reddish brown and contains inclusions. These inclusions are probably monazite, and each is surrounded by a halo that is dark but not pleochroic. Rocks having more than about 1.1 percent CaO contain biotite that is pleochroic from straw colored to dark olive green. Some of this biotite contains inclusions of accessory minerals, mostly apatite, but none of these inclusions is surrounded by a halo.
7. Hornblende is observed only in the larger masses of xenolithic material. In all other members of the rock series, including those xenoliths no more than 1 foot in greatest dimension, hornblende is completely absent and biotite is present instead.
8. In the larger masses of xenolithic material, where assimilation was so incomplete that hornblende still remains, the general tendency for abundance of accessory minerals to increase with CaO content of the rock fails; and zircon, epidote, allanite, sphene, and magnetite are present in relatively small amounts.
9. In both lime-poor and lime-rich rocks, the accessory minerals tend to be associated with biotite. Apatite is the only accessory mineral that does not always follow this pattern, especially in the more mafic rocks (CaO>2.5 percent), where acicular euhedra of apatite are readily found in all the essential minerals.
10. Almost all the quartz shows some degree of strain.

## PETROLOGY

Many types of plots have been devised for discussion and comparison of data such as those in table 5, and one of the most common of these, the Harker variation diagram, has already been presented (fig. 4).

We plotted (fig. 13) values for rocks from the Snake Creek-Williams Canyon area (table 5) to determine Peacock's (1931) alkali-lime index. For only one rock, a xenolith (sample 87) containing 60.2 percent $SiO_2$, does percent CaO exceed percent $K_2O+Na_2O$, and the excess is only 0.3 percent. Of course, if the alkali-lime index were less than 57, this would not be surprising, but we did not find more mafic (less than 57 percent $SiO_2$) representatives of rocks from the Snake Creek-Williams Canyon area. Extrapolations based on the more felsic members of the series point toward an alkali-lime index of about 64 (fig. 13), characteristic of the calcic rock series of orogenic regions, which commonly involve magmas contaminated by sedimentary materials (Barth, 1962, p. 173).

Rittmann's (1960) serial index $s$, defined as:

$$s=\frac{(Na_2O+K_2O)^2}{SiO_2-43}$$

throws light on magmatic processes (Barth, 1962, p. 168). By plotting $s$ against the $SiO_2$ values, Rittmann distinguished among the following:

| Process | $s$ | $SiO_2$ content |
|---|---|---|
| Crystal settling | Constant | Increasing. |
| Gas transfer, top (+ alkalis) | Increasing | Oscillating. |
| Gas transfer, bottom (− alkalis). | Decreasing | Increasing. |
| Assimilation of clastic sediments. | Increasing to 2.3. | Do. |
| Assimilation of limestone | Increasing | Decreasing. |

We have plotted $s$ against $SiO_2$ for rocks of the Snake Creek-Williams Canyon area (fig. 14), and results support the idea of assimilation. Thus $s$ tends to increase with decreasing $SiO_2$ near the mafic end of the series where there has been assimilation of limestone, whereas the two increase together where there has been assimilation of clastic sediments.

The plots of $(K_2O+Na_2O)$ and $s$—both with respect to $SiO_2$ (figs. 13, 14)—are similar, but trends are more pronounced in the latter, as is to be expected from the algebra involved. Rocks of the Snake Creek-Williams

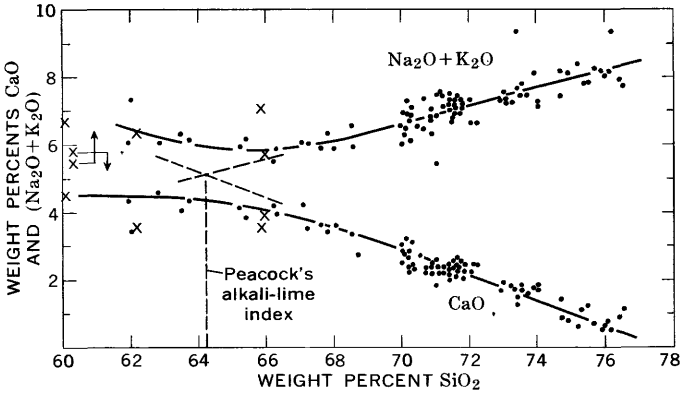


FIGURE 13.—Silica variation diagram for CaO and $Na_2O+K_2O$ in granitoid rocks of the Snake Creek-Williams Canyon area (table 5). ●, sample from main intrusive phase; ×, xenolith.

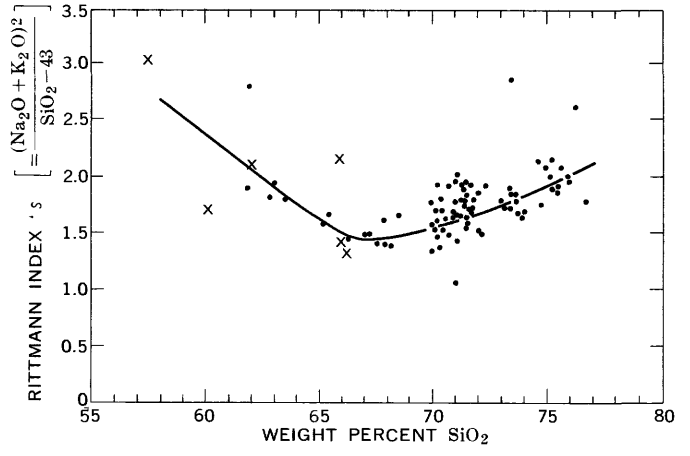


FIGURE 14.—Relation between Rittmann index $s$ and $SiO_2$ content for granitoid rocks of the Snake Creek-Williams Canyon area. ●, sample from main intrusive phase; ×, xenolith.

Canyon area resemble part of the classic magmatic differentiation sequence, but figure 14 suggests that assimilation was more important than differentiation in the history of these rocks.

The triangular diagrams (figs. 15–17) showing distribution of normative albite, orthoclase, and quartz in the analyzed rocks (tables 5–7) indicate crystallization of granite from a magmatic liquid. The analyses concentrate in and near Bowen's (1937) thermal valley on the liquidus surface in the system $NaAlSi_3O_8$–$KAlSi_3O_8$–$SiO_2$. As emphasized by Tuttle and Bowen (1958), such a concentration is readily explained if the chemical compositions are controlled by liquid⇆crystal equilibria, but this concentration would be a remarkably fortuitous result of any mechanism not involving a magma.

Compared with a similar diagram (Tuttle and Bowen, 1958, fig. 42) for 571 analyzed plutonic rocks (80 percent or more Ab+Or+Q) in Washington's (1917) tables, the concentration of points for rocks of the Snake Creek-Williams Canyon area (table 5; fig. 15) is shifted away from the orthoclase apex, reflecting that series' somewhat lower contents of $K_2O$.

This same relative lack of $K_2O$ is apparent when modal analyses of the Snake Creek-Williams Canyon rocks are compared with those of 260 "granites" from the Eastern United States (Chayes, 1951; Tuttle and Bowen, 1958). On a triangular diagram (fig. 18) featuring modal quartz, plagioclase, and orthoclase (=microcline), even the most-microcline-rich rocks of the Snake Creek-Williams Canyon area are farther away from the orthoclase apex than the main concentration of points for Chayes' granites. But the most striking feature of figure 18 is the shift of points toward the quartz-plagioclase sidelines with increasing CaO content of the rock, forming a continuous band of points from that sideline almost to the center of the diagram. This, of course, is a direct consequence of the fact that the biotite and CaO contents of these rocks increase together, as has been shown (fig. 8). With increased biotite content, less and less $K_2O$ is available for microcline, until much of the granitoid rock nearest the limestone country rock in Snake Creek is virtually devoid of potassium feldspar. A number of previous studies pointed up the development of biotite in hybrid rocks, which we shall discuss in some detail in the following section on petrogenesis.

On the basis of the distribution of the sodium feldspar between the plagioclase and potassium feldspar components, Tuttle and Bowen (1958, p. 130) proposed a classification of igneous rocks having compositions within or near "petrogeny's residual system." This "residual system" is defined to include those rocks containing 80 percent or more normative Ab-Or-Q (albite-orthoclase-quartz). According to this classification, all the granitoid rocks in this study are:

II. Subsolvus
  C. Potassium feldspar Ab<15 percent
    (2) Microcline–low albite perthite

This conclusion is based partly on data in the earlier section on mineralogy and partly on preliminary analytical results for some of our purified microclines.

The major category designation—subsolvus—means in part that the rocks are characterized by both potassium feldspar and plagioclase as discrete phases, as opposed to hypersolvus rocks where all or most of the plagioclase component is present in solid solution with potassium feldspar. The second designation—albite content of potassium feldspar less than 15 weight percent—indicates that the rocks completed crystallization or recrystallization at low temperatures. It is important to remember that metamorphism of a crystallized intru-

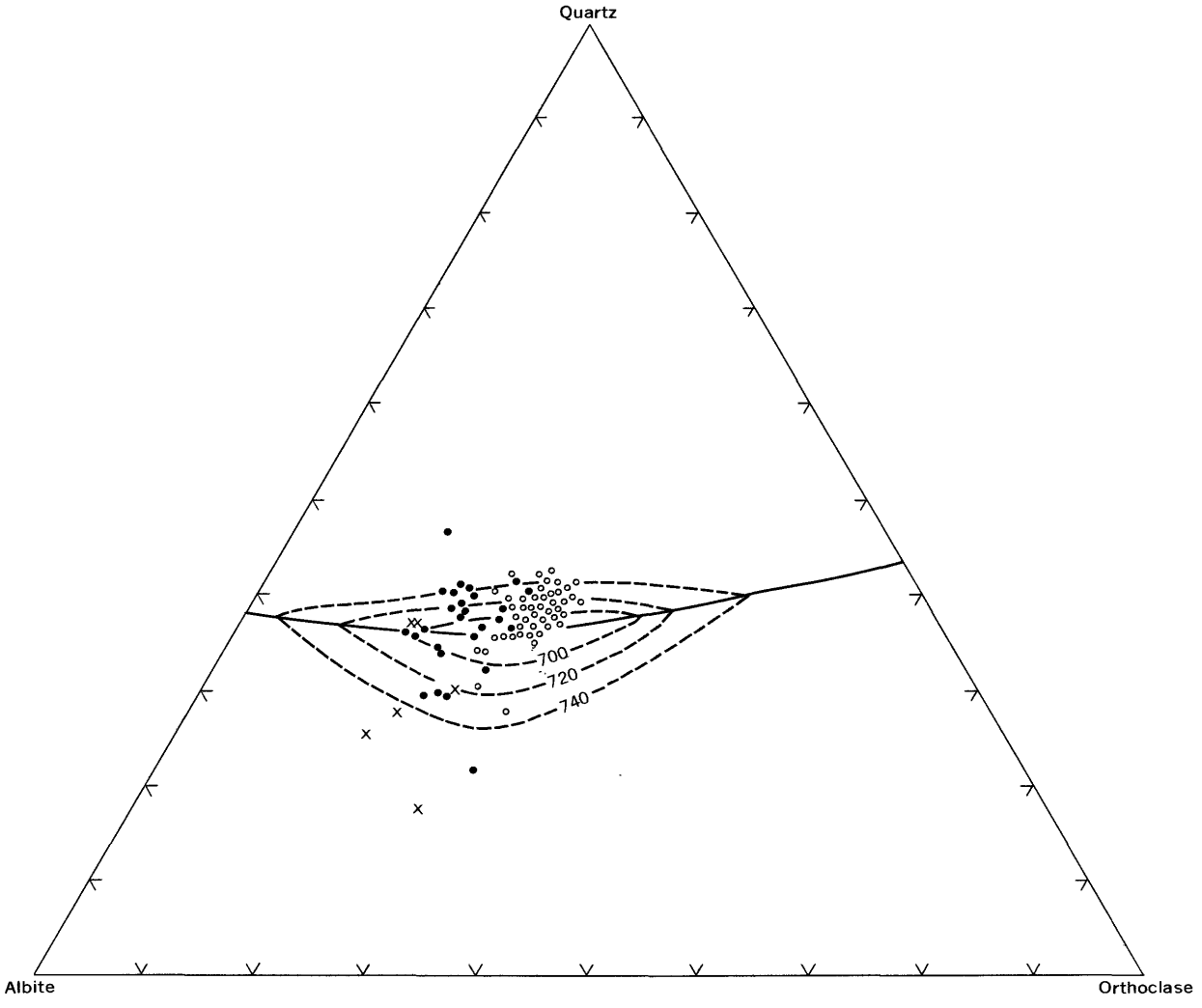


FIGURE 15.—Normative albite, orthoclase, and quartz in granitoid rocks of the Snake Creek-Williams Canyon area (table 5). Solid line shows position of the thermal valley, and dashed lines are isotherms (700°, 720°, and 740°C) on liquidus in the system albite-orthoclase-quartz at $P_{H_2O}$=2,000 kg/cm² (from Tuttle and Bowen, 1958, p. 55). Samples 31, 32, 35, 36, 53, and 54 are not plotted; they would fall in main concentration of points. ○, sample of main intrusive phase, normative Ab+Or+Q≥80 percent. ●, sample of main intrusive phase, normative Ab+Or+Q<80 percent. ×, xenolith; except for sample 46, each xenolith has normative Ab+Or+Q<80 percent.

sive would have promoted unmixing of the feldspars (Tuttle and Bowen, 1958, p. 101) and that these granitoid rocks were subjected to a low-grade regional metamorphism, perhaps during Mesozoic time (Lee and others, 1970). The third designation—the triclinicity of the potassium feldspar—suggests unmixing and recrystallization of the feldspars in the presence of excess water vapor.

Completing description of these rocks are sketches (fig. 19) of polished and stained slabs of four representative specimens. Sketches *A*, *B*, and *C* illustrate the mineralogical composition of increasingly mafic rocks in the Snake Creek-Williams Canyon area. In general, their textures are similar to the texture of the subsolvus granite figured by Tuttle and Bowen (1958, pl. 6). The striking reversal of the microcline-biotite ratio is well shown. Sketch *D* shows a typical rock from the Pole Canyon-Can Young Canyon area.

## PETROGENESIS

More than 30 years ago, Nockolds (1934) published a paper entitled "The Production of Normal Rock Types by Contamination and Their Bearing on Petrogenesis," in which he (p. 33) stated:

> Indeed, anyone familiar with recent literature on the subject cannot fail to be impressed with the number of intrusions, once thought to be normal, which are now known to be the result of assimilation; not to mention the number of "normal" intrusions known to be contaminated, but which have not yet been studied in detail.

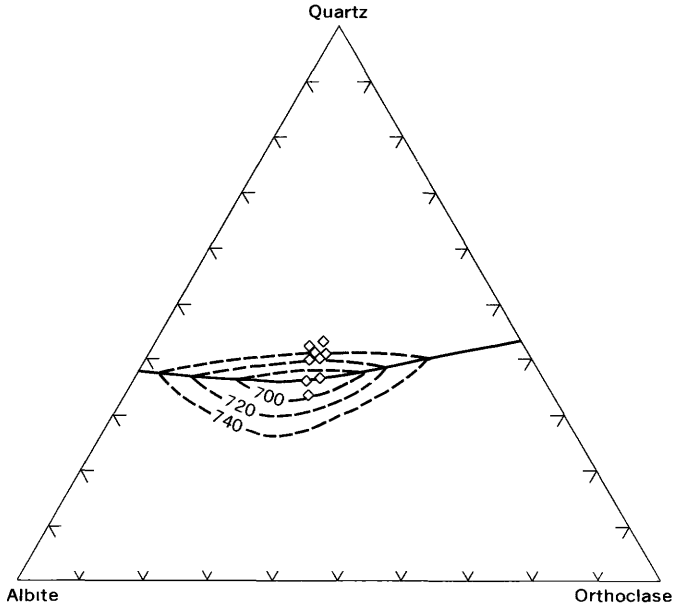


FIGURE 16.—Normative albite, orthoclase, and quartz in granitoid rocks of the Pole Canyon-Can Young Canyon area. Each sample has normative Ab+Or+Q>80 percent. Solid line shows position of the thermal valley, and dashed lines are isotherms (700°, 720°, and 740°C) on liquidus in the system albite-orthoclase-quartz at $P_{H_2O}$=2,000 kg/cm² (from Tuttle and Bowen, 1958, p. 55).

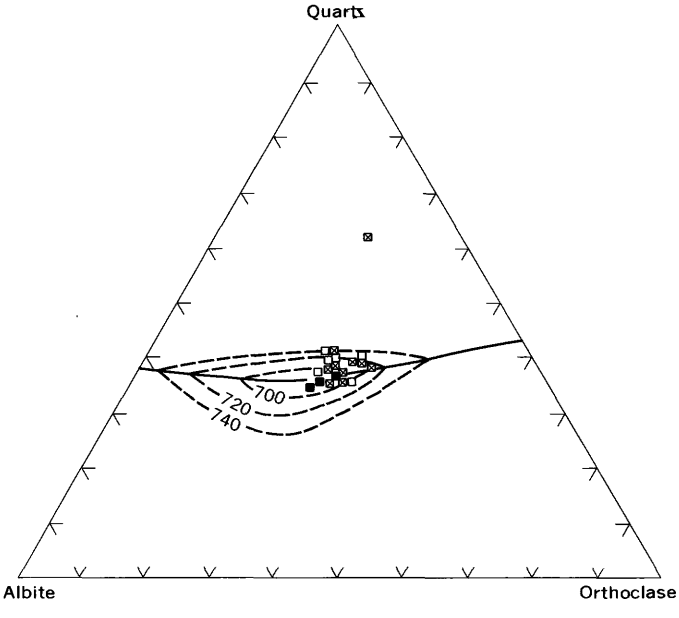


FIGURE 17.—Normative albite, orthoclase, and quartz in rocks of the Young Canyon-Kious Basin area (table 7). Solid line shows position of the thermal valley and dashed lines are isotherms (700°, 720°, and 740°C) on liquidus in the system albite-orthoclase-quartz at $P_{H_2O}$=2,000 kg/cm² (from Tuttle and Bowen, 1958, p. 55).

□, unsheared rocks; normative Ab+Or+Q>80 percent.
⊠, sheared rocks; normative Ab+Or+Q≥80 percent.
■, sheared rocks; normative Ab+Or+Q<80 percent.

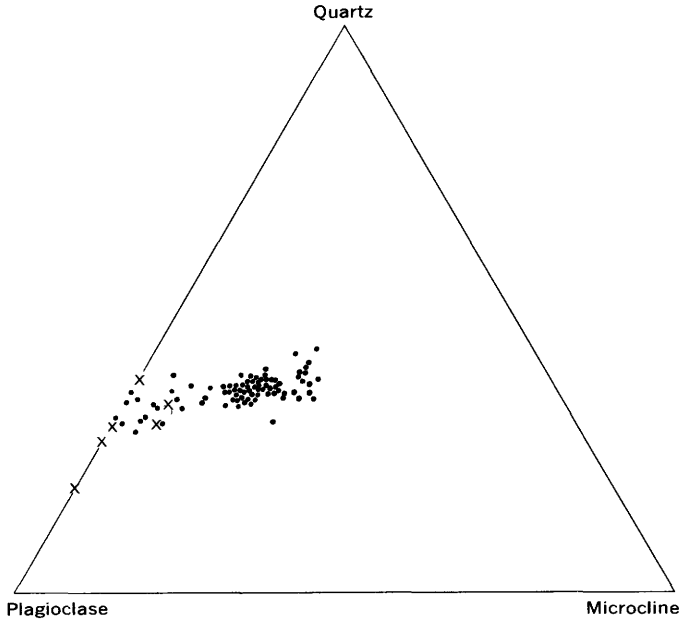


FIGURE 18.—Modal plagioclase, microcline, and quartz in granitoid rocks of the Snake Creek-Williams Canyon area (table 5). ●, sample from main intrusive phase; ×, xenolith.

Our study area was advantageous because it presented well-exposed granitoid rocks in contact with chemically distinct host rocks, which enabled us to relate the various concentration gradients and systematic mineralogical differences to host rock type. The granitoid rocks described are a good example of the "production of normal rock types by contamination."

Before proceeding, we shall anticipate some of the conclusions of this section and state what is implicit in much of the previous discussion of petrology. We are not concerned here with granitization (as opposed to magmatic action); nothing in our results requires that interpretation. Whether our "original, uncontaminated" magma was formed by palingenesis of sediments or differentiated from some more basic magma at depth, we are dealing with a crystallized magma and the results of liquid⇌crystal equilibria.

Although it is well known that normal rock types can result from contamination of an acid magma, most examples described in the literature involve assimilation of more basic igneous material such as gabbro, dolerite, or norite (Nockolds, 1934, p. 31). There are fewer descriptions of normal rock types having resulted from contamination of an acid magma by sedimentary rocks. Moreover, contamination by more basic material is much easier to treat theoretically because the principles of a continuous reaction series (calcic plagioclase→alkalic plagioclase) are more directly ap-

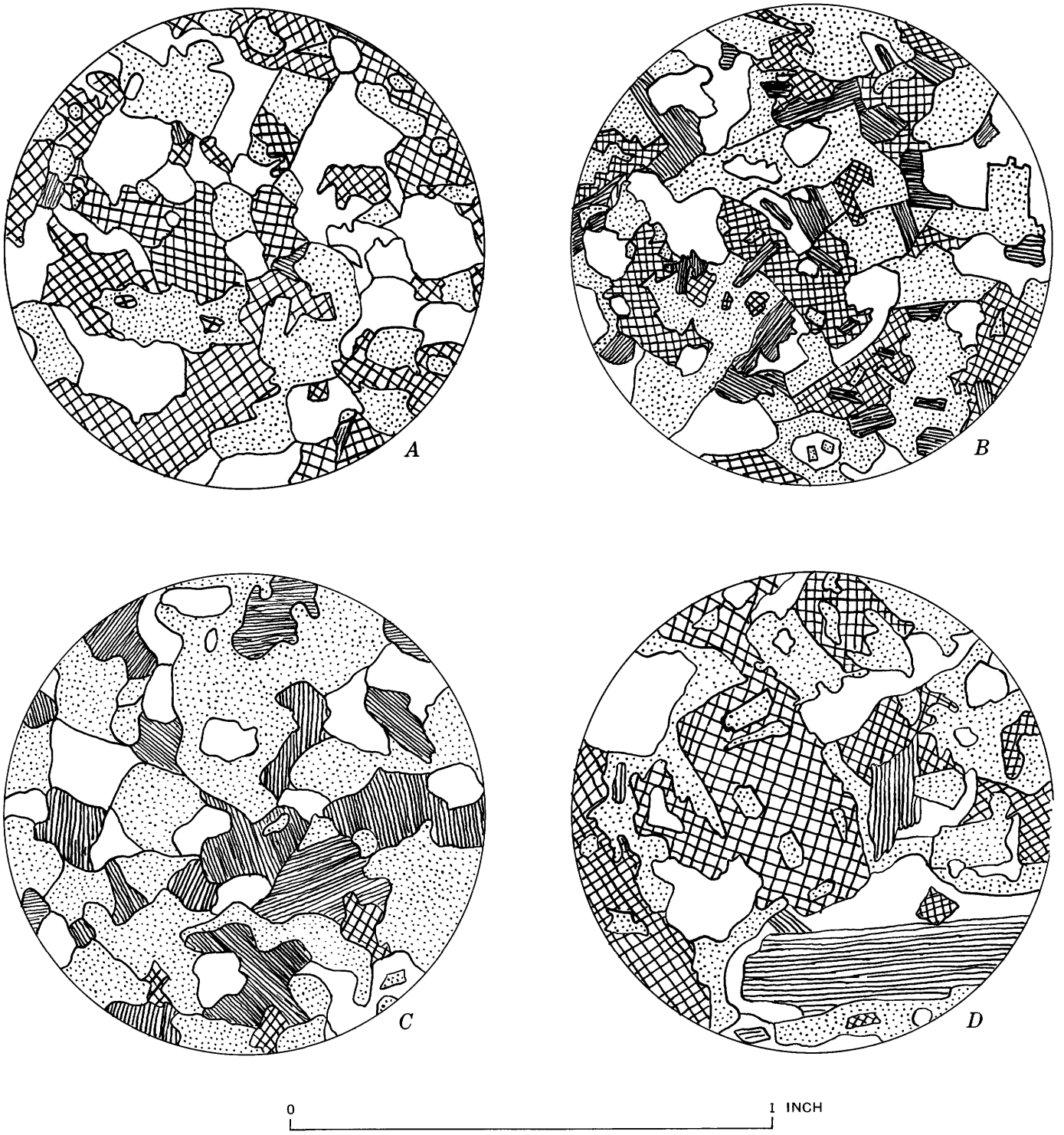


FIGURE 19.—Sketches of stained rocks. White, quartz; stippled, plagioclase; cross-hatched, microcline; ruled, biotite (and much muscovite in *D*). *A*, 0.78 percent CaO, sample 7, Williams Canyon; *B*, 2.2 percent CaO, sample 34, Snake Creek; *C*, 4.0 percent CaO, sample 79, Snake Creek; *D*, 0.98 percent CaO, sample 89, Can Young Canyon.

plicable. To quote from the classic account by Bowen (1922, p. 531):

> Summing up the result of adding to a liquid various members of a solid solution series with which it is saturated we find that if the added inclusion is nearer the high temperature end of the series than the crystals with which the liquid is saturated the reaction is such as to *decrease the amount of liquid and is exothermic.* If the inclusion is nearer the low-temperature end of the series than the crystals with which the liquid is saturated, the reaction is such as to *increase slightly the amount of liquid and is endothermic.* The liquid, too, is enriched in this case in the constituents of the low-temperature end of the crystallization series. Even inclusions consisting of the precise crystals with which the liquid is in equilibrium must react with the liquid as the temperature falls. [Italics added.]

Later in his discussion, Bowen (1922, p. 535–537) showed that results for corresponding members of a discontinuous reaction series (olivines→pyroxenes→amphiboles→biotites) are virtually the same.

Regarding magmatic assimilation of sedimentary rocks, Bowen stated (1922, p. 543–544):

> The general problem of the effects of magma upon inclusions of sedimentary origin is much more difficult than the similar problem in connection with igneous inclusions. Sedimentary rocks have their compositions determined by processes wholly independent of igneous action and do not correspond in composition with the products precipitated from magmas at any stage of their career, that is, cannot be placed definitely in the reaction series. However, certain minerals that can be formed in magmas do occur in the sedimentary rocks and often the composition of a sediment is such that by mere heating it can be transformed into a aggregate made up exclusively or almost exclusively of igneous rock minerals. Again sediments exhibit extremes of composition, being very rich in calcium carbonate, aluminum silicate or silica itself, and these present a special problem. *Yet it is perhaps not generally realized how much even of these extreme sediments might be incorporated in an igneous rock without changing its mineralogy.* [Italics added.]

We now consider the chemistry of the sedimentary rocks in contact with the granitoid rocks of the Snake Creek-Williams Canyon area. Sedimentary-rock analyses listed in tables 1 and 2 are averaged in table 9, where $CO_2$ is omitted and major- and minor-element values have been adjusted accordingly. Also, minor-element figures are rounded to the nearest semiquantitative value, using the same scale as in tables 1 and 2. In view of the great stratigraphic thickness involved and the stratigraphic and structural complexities, the average analyses in table 9—which represent only 34 individual analyses—must be used with caution; nevertheless, the differences among these average analyses are so pronounced that some general quantitative comparisons are justified.

Shale is a sedimentary rock similar to diorite or granodiorite in chemical composition. In most respects, the Pioche Shale major-element average listed in table 9 is remarkably similar to the average for the most-lime-rich members of the Snake Creek-Williams Canyon granitoid rocks. The most striking difference involves $Na_2O$, which is much higher in the granitoid rock than in the shale. Lime and alumina each are somewhat higher in the mafic granitoid phase than in the sale, and $K_2O$ is somewhat lower. The Wheeler limestone probably constitutes 5–10 percent of the thickness of the Pioche Shale. If we assume a mixture of Pioche Shale and Wheeler limestone of about 15 to 1 (or about 30 to 1 of the $CO_2$—free averages in table 9), the qualitative comparisons above can be improved for $K_2O$ and (especially) lime, but the discrepancies for alumina and (especially) $Na_2O$ are increased.

The Pole Canyon Limestone is a rather pure calcium carbonate, as shown by data in table 2 and the $CO_2$—free average in table 9. This average can be made to resemble analyses of the mafic (dioritic) phase with which the limestone is in contact only by a sharp de-

TABLE 9.—*Average compositions of sedimentary rocks studied*

[Analyses of individual samples given in tables 1 and 2. 0, below limit of detection]

| | Argillite [1] | Quartzite [2] | Shale [3] | Limestone | |
|---|---|---|---|---|---|
| | | | | Wheeler [4] | Pole Canyon [5] |
| **Chemical analyses (weight percent)** | | | | | |
| $SiO_2$ | 62.9 | 91.6 | 63.6 | 31.4 | 4.5 |
| $Al_2O_3$ | 16.2 | 4.1 | 15.9 | 2.9 | 1.1 |
| $Fe_2O_3$ | 4.3 | .79 | 3.8 | 1.6 | .33 |
| FeO | 1.9 | .25 | 3.3 | 5.2 | .25 |
| MgO | 2.2 | .23 | 1.8 | 16.5 | 2.0 |
| CaO | 4.7 | .01 | 1.9 | 39.6 | 91.0 |
| $Na_2O$ | 1.5 | .13 | .58 | .30 | .12 |
| $K_2O$ | 3.0 | 2.1 | 5.3 | .42 | .37 |
| $H_2O$ | 2.2 | .38 | 2.7 | .19 | .07 |
| $TiO_2$ | .71 | .36 | .64 | .13 | .05 |
| $P_2O_5$ | .13 | .03 | .31 | .35 | .04 |
| MnO | .16 | .01 | .09 | 1.3 | .06 |
| Cl | .00 | .00 | .00 | .02 | .00 |
| F | .07 | .02 | .13 | .08 | .04 |
| Total | 100 | 100 | 100 | 100 | 100 |
| **Semiquantitative spectrographic analyses (parts per million)** | | | | | |
| B | 15 | 0 | 30 | 0 | 0 |
| Ba | 1,000 | 500 | 1,000 | 50 | 300 |
| Be | 5 | 0 | 5 | 0 | 0 |
| Ce | <150 | 0 | 150 | 0 | 0 |
| Co | 20 | 3 | 20 | 5 | 0 |
| Cr | 150 | 7 | 100 | 15 | 20 |
| Cu | 30 | 30 | 50 | 10 | 20 |
| Ga | 50 | 5 | 30 | 5 | <5 |
| La | 70 | 0 | 100 | 0 | 0 |
| Mo | 0 | <3 | <3 | 0 | 0 |
| Nb | 20 | 0 | 20 | 0 | 0 |
| Ni | 70 | 7 | 50 | 10 | 7 |
| Pb | 70 | <10 | 50 | 50 | 20 |
| Sc | 20 | <5 | 20 | 0 | 0 |
| Sr | 300 | 15 | 150 | 1,000 | 3,000 |
| V | 150 | 20 | 150 | 20 | 15 |
| Y | 50 | 10 | 70 | 30 | 7 |
| Yb | 5 | 1 | 7 | 3 | 0 |
| Zr | 300 | 500 | 300 | 70 | 30 |

[1] Osceola Argillite of Misch and Hazzard (1962): average of 6 analyses on $CO_2$-free basis.
[2] Prospect Mountain Quartzite: average of 4 analyses.
[3] Pioche Shale: average of 8 analyses on $CO_2$-free basis. Sample S3 (which contains fluorite) excluded.
[4] Wheeler limestone of local usage: average of 6 analyses on $CO_2$-free basis.
[5] Pole Canyon Limestone: average of 9 analyses on $CO_2$-free basis.

crease in lime and an increase in almost all other oxides, except MgO.

A similar comparison of the "average quartzite" (table 9) with the most-lime-poor members of igneous rocks from the Snake Creek–Williams Canyon area shows that the quartzite is higher in silica and $TiO_2$ and lower in alumina, the alkalis, and lime.

If we extend these comparisons a step further and consider the whole Snake Creek–Williams Canyon area along with the sedimentary country rocks, the sedimentary rocks (quartzite, shale, and limestone) together appear to be much lower in $Na_2O$ and $Al_2O_3$ and higher possibly in $SiO_2$ (and, of course, in $CO_2$).

The major-element concentration gradients present in the contaminated granitoid rocks of the Snake Creek-Williams Canyon area are remarkably regular and well defined. Consider again the rock analyses in table 5 and the CaO contours on plate 1. Even the most felsic rocks contain 0.5 percent CaO, although the quartzite country rock is all but devoid of CaO. The most mafic members of the series contain only about 4.5 percent lime, much less than the contiguous Pole Canyon Limestone. Now consider the sympathetic increase of both $TiO_2$ and $P_2O_5$ with CaO (table 5; fig. 3*G*, *H*), along with the fact that the average Pole Canyon Limestone contains little of either $TiO_2$ or $P_2O_5$ (table 9). These and other relations involving major-element oxides point toward a central fact: while the magma was being contaminated by assimilation of country rock, local liquid⇄crystal equilibria became subordinate and were incorporated into well-defined concentration gradients extending over a horizontal distance as great as 3 miles. For some oxides such as CaO, the slope of the gradient in the granitoid rocks is that expected from the wall-rocks involved—that is, CaO increases toward the lime-rich country rock. For other oxides such as $TiO_2$ and $P_2O_5$, the slopes of the concentration gradients appear to have been reversed over horizontal distances of a mile or more.

Similar patterns can be shown with minor-element data. Zirconium is an example. As shown previously (Lee and Dodge, 1964; Lee and Bastron, 1967; Lee and others, 1968) and in tables 5 and 8 and figure 6*B*, zirconium increases with lime in these contaminated granitoid rocks. This is the opposite of what one might expect from the sedimentary rock data in table 9. On the other hand, the sympathetic increase of lime with strontium in the Snake Creek-Williams Canyon area (tables 5, 9; fig. 6*D*) is consistent with the increase from quartzite through shale to limestone shown in table 9.

What is the mechanism by which the ions concerned were exchanged between the magma and the assimilated country rocks to produce the results described for granitoid rocks from the Snake Creek-Williams Canyon area? The evidence leads us to the conclusion that this exchange was accomplished by a combination of diffusion and mechanical mixing, much as described by Nockolds (1933) in his study dealing specifically with the theoretical aspects of contamination in plutonic acid magmas. Nockolds' work seems almost to have anticipated the results of our study, and much of the discussion immediately following was influenced by his paper.

Nockolds concluded that contamination in acid magmas is intimately connected with the volatiles which they contain. As summarized by Turner and Verhoogen (1960, p. 156), Nockolds suggested "that the necessary ionic exchange is effected through the medium of a mobile aqueous fluid (perhaps a simple ionic solution of such compounds as sodium and potassium silicates), which is assumed to separate from the magma and penetrate the xenolith freely." Nockolds (1933, p. 563) wrote:

> This conclusion was based partly on the relative abundance of apatite found in the xenoliths and more contaminated portions of the magma *when compared with the amount present in the invaded or invading rock.* This apatite is characteristically present as *thin needles* penetrating the other minerals and often of exceedingly small dimensions. [Italics added.]

This accurately describes the apatite present in our contaminated rocks. Moreover, Nockolds cited 14 references describing the relative abundance of apatite in hybrid rocks. The earliest was Harker (1895), and many of the other writers mentioned "apatite needles" or otherwise referred to the acicular habit of the apatite.

Biotite and hornblende are other hydroxyl-bearing minerals typical of hybrid rocks. For instance, granophyres in west Scotland usually are augite bearing, but when they are contaminated, they develop hornblende and even biotite (Nockolds, 1933, p. 565). Turner and Verhoogen (1960, p. 156) noted that biotite is conspicuous in hybrid rocks. Just as we found in the Snake Creek area, Deer, Howie, and Zussman (1962, p. 78) wrote that "the progressive alteration of hornblende to biotite with the increasing modification of basic xenoliths in rocks of both intermediate and acid composition has been noted by many workers." Thus, in addition to our results, there is much evidence in the literature that volatiles are concentrated in xenoliths and in the more contaminated portions of acid magmas.

The relation between volatiles and the process of contamination in our granitoid rocks is emphasized by the plot of $H_2O(+)$ versus CaO for the Snake Creek-Williams Canyon area (fig. 20), based on the quantitative $H_2O(+)$ data from table 5. The increase of F with CaO in these rocks has already been illustrated (fig. 7).

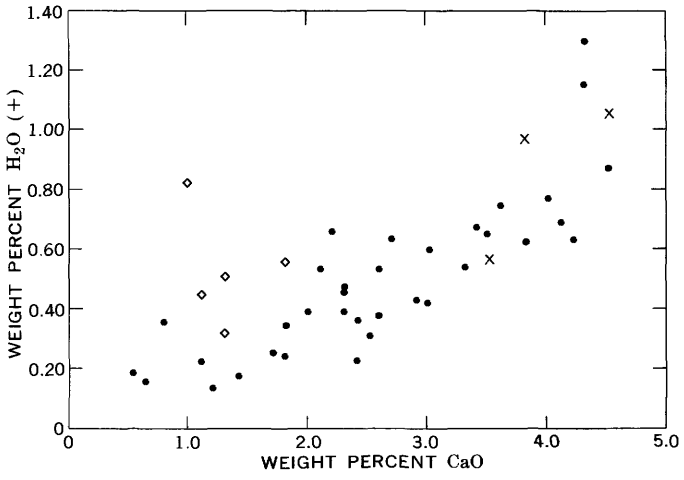


FIGURE 20.—Relation between CaO content and $H_2O(+)$ content in selected granitoid rocks. ●, sample from Snake Creek-Williams Canyon area (table 5); ×, xenolith (table 5); ♦ sample from Pole Canyon-Can Young Canyon area (table 6).

Although there is a concentration of volatiles (mainly water) in the final product, the $P_{H_2O}$ was not necessarily higher in the more mafic parts of the magma during alteration of the xenolithic material. Instead, the relative concentration resulted when some of the volatiles were fixed in solid phases as an integral part of the process of assimilation. As the volatiles (essentially in an ionic solution) moved from the magma into the xenolith to effect alteration, some were used to form hydrous minerals. As these volatiles were removed, a pressure gradient resulted, and more volatiles moved in from the surrounding magma. The dissolved substances carried with the volatiles were deposited during alteration of the xenolith, and the elements displaced by this alteration were freed to diffuse out into the magma. This reciprocal action was discussed at length by Nockolds (1933), and there is nothing in his discussion that is not in agreement with the field and laboratory evidence already presented for the Mount Wheeler mine area.

Material removed from the xenolith by this reciprocal action thus was incorporated into phases crystallizing from the contaminated magma. Material was also gained by the magma through other methods that may be loosely described as "mechanical." These methods disintegrated the xenoliths and freed their constituent minerals in the magma (Nockolds, 1933, p. 589).

In the earlier section on chemistry, we noted certain groupings of elements. The association involving CaO, MgO, FeO, $P_2O_5$, $TiO_2$, and MnO, so clearly shown by our data, may be of rather widespread geologic significance and has also been noted by other investigators. For example, Nockolds (1933, p. 570) mentioned the tendency of lime, magnesia, and ferrous iron to be transferred together. Tuttle and Bowen (1958, p. 2) reported:

> The vapor in equilibrium with hydrous granitic liquids can remove the silica, feldspars and quartz from the liquid phase by vapor transport or by diffusion through the vapor, and in the long runs these materials were transferred to the cooler part of the pressure vessel. CaO, MgO, FeO, and $P_2O_5$ were concentrated by this process, and in one experiment with the Westerly granite the vapor removed essentially all the feldspar and quartz, leaving a residue of garnet, pyroxene and apatite. This tendency for the oxides abundant in the basic and ultrabasic rocks to be relatively insoluble in the vapor suggests that such a mechanism may produce the basic zones commonly found at granite contacts.

Recalling the earlier quotation (p. 36) from Bowen (1922, p. 531), it is obvious that these constituents also are concentrated in rocks of the Snake Creek area where magmatic temperatures were highest.

The tendency for CaO, MgO, FeO, $P_2O_5$, $TiO_2$, and MnO all to be associated in the diffusion of material also was recognized by Reynolds (1946). In the last part of Reynolds' (1946) paper, H. H. Read (p. 438) and A. Holmes (p. 440) each commented on the compatibility of this chemical association with the doctrine of basic fronts.

Still undetermined is the composition of the "original, uncontaminated" magma. Related to this question is another: What was the origin of the large amounts of $Na_2O$ and $Al_2O_3$ that (according to our earlier quantitative comparisons) apparently were supplied along with wallrock contaminants to the original magma to result in the hybrid rocks exposed? Since our data were gathered from the top part of an intrusive and we do not know the overall form of the body, speculating on the answers to these questions is probably pointless. Quantitatively, the granitoid rocks described may represent relatively minor compositional variants of a larger mass at depth. However, if the intrusive mass is sill-like and for some reason localized near the level of the Snake Range décollement, these questions are more difficult to answer. In either case, the late albitic rims present on some of the plagioclase crystals in these rocks might be interpreted to support the idea of introduction of $Na_2O$, at least during the latter part of the magmatic activity.

## POLE CANYON-CAN YOUNG CANYON AREA

Sample 89 is representative of the host intrusive (as opposed to aplitic) phase of the Pole Canyon-Can Young Canyon area. The rock is coarse grained, being made up mostly of crystals more than 5 mm across. The texture is porphyritic, with some phenocrysts of microcline and muscovite more than 2 cm across. The large muscovite flakes usually contain small biotite euhedra that are easily visible with a hand lens. It is common to find as many as 20 biotite crystals included within a single grain of muscovite.

The rock appears fresh in thin section, despite the fact that it looks somewhat altered in hand specimen and does not form very good outcrops. The plagioclase (near $An_{20}$) carries few alteration products. Polysynthetic twinning is much less well developed than in most representatives of the Snake Creek-Williams Canyon area. Many grains show almost no zoning. Some crystals exhibit an optical effect that resembles a subtle unsystematic zonation, but that might be due to strain. A few crystals show a series of poorly defined concentric zones. The thin sections show much myrmekite, most of which appears to have developed where plagioclase and microcline were originally adjacent. Some of the larger microcline grains contain zonally oriented euhedra of plagioclase identical with the larger scale example sketched in figure 19*D*. Some of these plagioclase euhedra have developed a rim of late albitic material, but some show no evidence of reaction with the microcline oikocryst. The microcline is perthitic and rather fresh looking, even in reflected light. It shows a wavy extinction that probably results from strain. The quartz is badly strained, and it tends to develop serrate boundaries with itself and with the feldspars. Muscovite and biotite, both of which are very fresh looking, are associated and often intergrown. They appear to have formed in equilibrium. The muscovite contains no fine-grained inclusions nor any other evidence that it is secondary after biotite. A few prisms of apatite are associated with the micas.

Thus, megascopically and petrographically, the granitoid rocks of the Pole Canyon-Can Young Canyon area are distinct from all other igneous rocks considered in this study. Mineralogically, too, they are different in both essential and accessory minerals. The plagioclase feldspar compositions fall outside the Snake Creek-Williams Canyon field (fig. 21). Muscovite is an essential mineral in these rocks, whereas in the Snake Creek-Williams Canyon area, muscovite either is absent or is present only as a minor accessory or secondary mineral. Analytical data show that biotites in the Pole Canyon-Can Young Canyon area are consistently higher in iron and lower in MgO than those in the Snake Creek-Williams Canyon area (Lee and Van Loenen, 1970). Mineral separation work has shown that rocks in the Pole Cayon-Can Young Canyon area are different in that they are devoid of magnetite, ilmenite, and sphene. One of the most striking mineralogical distinctions of these rocks in the apatite-zircon relationship mentioned earlier. The apatite has a stubby habit, and almost all of the zircon in these rocks is present as tiny needlelike inclusions within this apatite. This is different from anything observed in the Snake Creek-Williams Canyon area, except in one small area north of Williams Canyon on the west side of the range, where (locs. 27, 28 and

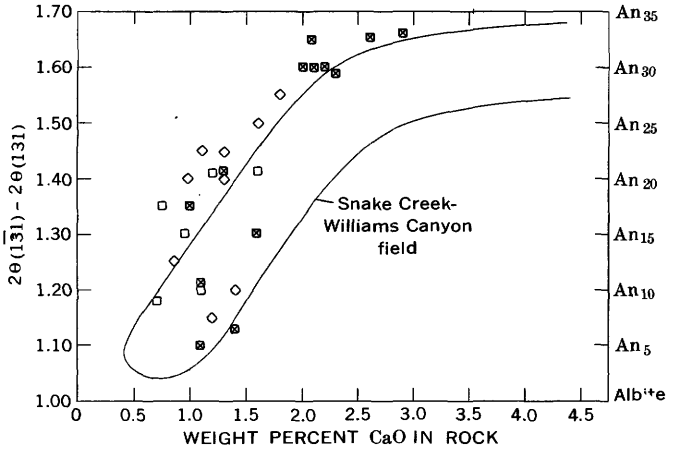


FIGURE 21.—Relation between CaO content of rock and angular difference between $2\theta_{(\bar{1}31)}$ and $2\theta_{(131)}$ X-ray reflections of constituent plagioclase. Equivalent low-temperature plagioclase compositions (right ordinate) from Tuttle and Bowen (1958). ◇, sample from Pole Canyon-Can Young Canyon area. □, undeformed portion, Young Canyon-Kious Basin area. ⊠, deformed portion, Young Canyon-Kious Basin area. Snake Creek-Williams Canyon field (fig. 9) outlined for comparison.

59, pl. 1) the intrusive is exposed in contact with the Osceola Argillite. In this restricted area, the apatite carries a few grains of acicular zircon, but most of the zircon is present as free and discrete grains of the type described for the more mafic rocks (Lee and others, 1968).

Chemically, the ratio of various other oxides to lime may tend to be somewhat different for rocks of the Pole Canyon-Can Young Canyon area than for rocks previously described (fig. 3). This is especially evident in the plot of CaO versus $Al_2O_3$ (fig. 3*B*). The chemistry and mineralogy of these rocks are variable from place to place, but the nine samples analyzed (pl. 1; table 6) do not express any general compositional trend in the field. The six samples of Osceola Argillite (table 1) show a wide range of composition within the 750-foot-thick unit. The "average" analysis of this argillite (table 9) may indicate that the distinctive intrusive resulted from magmatic assimilation of some mixture of this argillite and quartzite. The stratigraphic position of this granitoid rock is in accord with this idea. Other rather compelling evidence, presented previously, in favor of assimilation is the unusual apatite-zircon relationship, similar to but much more pronounced than what is observed where the granitoid rock is in contact with argillite on the west side of the range. Finally, it is logical to suppose that contamination played an important role in the history of this intrusive in view of the hybrid nature of the granitoid rocks of the Snake Creek-Williams Canyon area immediately to the south.

### YOUNG CANYON-KIOUS BASIN AREA

Instead of describing one or two particular samples from the Young Canyon-Kious Basin area, we present a more general discussion based on study of all the cataclastically deformed rocks represented in table 7.

In hand specimen, the rock is mostly dull grayish green mottled with light gray. The rock tends to break into splinterlike forms elongated parallel to the north-northwest directional element already described. On a surface sawed normal to this directional element, broken masses of quartz up to about 5 mm across are set in a matrix of smaller irregularly shaped masses of feldspar mixed with structureless light-green stringers. When we first saw this rock in the field, we attributed its green color to the presence of chlorite, and this is a good description of its appearance, even though subsequent petrographic study shows that most samples of the rock actually contain very little chlorite. The presence of relatively undeformed masses within the more cataclastic and even mylonitic rock was noted in an earlier section. At the other extreme, the most complete cataclasis has produced a few dikelike forms of massive dark-green pseudotachylite. One of these dikes (table 7, sample 113) is about 1 foot wide and persists over a horizontal distance of at least 15 feet. It strikes N. 10° W. (parallel to the shears) and dips about 55° W. Compositionally, this pseudotachylite is similar to the less completely deformed intrusive, but the X-ray mode (table 7) indicates that some of the rock has been reduced to material which is essentially isotropic to X-radiation.

In thin section, the pseudotachylite is isotropic, except for a few scattered birefringent specks. Somewhat less intensely deformed rock is a microbreccia in thin section, with fragments of angular to subangular quartz and feldspar set in a matrix of comminuted debris. Where no part of the rock has actually been pulverized, strain is nonetheless evident from bent albite twins, extremely wavy extinction of quartz and the feldspars, and the development of a serrate texture, much as in the cataclastic textures illustrated by Johannsen (1931, figs. 22, 25, 27; p. 22). Some thin sections exhibit relatively undeformed (but badly strained) fragments of the rock surrounded by mylonitic material, very similar to previously described relations that are visible on a megascopic scale in the field. Where cataclasis has been as complete as this, all the original micas are gone from the rock, and relatively small amounts of a fine-grained secondary muscovite are developed, mainly along grain boundaries. It is this material that was dated (age, 17–18 m.y.) to fix the time of deformation (Lee and others, 1970). Despite the development of this secondary muscovite, the feldspars (especially microcline) are fairly fresh. The rock was completely crystallized and "dry" at the time of deformation. Petrographic study of the least deformed parts of this rock and of its undeformed equivalent southwest of the projected Pioche Shale horizon (pl. 1) indicates that these granitoid rocks resemble the Snake Creek-Williams Canyon intrusive mass more than they do the granitoid rocks of the Pole Canyon-Can Young Canyon area, even though plagioclase feldspar compositions tend to fall outside the Snake Creek-Williams Canyon field (fig. 21).

The Young Canyon-Kious Basin area thus presents us with first-order evidence bearing on the time and spatial relation between the regional thrust faulting and the magmatic history of these granitoid rocks. Influence of wallrock on the composition of the intrusive also is shown. Cataclasis of the intrusive northeast of the projected position of the Pioche Shale has blurred some of the chemical relations; nevertheless, as shown on plate 1 and in table 6, the undeformed intrusive (for which the host rock was quartzite) below the projected Pioche Shale horizon contains less lime than the deformed intrusive (for which the host rock was limestone) above the projected shale.

## APLITES

The main effort of the investigation has been focused on the petrologic types already described, and, accordingly, our treatment here of the aplitic and micropegmatitic phases is relatively superficial. We have learned just enough about these phases to say with assurance that they would be a very rewarding subject for more detailed study. In the discussion to follow, the term "aplite" will be used to include both aplite and pegmatite, unless the two are specifically distinguished.

Aplites are widespread in all three areas described. On the basis of field occurrence, we have distinguished among three main aplitic types: fault zone aplites, aplite dikes, and border facies. Some of these aplites are, clearly, much older than others, and the fault zone aplites appear to be related to some of the aplite dikes.

The fault zone aplites owe their position to stresses resulting from movement on the Snake Range décollement. They are located along or near the fault (and (or) the projected position of the Pioche Shale) that separates undeformed from cataclastic granitoid rock in the eastern part of the mapped area (pl. 1). Where this fault splits at the northwestern corner of Kious Basin, the wedge-shaped area of intrusive rock between the two branches of the fault is aplite. Farther to the northwest (pl. 1, locs. 121–127), within a larger pie-shaped area bounded by the projections of these two faults (but where the faults themselves are not in evidence), all the exposed intrusive is aplitic.

There is no indication of any appreciable movement on these faults and, indeed, nothing to suggest more than a few inches of movement along any of the shears in the cataclastic part of the intrusive. Some evidence indicates absence of any movement. Although xenoliths are very uncommon in the cataclastic granitoid rock, one xenolith of Pioche Shale (loc. 85, pl. 1) was found. It is a well-formed ellipsoid about 1 foot long with no megascopic evidence of deformation or shearing, but in thin section, evidence of much strain is apparent.

Despite this apparent lack of displacement, these faults separate cataclastic from undeformed intrusive. We interpret this and the aplites themselves as evidence that these faults persist to a depth sufficient to have tapped late-stage aplitic material after the main intrusive was crystallized. According to this interpretation, the aplitic material was squeezed up by stresses resulting from late movement on the Snake Range décollement. Radiometric age data show this aplite to be about 32 m.y. old (Lee and others, 1970).

Aplite dikes are present within the main intrusive masses, usually as tabular bodies that tend to follow one or more sets of a joint system. Most are either in the Pole Canyon-Can Young Canyon area or in and around the Hub mine area north of Williams Canyon on the west side of the range. The host intrusive present in each of these areas appears to have been influenced by assimilation of the Osceola Argillite. Nonetheless, radiometric age data (Lee and others, 1970) show that the aplite dikes present in these two areas are related to two different epochs of mineralization.

Aplite dikes are present throughout the Pole Canyon-Can Young Canyon area. In some places their volume is subequal to that of the host intrusive. In most places the host intrusive is rather friable and is overlain by rubble slopes, except where massive outcrops are held up by the more resistant dikes of aplite and micropegmatite. Some of these dikes are more than 6 feet wide. It is not uncommon for them to be present in swarms that all but remake the host intrusive. Although local crosscutting relations are exposed, most of these dikes have a well-defined attitude, with a northeast strike and a near-vertical dip. Many feature symmetrical banding of aplitic and micropegmatitic material, with several sets of banding the rule. There is no particular relation between grain size and position of a band. Here and there barren veinlets of glassy quartz are associated with the felsic dikes. Some of these veinlets mark the center of symmetrically banded dikes. The mineralogy of these aplites and pegmatites is simple. Except for quartz, muscovite, and alkali feldspars, garnet is virtually the only mineral seen in the field. Fluorite is a common but minor accessory mineral. In addition, very careful mineral separation work on a few samples of aplite has revealed the presence of exceedingly minute amounts of gahnite, columbite-tantalite, and two unidentified minerals. Beryl is present in one aplite about 400 feet north of locality 93. This is the only beryl found in any of the aplites within the area shown on plate 1. Radiometric age data indicate that the aplites of this area are about 31 m.y. old (Lee and others, 1970), which is about the same age as the fault zone aplites described above. Thus, the fault zone aplites are related to the aplite dikes of the Pole Canyon-Can Young Canyon area.

The aplite dikes of the Hub mine area are about 150 m.y. old (Lee and others, 1970). They strike east-northeast and are nearly vertical. Almost all have a true aplitic or sugary texture. In contrast to the aplites described above, there is very little associated pegmatitic material. These aplites commonly flank veins of bull quartz, some of which are more than 10 feet wide. The trend of these veins of aplite and bull quartz—indeed even the topography—is dominated and controlled by a well-developed set of joints. Some of the Hub mine area aplites carry accessory garnet in addition to essential minerals (table 10); and mineral separation work turned up a few grains of an unknown mineral, but no fluorite was seen. The quartz veins are related to the aplites in time as well as space. The quartz veins carry a few widely scattered crystals of galena, and one of the veins carried most or perhaps all of the wolframite that was worked at the Hub tungsten mine about the time of World War I (pl. 1).

A few aplite dikes are exposed in the Snake Creek drainage. None was seen to be more than 1 foot wide or to persist in outcrop over a distance of more than a few tens of feet. Megascopically and petrographically, none was observed to carry any but essential minerals. No mineral separation work was done on these rocks.

Aplitic border facies are present locally near contacts of the intrusives. Most border facies dikes are only a few feet wide, but a larger mass is exposed south of locality 68 (pl. 1). No accessory minerals were noted in the field examination, but no mineral separation work was performed to confirm this.

The relatively few data available (table 10) suggest that our field classification of these aplites might be supported by differences in minor-element contents. For example, the three aplite dikes (samples 128–130, table 10) are relatively high in barium and strontium. Also, the fault zone aplites tend to be higher in tin and silver.

Only one lamprophyre was found within the mapped area. It is almost exactly at locality 19 (pl. 1). It does not crop not, but judged by the distribution of float on the ridge, it appears to be about 3 feet wide and less than 50 feet long.

TABLE 10.—*Analytical and other data for aplites*

[Samples 116–127, fault zone aplites; samples 128–130, border facies; and samples 131–133, simple aplite dikes. Sample localities shown on plate 1]

| Sample No. | 116 | 117 | 118 | 119 | 120 | 121 | 122 | 123 | 124 | 125 | 126 | 127 | 128 | 129 | 130 | 131 | 132 | 133 |
|---|---|---|---|---|---|---|---|---|---|---|---|---|---|---|---|---|---|---|
| **Chemical analyses (weight percent)** [1] | | | | | | | | | | | | | | | | | | |
| $SiO_2$ | 74.8 | 74.8 | 76.1 | 76.2 | 75.9 | 81.0 | 76.4 | 75.1 | 76.2 | 75.8 | 76.1 | 75.7 | 75.3 | 75.1 | 77.2 | 76.2 | 75.9 | 76.5 |
| $Al_2O_3$ | 14.1 | 14.1 | 13.3 | 13.7 | 13.5 | 10.5 | 13.6 | 14.0 | 13.0 | 14.1 | 14.2 | 14.0 | 13.4 | 13.4 | 13.0 | 13.8 | 13.9 | 13.2 |
| $Fe_2O_3$ | .42 | .29 | .52 | .30 | .33 | .59 | .46 | .49 | .41 | .18 | .48 | .30 | .59 | .61 | .44 | .19 | .21 | .21 |
| FeO | .20 | .32 | .88 | .20 | .28 | .08 | .14 | .20 | .32 | .36 | .22 | .28 | .12 | .28 | .20 | .12 | .28 | .08 |
| MgO | .07 | .05 | .10 | .10 | .10 | .04 | .12 | .13 | .10 | .10 | .10 | .05 | .24 | .57 | .13 | .08 | .10 | .11 |
| CaO | .42 | .31 | .28 | .50 | .35 | .24 | .36 | .56 | .63 | .55 | .54 | .35 | .40 | .30 | 1.3 | .28 | .72 | .48 |
| $Na_2O$ | 4.3 | 3.8 | 4.2 | 4.1 | 4.1 | 3.0 | 4.0 | 3.9 | 3.7 | 4.0 | 3.6 | 4.0 | 2.9 | 2.7 | 3.4 | 4.4 | 3.9 | 4.1 |
| $K_2O$ | 4.1 | 5.0 | 4.2 | 3.7 | 3.9 | 3.5 | 4.2 | 4.6 | 4.5 | 4.0 | 4.3 | 4.4 | 5.4 | 5.9 | 3.8 | 4.2 | 4.4 | 4.7 |
| $H_2O(+)$ | .55 | .49 | .50 | .62 | .73 | .72 | .58 | .41 | .51 | .64 | .44 | .52 | .62 | .82 | .45 | .50 | .47 | .44 |
| $H_2O(-)$ | .06 | .11 | .09 | .11 | .05 | .11 | .11 | .08 | .09 | .10 | .10 | .08 | .17 | .15 | .04 | .08 | .02 | .09 |
| $TiO_2$ | .10 | .01 | .04 | .10 | .06 | .00 | .01 | .10 | .06 | .06 | .01 | .03 | .35 | .21 | .02 | .10 | .04 | .05 |
| $P_2O_5$ | .05 | .03 | .02 | .00 | .02 | .06 | .00 | .00 | .03 | .02 | .00 | .00 | .18 | .02 | .00 | .00 | .00 | .00 |
| MnO | .15 | .34 | .15 | .13 | .21 | .07 | .14 | .13 | .17 | .12 | .09 | .25 | .08 | .01 | .02 | .06 | .04 | .03 |
| $CO_2$ | <.05 | <.05 | <.05 | <.05 | <.05 | <.05 | <.05 | <.05 | <.05 | <.05 | <.05 | .06 | <.05 | <.05 | <.05 | <.05 | .05 | <.05 |
| Cl | .00 | .00 | .00 | .00 | .01 | .00 | .00 | .01 | .00 | .00 | .00 | .01 | .00 | .00 | .00 | .00 | .00 | .00 |
| F | .02 | .05 | .03 | .09 | .07 | .03 | .04 | .07 | .09 | .09 | .13 | .03 | .04 | .07 | .01 | .04 | .01 | .01 |
| Total | 99 | 100 | 100 | 100 | 100 | 100 | 100 | 100 | 100 | 100 | 100 | 100 | 100 | 100 | 100 | 100 | 100 | 100 |
| **CIPW norms** | | | | | | | | | | | | | | | | | | |
| Quartz | 33.5 | 32.7 | 34.2 | 37.2 | 36.4 | 49.9 | 36.1 | 33.7 | 36.2 | 35.9 | 37.6 | 34.7 | 37.2 | 35.5 | 39.9 | 33.9 | 34.7 | 33.5 |
| Corundum | 2.0 | 2.1 | 1.5 | 2.3 | 2.1 | 1.6 | 1.9 | 1.8 | 1.2 | 2.5 | 3.0 | 2.3 | 2.6 | 2.3 | .96 | 1.6 | 1.6 | .52 |
| Zircon | | | | | | | .02 | | | | | | | .02 | | | .02 | |
| Orthoclase | 24.4 | 29.6 | 24.7 | 21.9 | 23.1 | 20.7 | 24.8 | 27.2 | 26.6 | 23.6 | 25.3 | 26.0 | 32.0 | 34.8 | 22.4 | 24.8 | 26.0 | 27.8 |
| Albite | 36.6 | 32.3 | 35.4 | 34.8 | 34.8 | 25.4 | 33.8 | 33.0 | 31.4 | 33.8 | 30.4 | 33.8 | 24.6 | 22.8 | 28.8 | 37.2 | 33.0 | 34.7 |
| Anorthite | 1.6 | .99 | 1.0 | 1.8 | 1.1 | .60 | 1.5 | 2.3 | 2.3 | 1.9 | 1.7 | 1.1 | .58 | .85 | 6.4 | 1.1 | 3.2 | 2.3 |
| Halite | | | | | .02 | | | .02 | | | | .02 | | | | | | |
| Enstatite | .18 | .13 | .25 | .25 | .25 | .10 | .30 | .32 | .25 | .25 | .25 | .12 | .60 | 1.4 | .32 | .20 | .25 | .27 |
| Ferrosilite | .14 | .97 | 1.4 | .20 | .54 | | .12 | .04 | .47 | .64 | .16 | .68 | | | .01 | .01 | .35 | |
| Magnetite | .61 | .42 | .75 | .44 | .48 | .49 | .67 | .71 | .60 | .26 | .69 | .44 | | .33 | .64 | .28 | .30 | .21 |
| Hematite | | | | | | .26 | | | | | | | .59 | .38 | | | | .07 |
| Ilmenite | .19 | .02 | .08 | .19 | .11 | | .02 | .19 | .11 | .11 | .02 | .06 | .43 | .40 | .04 | .19 | .08 | .10 |
| Apatite | .12 | .07 | .05 | | .05 | .14 | | | .07 | .05 | | | .43 | .05 | | | | |
| Fluorite | .04 | .10 | .06 | .19 | .14 | .06 | .08 | .14 | .18 | .18 | .27 | .06 | .07 | .14 | .02 | .08 | .02 | .02 |
| Calcite | | | | | | | | | | | | .14 | | | | | .11 | |
| $H_2O$ | .61 | .60 | .59 | .73 | .78 | .83 | .69 | .49 | .60 | .74 | .54 | .60 | .79 | 97 | .49 | .60 | .49 | .53 |
| Total | 100 | 100 | 100 | 100 | 100 | 100 | 100 | 100 | 100 | 100 | 100 | 100 | 100 | 100 | 100 | 100 | 100 | 100 |
| **Partial modal analyses** [2] | | | | | | | | | | | | | | | | | | |
| Quartz | 34 | 38 | 37 | 35 | 38 | 52 | 38 | 37 | 37 | 38 | 39 | 35 | 47 | 40 | 35 | 36 | 39 | 35 |
| Microcline | 22 | 21 | 23 | 20 | 20 | 16 | 20 | 20 | 21 | 20 | 20 | 23 | 21 | 25 | 21 | 22 | 23 | 25 |
| Plagioclase | 35 | 34 | 36 | 38 | 37 | 27 | 34 | 36 | 36 | 35 | 31 | 32 | 22 | 24 | 33 | 38 | 35 | 38 |
| Muscovite | 8 | 9 | 5 | 6 | 7 | 6 | 5 | 6 | 7 | 6 | 7 | 8 | 7 | 10 | 7 | 5 | 6 | 3 |
| **Semiquantitative spectrographic analyses (parts per million)** [3] | | | | | | | | | | | | | | | | | | |
| Ag | 0 | <0.7 | 0 | 0 | <0.7 | 0 | 0 | 0 | 0 | 0 | <0.7 | <0.7 | 0 | 0 | 0 | 0 | 0 | 0 |
| B | 0 | 0 | 0 | 0 | 0 | 10 | 15 | 10 | 0 | 0 | 15 | 15 | 10 | 0 | 0 | 10 | 0 | 10 |
| Ba | 30 | 10 | 70 | 70 | 70 | 50 | 100 | 100 | 70 | 100 | 100 | 20 | 200 | 500 | 700 | 20 | 300 | 50 |
| Be | 5 | 3 | 7 | 7 | 7 | 50 | 10 | 7 | 5 | 10 | 10 | 7 | 7 | 2 | 5 | 10 | 5 | 10 |
| Bi | 0 | 0 | 0 | 0 | 0 | 0 | 0 | 0 | 0 | 0 | 20 | 0 | 0 | 0 | 0 | 0 | 0 | 0 |
| Cr | 5 | 5 | 5 | 7 | 5 | 50 | 70 | 30 | 15 | 3 | 70 | 50 | 15 | 7 | 7 | 30 | 3 | 50 |
| Cu | 70 | 5 | 7 | 20 | 50 | 10 | 3 | 3 | 2 | 7 | 30 | 30 | 5 | 20 | 7 | 7 | 20 | 15 |
| Ga | 50 | 50 | 50 | 50 | 70 | 30 | 50 | 50 | 50 | 50 | 70 | 50 | 50 | 30 | 20 | 50 | 30 | 50 |
| Li | 0 | 0 | 0 | 0 | 0 | 0 | 0 | 0 | 0 | <200 | 0 | 0 | 0 | 0 | 0 | 0 | 0 | 0 |
| Mo | 0 | 0 | 0 | 0 | 0 | 0 | 0 | 0 | 0 | 0 | 0 | 0 | 5 | 0 | 0 | 0 | 0 | 0 |
| Nb | 50 | 70 | 50 | 70 | 70 | 50 | 70 | 50 | 70 | 70 | 70 | 70 | 30 | 10 | 15 | 70 | 30 | 50 |
| Ni | 3 | 5 | 5 | 3 | 5 | 15 | 20 | 7 | 5 | 3 | 20 | 20 | 5 | 3 | 5 | 15 | 0 | 15 |
| Pb | 50 | 50 | 70 | 50 | 50 | 50 | 100 | 100 | 70 | 70 | 100 | 50 | 70 | 50 | 150 | 70 | 70 | 100 |
| Sc | 7 | 0 | 10 | 15 | 15 | 10 | 10 | 15 | 10 | 7 | 7 | 10 | 7 | 5 | 5 | 10 | 5 | 0 |
| Sn | 5 | 0 | 0 | 15 | 20 | 0 | 0 | 0 | 15 | 7 | 20 | 15 | 0 | 0 | 7 | 0 | 0 | 7 |
| Sr | 30 | 10 | 50 | 30 | 30 | 50 | 70 | 50 | 50 | 50 | 50 | 10 | 100 | 200 | 300 | 10 | 150 | 30 |
| V | 3 | 0 | 5 | 3 | 7 | 7 | 7 | 7 | 7 | 5 | 10 | 7 | 15 | 30 | 15 | 0 | 5 | 10 |
| Y | 30 | 50 | 30 | 30 | 50 | 15 | 30 | 50 | 30 | 30 | 50 | 50 | 30 | 7 | 15 | 30 | 50 | 30 |
| Yb | 3 | 3 | 5 | 5 | 5 | 2 | 5 | 5 | 3 | 3 | 5 | 5 | 3 | 1 | 2 | 5 | 5 | 5 |
| Zr | 30 | 20 | 50 | 30 | 20 | 20 | 100 | 70 | 50 | 70 | 50 | 20 | 70 | 100 | 50 | 70 | 150 | 50 |

[1] Cl and F determinations by Vertie C. Smith. All other determinations by Paul Elmore, Samuel Botts, Gillison Chloe, Lowell Artis, and H. Smith, using methods similar to those developed by Shapiro and Brannock (1956).

[2] Based mainly on calibrated X-ray diffraction patterns. See text for discussion. Muscovite figures for samples 128 and 129 include some kaolinite.

[3] Analyses by Chris Heropoulos and R. E. Mays. 0, below limit of detection. Table 4 lists the 45 minor elements sought, together with limits of detection. General limitations of method are given in text.

## AGE RELATIONS OF THE INTRUSIVE TYPES

First efforts to apply radiometric age dating techniques to an understanding of the history of these intrusive rocks met with several puzzling inconsistencies. Gradually, by means of more than 80 age determinations based on K-Ar, Pb/$\alpha$, Rb-Sr, and U-Th-Pb isotope methods, we unraveled a sequence of events that fits the well-exposed field relations. The details of this age dating and the causes of the earlier inconsistences mentioned above are given by Lee, Stern, Mays, and Van Loenen (1968) and Lee, Marvin, Stern, and Peterman (1970).

Briefly, this was the sequence of events. Emplacement and crystallization of the main intrusive bodies took place in Middle Jurassic time, about 160 m.y. ago. About 150 m.y. ago, the aplite dikes and quartz veins of the Hub mine area were formed. Regardless of when the Snake Range décollement came into existence, the latest movement on it appears to have taken place 17–18 m.y. ago. Prior to this latest movement stresses related to this faulting were at least partly responsible for squeezing up a mass of late aplitic material. This aplitic phase and its associated micropegmatite are rather widely exposed in the eastern part of the mapped area.

## SOURCE OF BERYLLIUM MINERALIZATION

This study grew out of an attempt to test the idea of a relation between the granitoid rocks described and the nonpegmatite beryllium mineralization exposed at the Mount Wheeler mine. What then can be said regarding the source of this mineralization?

First, consider briefly some of the other concentrations of metals that might logically be related to the history of the intrusive rocks described. (All subsequent references to age are based on the radiometric age data presented by Lee and others (1970).) A partial list of area deposits covering a representative suite of metals is:

1. The Hub mine wolframite deposit (about 150 m.y.).
2. The Johnson mine scheelite deposits, near the crest of the range above Johnson Lake (about 140 m.y.).
3. The St. Lawrence mine galena deposits, about 1 mile east of the adit of the Mount Wheeler mine.
4. The Osceola gold mining district (fig. 1; Weeks, 1908), about 10 miles north of the mapped area.

Except for the quartz veins that carry the wolframite in the Hub mine area (about 150 m.y.), and the quartz veins that carry scheelite at the Johnson mine (about 140 m.y.), radiometric age dates are not available for the deposits mentioned above. However, the few age data available for the tungsten-bearing quartz veins and the sparse distribution of scheelite in the low-grade contact rocks on the crest of the range (p. 5) are both evidence that tungsten was present during the magmatic history of this Jurassic intrusive. Moreover, other evidence suggests a genetic relation between this mineralization and the Jurassic granitoid rocks; small amounts of tungsten, gold, and mercury were detected spectrographically in zircons recovered from some of the lime-poor rocks of the Snake Creek-Williams Canyon area (Lee and others, 1968). Thus, it appears that these metals were available in the magma and probably were concentrated in some of the hydrothermal end products of crystallization. Similar evidence bearing on the introduction of beryllium at the Mount Wheeler mine by the (Jurassic) intrusive is less clear. Although some of the accessory monazite carries small amounts of beryllium, accessory allanite does not, even though allanite from other occurrences has been reported to carry significant amounts of beryllium (Lee and Bastron, 1962, 1967).

Results of this study point toward a genetic relationship between the nonpegmatite beryllium deposits at the Mount Wheeler mine and the Oligocene aplite—that is, the fault zone aplites (about 32 m.y.) and the aplite dikes of the Pole Canyon-Can Young Canyon area (about 31 m.y.). The evidence for this is mostly chemical and mineralogical:

1. Beryl is present (but surely not widespread) in these aplites.
2. Fluorite is a common accessory mineral in these aplites (but apparently not in the Jurassic aplites and quartz veins of the Hub mine area). The association of beryllium with fluorine in hydrothermal deposits is well known and is taken as evidence of the role of fluorides in the transportation of beryllium. (See Beus, 1962, p. 38.) Fluorite is a common gangue mineral of the beryllium deposits at the Mount Wheeler mine (Stager, 1960).
3. Tin is present in the fault zone aplites in amounts up to 20 ppm (parts per million) (table 10). The Sn-Be-F association was emphasized by Sainsbury (1964, p. 920). (See also Beus, 1962, p. 39.)
4. Boron is present in some of the fault zone aplites and also is associated with beryllium minerals at the Mount Wheeler mine. Three samples of phenakite ($Be_2SiO_4$) from these ores contained 200, 300, and 600 ppm boron (Lee and Erd, 1963).

At the present level of erosion, the beryllium deposit at the Mount Wheeler mine is 7 miles or more from the Oligocene aplite, but this aplite appears to be rather widespread at the surface and could easily extend to the southwest at depth. About 5 miles north of the mapped area, scattered outcrops of a beryl-bearing aplite phase occur over an area of several square miles north of

Strawberry Creek. Moreover, about 2 miles west of this Strawberry Creek aplite, the tourmaline-coated (boron) joint surfaces described by Lee and Erd (1963) are exposed.

## SUMMARY AND CONCLUSIONS

The region of this study is ideal for a study of igneous processes due to a fortuitous combination of circumstances:

1. The area has already been carefully mapped, so the field setting is well known.
2. The size of the intrusive outcrop, about 20 square miles, is amenable to this type of study. Chemical and mineralogical trends are developed over large enough distances to be defined with assurance, but the distances are small enough to allow detailed field study of the concentration gradients.
3. The area is well exposed and accessible.
4. The intrusive is in contact with chemically distinct host rocks.
5. The intrusive has not been deeply unroofed. Probably it has not been eroded to a depth of more than 1,000 feet anywhere.

The chemistry and mineralogy of these granitoid rocks are highly variable from place to place; and these variations, involving major elements and minor elements, essential minerals and accessory minerals, are systematic and for the most part interrelated in an orderly way. The discovery of these chemical and mineralogical relations in this geological environment is the main contribution of this study. We regard these features as resulting from assimilation.

For various reasons, we have chosen to relate other variables to lime content of the granitoid rock, but this choice is arbitrary inasmuch as the major-element oxides are interrelated much as one would expect to find in a sequence of differentiated rocks. Thus, if a given trend can be shown for CaO, the same or an opposite trend may accordingly be shown for one of the other major oxides.

Where trends are best defined, CaO content of the intrusive ranges from about 4.5 percent (host rock limestone) to about 0.6 percent (host rock quartzite). The complete transition from lime rich (granodiorite) to lime poor (quartz monzonite) is best exposed over a horizontal distance of about 3 miles. As the overall chemistry changes, amounts of the essential minerals present also change, and the trends have much in common with those expectable in a series of differentiates.

If so much of the chemistry and mineralogy of this transition from granodiorite to quartz monzonite fits the idea of magmatic differentiation, why not simply accept such differentiation as the best explanation of the gradients described? There is, of course, the negative argument that a diligent search in the field failed to turn up any contact relations among the "differentiates" (except aplites), but this in itself is hardly an adequate reason to turn instead to the idea of assimilation.

The positive arguments for assimilation are based on separate lines of evidence involving mineralogical and geochemical features. The more lime rich part of the intrusive contains acicular zircon and apatite, the same as the crystals of these minerals described in the literature as being typical of many other hybrid rocks. The main geochemical argument for assimilation involves distribution of the rare-earth elements. Whether we consider the rocks themselves or some of their constituent minerals (allanite, monazite, zircon, or apatite), the lighter, more basic rare earths tend to be concentrated in the more mafic parts of the intrusive—just the opposite of what might be expected in a series of differentiates. The tendency for barium to increase with decrease of $K_2O$ in these rocks also is contrary to what might be expected from differentiation.

Part of the granitoid outcrop contains coarse muscovite and is chemically and mineralogically different from the rest of the intrusive. The distinctive nature of this rock is most logically attributed to assimilation of the Osceola Argillite.

The chemistry of these hybrid rocks is in some ways similar to that of alkalic rocks and carbonatites (although these rare rock types are not known in this area). Allanites from the most-calcium-rich rocks show a pronounced concentration of the most basic rare earths, and whole-rock concentrations of such rare constituents as total cerium earths, Zr, P, Ti, Ba, Sr, and F increase sympathetically with whole-rock calcium. Moreover, thorium content of the constituent monazite tends to decrease as CaO content of the rock rises. These similarities along with the obviously strong influence of limestone and shale assimilation on the chemistry of the intrusive rock are certainly consistent with the limestone syntexis hypothesis for the origin of alkalic rocks and carbonatites.

The hybrid intrusive rocks described are near the level of a major thrust fault, and their emplacement seems to have been almost contemporaneous with some of the main movement on this thrust. However, the most recent movement postdates the main igneous activity and has caused cataclasis of some of the granitoid rocks.

The main intrusive, along with some associated aplite, crystallized during Middle Jurassic time, about 160 m.y. ago. There is also a rather extensive aplitic phase about 28–33 m.y. old that is, in part, localized near a normal fault in the intrusive. Judging from some rather

meager mineralogical and chemical evidence, we conclude that the nonpegmatite beryllium mineralization at the Mount Wheeler mine probably resulted from hydrothermal activity related to this 30-m.y. aplite.

The results of our study reaffirm what other workers have shown before. Normal igneous rock types may develop in any of several ways, and it is sometimes difficult to deduce the process from the end product. Of course, any "granite" must have undergone assimilation and contamination at some stage in its history. However, the late magmatic history of these rocks is often of economic as well as academic importance. We present, therefore, the following list of features, based upon the results of our studies, that may help to reveal the hybrid nature of other granitoid rocks and indicate contamination (of an acid magma) at or near the level of solidification. This list is not meant to be exhaustive, and most of these features have been mentioned individually by other workers, as is apparent from the references cited.

1. Acicular zircon is typical of a hybrid rock (Wyatt, 1954; Lee and others, 1968). In our study area, zircon also is more abundant in the more mafic phases (Lee and Dodge, 1964).
2. Acicular apatite is abundant in contaminated granites (Harker, 1895; Nockolds, 1933).
3. Biotite is conspicuous in hybrid rocks. (See Turner and Verhoogen, 1960, p. 156; Deer and others, 1962, p. 78.)
4. In accord with the abundance of apatite and biotite, hybrid rocks are likely to be relatively rich in $H_2O$ and F.
5. The most basic rare earths tend to be concentrated in hybrid rocks (Lyakhovich, 1962; Lee and Bastron, 1967).
6. The more mafic hybrid phases have a higher total content of accessory minerals than the associated felsic phases. Accessory minerals found in the more mafic phases are—in addition to apatite and zircon —allanite, epidote, sphene, and magnetite. The sparse suite of accessory minerals in the more felsic phases is more likely to be made up of monazite, ilmenite, and garnet (Lee and Dodge, 1964).
7. Owing to their unusual suite of accessory minerals, lime-rich hybrid rocks are likely to be richer in total cerium earths, Zr, P, Ti, Ba, and Sr than associated felsic rocks.

## REFERENCES CITED


Armstrong, R. L., 1968, Sevier orogenic belt in Nevada and Utah: Geol. Soc. America Bull., v. 79, no. 4, p. 429–458.

Barth, T. F. W., 1962, Theoretical petrology [2d ed.]: New York, John Wiley & Sons, Inc., 416 p.

Beus, A. A., 1962, Beryllium—Evaluation of deposits during prospecting and exploratory work [translated from Russian]: San Francisco, W. H. Freeman & Co., 161 p.

Bowen, N. L., 1922, The behavior of inclusions in igneous magmas: Jour. Geology, v. 30, supp. to no. 6, p. 513–570.

——— 1937, Recent high-temperature research on silicates and its significance in igneous geology: Am. Jour. Sci., v. 33, no. 193, p. 1–21.

Chayes, F., 1951, Modal composition of granites: Carnegie Inst. Washington Year Book, no. 50, p. 41.

Deer, W. A., Howie, R. A., and Zussman, J., 1962, Sheet silicates, v. 3 *of* Rock-forming minerals: New York, John Wiley & Sons, Inc., 270 p.

Drewes, H. D., 1958, Structural geology of the southern Snake Range, Nevada: Geol. Soc. America Bull., v. 69, no. 2, p. 221–239.

——— 1967, Geology of the Connors Pass quadrangle, Schell Creek Range, east-central Nevada: U.S. Geol. Survey Prof. Paper, 557, 93 p.

Drewes, H. D., and Palmer, A. R., 1957, Cambrian rocks of southern Snake Range, Nevada: Am. Assoc. Petroleum Geologists Bull, v. 41, no. 1, p. 104–120.

Gilluly, James, 1963, The tectonic evolution of the western United States—17th William Smith lecture: Geol. Soc. London Quart. Jour., v. 119, no. 2, p. 133–174.

Goldschmidt, V. M., Hauptmann, H., and Peters, C., 1933, Über die Berücksichtigung "seltener" Elemente bei Gesteins-Analysen: Naturwissenschaften, v. 21, no. 20, p. 362–365.

Haberlandt, Herbert, 1947, Die Bedeutung der Spurenelemente in der geochemischen Forschung: Österreichische Akad. Wiss. Sitzungsber., Math.-Naturw. Kl., Abt. 2b, v. 156, nos. 1–10, p. 293–323.

Harker, A., 1895, The Carrock Fell granophyre, pt. 2 *of* Carrock Fell—A study in the variation of igneous rock masses: Geol. Soc. London Quart. Jour., v. 51, p. 125–139.

Howell, E. E., 1875, Report on the geology of portions of Utah, Nevada, Arizona, and New Mexico: U.S. Geog. Surveys west 100th meridian (Wheeler), v. 3, pt. 3, p. 227–301.

Johannsen, Albert, 1931, Introduction, textures, classifications and glossary, v. 1 *of* A descriptive petrography of the igneous rocks: Chicago Univ. Press, 267 p.

Lee, D. E., and Bastron, Harry, 1962, Allanite from the Mount Wheeler area, White Pine County, Nevada: Am. Mineralogist, v. 47, nos. 11–12, p. 1327–1331.

——— 1967, Fractionation of rare-earth elements in allanite and monazite as related to geology of the Mount Wheeler mine area, Nevada: Geochim. et Cosmochim. Acta, v. 31, no. 3, p. 339–356.

Lee, D. E., and Dodge, F. C. W., 1964, Accessory minerals in some granitic rocks in California and Nevada as a function of calcium content: Am. Mineralogist, v. 49, nos. 11–12, p. 1660–1669.

Lee, D. E., and Erd, R. C., 1963, Phenakite from the Mount Wheeler area, Snake Range, White Pine County, Nevada: Am. Mineralogist, v. 48, nos. 1–2, p. 189–193.

Lee, D. E., Marvin, R. F., Stern, T. W., and Peterman, Z. E., 1970, Modification of potassium-argon ages by Tertiary thrusting in the Snake Range, White Pine County, Nevada, *in* Geological Survey research 1970; U.S. Geol. Survey Prof. Paper 700–D, p. D92–D102.

Lee, D. E., Mays, R. E., Van Loenen, R. E., and Rose, H. J., Jr., 1969, Accessory sphene from hybrid rocks of the Mount Wheeler mine area, Nevada, *in* Geological Survey research 1969: U.S. Geol. Survey Prof. Paper 650–B, p. B41–B46.

——— 1971, Accessory epidote from hybrid granitoid rocks of the Mount Wheeler mine area, Nevada, *in* Geological Survey reseach 1971: U.S. Geol. Survey Prof. Paper 750–C (in press).

Lee, D. E., Stern, T. W., Mays, R. E., and Van Loenen, R. E., 1968, Accessory zircon from granitoid rocks of the Mount Wheeler mine area, Nevada, *in* Geological Survey research 1968: U.S. Geol. Survey Prof. Paper 600–D, p. D197–D203.

Lee, D. E., and Van Loenen, R. E., 1969, Phengitic micas from the Cambrian Prospect Mountain Quartzite of eastern Nevada, *in* Geological Survey research 1969: U.S. Geol. Survey Prof. Paper 650–C, p. C45–C48.

——— 1970, Biotites from hybrid granitoid rocks of the southern Snake Range, Nevada, *in* Geological Survey research 1970: U.S. Geol. Survey Prof. Paper 700–D, p. D196–D206.

Lyakhovich, V. V., 1962, Rare earth elements in the accessory minerals of granitoids: Geochemistry (a translation of Geokhimiya), no. 1, p. 39–55.

Misch, Peter, and Hazzard, J. C., 1962, Stratigraphy and metamorphism of Late Precambrian rocks in central northeastern Nevada and adjacent Utah: Am. Assoc. Petroleum Geologists Bull., v. 46, no. 3, pt. 1, p. 289–343.

Murata, K. J., Rose, H. J., Jr., Carron, M. K., and Glass, J. J., 1957, Systematic variation of rare-earth elements in cerium-earth minerals: Geochim. et Cosmochim. Acta, v. 11, no. 3, p. 141–161.

Myers, A. T., Havens, R. G., and Dunton, P. J., 1961, A spectrochemical method for the semiquantitative analysis of rocks, minerals, and ores: U.S. Geol. Survey Bull. 1084–I, p. 207–229.

Nockolds, S. R., 1932, The contaminated granite of Bibette Head, Alderney: Geol. Mag., v. 69, no. 10, p. 433–452.

——— 1933, Some theoretical aspects of contamination in acid magmas: Jour. Geology, v. 41, no. 6, p. 561–589.

——— 1934, The production of normal rock types by contamination and their bearing on petrogenesis: Geol. Mag., v. 71, p. 31–39.

Palmer, A. R., 1958, Morphology and ontogeny of a Lower Cambrian ptychoparioid trilobite from Nevada: Jour. Paleontology, v. 32, no. 1, p. 154–170.

Peacock, M. A., 1931, Classification of igneous rock series: Jour. Geology, v. 39, no. 1, p. 54–67.

Pecora, W. T., 1956, Carbonatites—a review: Geol. Soc. America Bull., v. 67, no 11, p. 1537–1555.

Pirsson, L. V., 1947, Rocks and rock minerals [3d ed., revised by Adolph Knopf]: New York, John Wiley & Sons, Inc., 349 p.

Prince, A. T., 1943, The system albite-anorthite-sphene: Jour. Geology, v. 51, no. 1, p. 1–16.

Rankama, K. K., and Sahama, Th. G., 1950, Geochemistry: Chicago Univ. Press, 912 p.

Reynolds, D. L., 1946, The sequence of geochemical changes leading to granitization: Geol. Soc. London Quart. Jour., v. 102, no. 407, pt. 3, p. 389–446.

Rittmann, Alfred, 1960, Vulkane und ihre Tätigkeit [2d ed.]: Stuttgart, Ferdinand Enke, 336 p.

Sainsbury, C. L., Association of beryllium with tin deposits rich in fluorite: Econ. Geology, v. 59, no. 5, p. 920–92?.

Shapiro, Leonard, and Brannock, W. W., 1956, Rapid analysis of silicate rocks: U.S. Geol. Survey Bull. 1036–C, p. 19–56.

Shawe, D. R., 1966, Arizona-New Mexico and Nevada-Utah beryllium belts, *in* Geological Survey research 1966: U.S. Geol. Survey Prof. Paper 550–C, p. C206–C213.

Spurr, J. E., 1903, Descriptive geology of Nevada south of the fortieth parallel and adjacent portions of California: U.S. Geol. Survey Bull. 208, 229 p.

Stager, H. K., 1960, A new beryllium deposit at the Mount Wheeler mine, White Pine County, Nevada, *in* Short papers in the geological sciences: U.S. Geol. Survey Prof. Paper 400–B, p. B70–B71.

Tatlock, D. B., 1966, Rapid modal analysis of some felsic rocks from calibrated X-ray diffraction patterns: U.S. Geol. Survey Bull. 1209, 41 p.

Turekian, K. K., and Kulp, J. L., 1956, The geochemistry of strontium: Geochim. et Cosmochim. Acta, v. 10, nos. 5–6, p. 245–296.

Turner, F. J., and Verhoogen, John, 1960, Igneous and metamorphic petrology [2d ed.]: New York, McGraw-Hill Book Co., 694 p.

Tuttle, O. F., and Bowen, N. L., 1958, Origin of granite in the light of experimental studies in the system $NaAlSi_3O_8$–$KAlSi_3O_8$–$SiO_2$–$H_2O$: Geol. Soc. America Mem. 74, 153 p.

Washington, H. S., 1917, Chemical analyses of igneous rocks: U.S. Geol. Survey Prof. Paper 99, 1201 p. (a revision and expansion of Prof. Paper 14).

Weeks, F. B., 1908, Geology and mineral resources of the Osceola mining district, White Pine County, Nevada: U.S. Geol. Survey Bull. 340–A, p. 117–133.

Whitebread, D. H., 1968, Snake Range décollement and related structures in the southern Snake Range, eastern Nevada, *in* Abstracts for 1966: Geol. Soc. America Spec. Paper 101, p. 345–346.

Whitebread, D. H., Griggs, A. B., Rogers, W. B., and Mytton, J. W., 1962, Preliminary geologic map and sections of the Wheeler Peak quadrangle, White Pine County, Nevada: U.S. Geol. Survey Mineral Inv. Field Studies Map MF–244.

——— 1970, Geologic map of the Wheeler Peak and Garrison quadrangles, White Pine County, Nevada, and Milford County, Utah: U.S. Geol. Survey Misc. Geol. Inv. Map I–578.

Whitebread, D. H., and Lee, D. E., 1961, Geology of the Mount Wheeler mine area, White Pine County, Nevada, *in* Short papers in the geologic and hydrologic sciences: U.S. Geol. Survey Prof. Paper 424–C, p. C120–C122.

Wyatt, Michael, 1954, Zircons as provenance indicators: Am. Mineralogist, v. 39, nos. 11–12, p. 983–990.

# INDEX

[Italic page numbers indicate major references]

U. S. GOVERNMENT PRINTING OFFICE : 1971 O - 416-715